HEC MONTRÉAL
École affiliée à l'Université de Montréal

Essays on the valuation and the management of counterparty risk

par
Oussama Marzouk

Thèse présentée en vue de l'obtention du grade de Ph. D. en administration
(option Ingénierie financière)

Juin 2017

HEC MONTRÉAL

École affiliée à l'Université de Montréal

Cette thèse intitulée :

Essays on the valuation and the management of counterparty risk

Présentée par :

Oussama Marzouk

a été évaluée par un jury composé des personnes suivantes :

Érick Delage

HEC Montréal

Président-rapporteur

Michèle Breton

HEC Montréal

Directrice de recherche

Chantal Labbé

HEC Montréal

Membre du jury

Damiano Brigo

Imperial College, London

Examinateur externe

Valérie Bélanger

HEC Montréal

Représentante du directeur de HEC Montréal

Résumé

Cette thèse concerne l'évaluation et la gestion du risque de contrepartie. Dans le premier essai, nous introduisons une nouvelle approche pour évaluer le risque de contrepartie en se basant sur une formulation récursive du credit valuation adjustment (CVA) d'un produit dérivé exotique. Nous tenons compte de la relation entre le CVA et le mécanisme d'exercice lorsque ce mécanisme est à la discrétion de l'une des parties dans le contrat. En particulier, nous montrons que le CVA pour les produits offrant l'exercice anticipé ne peut pas être réduit à une perte espérée, en raison du changement dans la stratégie de l'exercice causé par la présence du risque de contrepartie. Notre formulation donne lieu à un algorithme de programmation dynamique (PD) qui peut être utilisé pour évaluer le risque de contrepartie correspondant à n'importe quelle stratégie d'exercice ou temps d'arrêt exogène. Lorsque la dimension de l'espace d'états n'est pas grande, cet algorithme est beaucoup plus efficace que les méthodes actuellement disponibles, fournissant une évaluation précise sans qu'il soit nécessaire de faire des simulations coûteuses. L'approche est flexible et incorpore facilement le risque de corrélation et divers modèles pour les facteurs sous-jacents.

Dans le deuxième essai, nous proposons une méthode efficace pour estimer la valeur à risque du CVA (CVA VaR). L'algorithme d'évaluation suggéré dans le premier essai fournit plus qu'une estimation ponctuelle: il donne le CVA pour tous les états et toutes les dates en une seule exécution. En d'autres termes, l'algorithme permet de caractériser le CVA comme une fonction connue des facteurs de risque, et ce pour différentes dates. Cette propriété puissante permet d'éviter le recours à des simulations imbriquées et permet d'estimer la CVA VaR en une seule simulation. Nous présentons des expériences numériques illustratives dans lesquelles nous appliquons la procédure proposée. En particulier, nous montrons que les hypothèses ad-hoc utilisées par les praticiens peuvent sous-estimer fortement la CVA VaR. De plus, nous analysons les effets non-linéaires qui découlent de la nature de la fonction du CVA, et nous relions ces effets aux sensitivités du CVA. Nous examinons aussi dans quelle mesure une distorsion entre les mesures de probabilité risque-neutre et physique peut affecter la CVA VaR, et nous étudions l'impact du risque de corrélation. Dans le troisième essai, nous étudions l'impact de deux types de corrélation sur le risque de corrélation dans le marché du taux d'intérêt. La première corrélation quantifie la dépendance entre le niveau du taux d'intérêt et la probabilité de défaut, tandis que la seconde introduit une dépendance entre la volatilité du taux d'intérêt et la probabilité de défaut. Nous considérons un modèle du taux d'intérêt avec volatilité stochastique cachée afin d'analyser les effets des corrélations sur les produits insensibles à la volatilité tels que les swaps de taux d'intérêt et sur les instruments sensibles à la volatilité tels que les options sur taux. Nous étudions également les effets des corrélations sur les instruments collatéralisés où le risque d'écart devient pertinent. Nous constatons que, dans l'ensemble, l'effet de la corrélation entre la volatilité du taux d'intérêt et l'intensité du défaut n'est pas signifcatif, et il est largement dominé par celui de la corrélation entre le niveau du taux d'intérêt et l'intensité du défaut pour les instruments non-collatéralisés.

Mots clés: Risque de contrepartie, CVA, Exercice anticipé, Programmation dynamique, CVA VaR, Risque de corrélation

Méthodes de recherche: Recherche quantitative, Modélisation mathématique, Analyse numérique

Abstract

This thesis deals with the pricing and the management of counterparty risk. In the first essay, we introduce a new approach to price counterparty risk based on a recursive formulation for the credit valuation adjustment (CVA) of a derivative security with early-exercise features. We account for the relation between the CVA and the exercise mechanism when this mechanism is at the discretion of one of the parties in the contract. In particular, we show that the CVA for early-exercise products cannot be reduced to a standard expected loss, because of the change in the exercise strategy as a result of the presence of counterparty risk. Our formulation gives rise to a dynamic programming (DP) algorithm that may be used to evaluate counterparty risk corresponding to any exercise strategy or exogenous stopping time. When the dimension of the state space is low, this algorithm is much more efficient than presently available methods, providing an accurate evaluation without the need for costly simulation. The approach is flexible and can account for wrong-way risk (WWR) and various models for the underlying factors.

In the second essay, we propose an efficient method to estimate the CVA VaR. The pricing algorithm suggested in the first essay provides more than a point estimate: it yields the CVA for all states and all dates in just one execution. In other terms, the algorithm yields the CVA as a known function of the market risk factors for different future dates. Such powerful property allows to avoid nested simulations and makes it possible to estimate the CVA VaR in just one simulation. We present illustrative numerical experiments in which we apply the suggested procedure. In particular, we show that ad-hoc assumptions used by practitioners can strongly misestimate the CVA VaR. Moreover, we analyze the non-linearity effects that arise as a consequence of the nature of the CVA function, and we link these effects to the CVA sensitivities (the CVA greeks). We also examine to which extent a distortion between the risk-neutral and the physical probability

measures can affect the CVA VaR, and we investigate the impact of right-way/wrong-way risk.

In the third essay, we investigate the impact of two kinds of correlation on the right-way/wrong-way risk in the interest-rate market. The first correlation depicts the dependence between the interest-rate level and the default probability, while the second introduces the dependence between the interest-rate volatility and the default probability. We consider an interest-rate model featuring unspanned stochastic volatility (USV) behavior in order to analyze the effects of correlations on both volatility-insensitive products such as interest-rate swaps and volatility-sensitive instruments such as interest-rate caps and floors. We also investigate the effects of correlations on collateralized instruments where gap risk becomes relevant. We find that, overall, the wrong-way effect of the correlation between the interest-rate volatility and the default intensity is not signifcant, and it is largely dominated by that of the correlation between the interest-rate level and the default intensity for non-collateralized instruments.

Key words: Counterparty risk, CVA, Early-exercise, Dynamic programming, CVA VaR, Wrong-way risk

Research methods: Quantitative research, Mathematical modeling, Numerical analysis

Contents

List of Tables

List of Figures

List of Abbreviations

CDS	Credit default swap
CIR	Cox-Ingersoll-Ross
CVA	Credit valuation adjustment
DP	Dynamic programming
FFT	Fast Fourier transform
GBM	Geometric Brownian motion
LSMC	Least-squares Monte-Carlo
NSS	Nelson-Siegel-Svensson
USV	Unspanned stochastic volatility
VaR	Value at Risk
WWR	Wrong-way risk

To my beloved mother Radhia,

To my beloved wife Wiem,

To my brother Jihed,

To my sister Nesrine.

Acknowledgments

I am deeply thankful to my supervisor Prof. Michèle Breton for her unlimited support, motivation, and valuable guidance. She has been always there to listen, help and make stimulating suggestions. Without her, this work would not have seen light. Michèle, I am forever indebted to you, merci infiniment !

I would also like to thank Prof. Ramzi Ben Abdallah and Prof. Chantal Labbé, the two other members of my advisory committee, for their time and their high-quality comments and suggestions.

I am also thankful to Ali Boudhina, who encouraged me to pursue this doctoral degree and suggested that I work on counterparty risk topics.

I am grateful to the Montréal Exchange for their financial support through the Canadian Derivatives Exchange Scholars Program, to HEC Montréal, the J.A. DeSève foundation, the Institut des Sciences Mathématiques (ISM), the Montreal Institute of Structured Finance and Derivatives (IFSID) and the Natural Sciences and Engineering Research Council of Canada (NSERC) for their generous financial support.

My sincere gratitude goes to my wonderful mother Radhia, my brother Jihed and my sister Nesrine for their unconditional support and encouragement.

Special thanks to my beloved wife Wiem. Nothing can describe her precious presence in my life. Her unlimited support, patience and care have contributed to the completion of this thesis.

Finally, I would like to thank my family, my friends and my colleagues of Deloitte for their moral support.

Chapter 1

General introduction

The financial crisis of 2007-2008 highlighted a number of shortcomings in the regulation of financial institutions. One of these was the misestimation of counterparty risk, defined as the risk of incurring losses in mark-to-market derivative positions at a counterparty default event. In other words, it is the risk that a counterparty would not fulfill her future payment obligations. Counterparty risk has been a hot topic in both academic and professional environments since the financial crisis. The magnitude of systemic credit risk that exploded during the financial crisis has led researchers and practitioners to rethink the very basic foundations of derivative pricing and risk management. Counterparty risk is particularly relevant in over-the-counter markets, which are not subject to the same tight regulatory requirements as for exchange markets. It is a hybrid type of risk, that can be seen as a complex combination of default risk and market risk. Default risk is related to default probabilities, while market risk is related to the movements of market factors. The potential amount that can be lost is random due to market risk, while the likelihood of a counterparty default is driven by default risk. Intuitively, what is relevant as a market risk is only the positive part of the future mark-to-market value. This is what we call the exposure, which is defined in most common situations as the maximum between the mark-to-market value and zero. This introduces non-linearities and a kind of optionality when it comes to pricing counterparty risk.

There are two common ways of mitigating counterparty risk. The first one is netting. Rather than considering counterparty risk at a single trade level, it is interesting to consider the aggregate exposure over all trades with a given counterparty through a netting agreement. In more colloquial terms, in the event of a counterparty default, outstanding trades are not treated separately. A positive mark-to-market value would cancel a negative one, resulting in an overall exposure that is less than the sum of individual exposures. Thus, netting can be an important mitigant of counterparty risk. However, netting makes the pricing and management of counterparty risk a real conceptual and technological challenge, as the overall exposure would depend on too many risk factors driving a large set of trades with a given counterparty. The second way of mitigating counterparty risk is the use of collateral. Collateral is a security (cash in general) that is posted by the party whose mark-to-market is negative as a guarantee for the party whose mark-to-market is positive. Collateral may be the most efficient way of reducing counterparty risk. However, even if collateral is posted very frequently, there could be still a good probability that the mark-to-market value moves so quickly in a short period of time that the most recently posted collateral would not cover the new mark-to-market value. This is what we call gap risk, which can be particularly relevant during turbulent periods.

The credit valuation adjustment (CVA) is the price of counterparty risk. It is a positive adjustment which is subtracted from the default-free value of a derivative position in order to have a fair value that accounts for the possible default of the counterparty. The CVA is a complex hybrid product, that is sensitive to the counterparty default probability and to the underlying market risk factors. In general situations, it can be equated to a zero-strike call option on the default-free value with a random maturity corresponding to the counterparty default date, or equivalently to an expected discounted loss. The optionality arises from the fact that only positive mark-to-market values contribute to the exposure profile. Hence, pricing the CVA of an instrument is at least as complex as pricing the instrument itself. For very simple vanilla products such as bonds or european options, the CVA computation is generally straightforward, making use of analytical formulas. However, for exotic instruments and netted portfolios, the CVA computation is a challenging task. Exotic instruments introduce path-dependency, while the number of risk factors can be too high for large netting sets. In particular, for products having early-exercise features, the computation of the CVA is problematic, since the presence of counterparty risk may alter the exercise strategy; and in such a case, the CVA can not be equated to a simple expected loss. In most practical cases, the

CVA is calculated using simulation-based methods.

Wrong-way Risk (WWR) is the additional risk induced by a dependence between the default probability and the underlying risk factors. The presence of a correlation between the exposure and the default probability can significantly change the price of counterparty risk. On one hand, a positive correlation would result in an increase in the CVA, since the exposure is higher in scenarios with defaults. In such a case, we talk about wrong-way risk. On the other hand, a negative correlation would decrease the CVA. In this situation, we talk about right-way risk. Wrong-way risk can be particularly significant in periods of systemic credit risk, where default risk becomes contagious. Besides, wrong-way risk makes the valuation of the CVA a more challenging task, because of the additional complexity introduced by correlations.

The CVA pricing charge was advocated by regulators since the second installment of the Basel Accords (Basel II). However, during the financial crisis, the major losses were caused by CVA movements rather than actual defaults. In more colloquial terms, the volatility of the price of counterparty risk caused much more damage than default risk itself. This led the third installment of the Basel Accords (Basel III) to introduce a capital charge against CVA variability. From a practical point of view, this implies the computation of a risk measure for the CVA process; we talk about a Value at Risk of the CVA (CVA VaR). The computation of the CVA VaR is extremely challenging, since the calculation of just one instance of the CVA is already intensive. Such numerical complexity led regulators and practitioners to consider very simplifying assumptions for the computation of the CVA VaR.

This thesis provides various contributions on the evoked topics of counterparty risk, and it is composed of three essays. In the first essay, we propose a new approach to compute the CVA for derivatives with early-exercise features. This new method is based on a recursive formulation of the CVA, and it is implemented using dynamic programming (DP) techniques. In particular, the suggested method takes into account the alteration of the exercise strategy caused by counterparty risk, in contrast to standard simulation methods which do not account for it. Moreover, it easily accomodates a variety of market models as well as wrong-way risk. Numerical experiments show the efficiency of the proposed DP algorithm with comparison to standard simulation approaches.

In the second essay, we capitalize on a powerful property of the DP algorithm developed in the first essay to significantly reduce the computational burden of computing the CVA VaR. In fact, the DP algorithm yields the CVA for all states and all dates in just one execution. This property allows to compute the CVA VaR by running only one simulation and without making any simplifying assumptions. We present several numerical experiments in which we show that the CVA VaR presents complex patterns and that the ad-hoc assumptions adopted by practioners may underestimate the CVA VaR. In the third essay, we investigate the impact of a correlation between the interest-rate volatility and the default probability on the right-way/wrong-way risk in the fixed-income market. We study the effect of this correlation on both collateralized and non-collateralized instruments and we compare it to the effect of a correlation between the interest-rate level and the default probability, which is the common way of considering right-way/wrong-way risk in the interest-rate derivative market.

The rest of this thesis is divided in 4 chapters. Chapter 2 presents our first essay on the valuation of counterparty risk for derivatives with early-exercise features. Chapter 3 presents our second essay on the estimation of the CVA VaR. Chapter 4 presents our third essay on the investigation of right-way/wrong-way risk in the interest-rate market. Finally, Chapter 5 is a general conclusion.

Chapter 2

Evaluation of counterparty risk for derivatives with early-exercise features

2.1 Introduction

The credit valuation adjustment (CVA) is the market value of counterparty risk. It is a pricing adjustment applied to the default-free value of the contract in order to obtain a fair value that accounts for the possible default of the counterparty. This adjustment can differ significantly when considering wrong-way risk (WWR), which is the risk faced when the underlying risk factors and the default of the counterparty are correlated. For a broad introduction on counterparty risk and CVA computation, we refer Brigo et al. (2013).[1]

The CVA caught the attention of researchers in quantitative finance due to the complexity underlying its evaluation. Brigo and Masetti (2006) give a general pricing formula for the CVA, which can be seen as a call option on the derivative portfolio value with a random maturity corresponding to the counterparty default date, or equivalently as an expected discounted loss from counterparty default. While the computation of the CVA is generally straightforward for European-style derivatives, this is not the case for derivatives with early-exercise opportunities, because the CVA is then path-dependent (for instance, the exposure of a Bermudan option falls to zero after exer-

[1] Specifically, Chapter 1 in Brigo et al. (2013) is a set of questions and answers reviewing current issues in counterparty risk and CVA valuation.

cise). Complexity is again increased when considering WWR, that is, when allowing correlation between the default process and the derivatives' underlying risk factors to exist (see Gregory (2012) (Chapter 15) for an overview and Brigo et al. (2013) for instances in various asset classes).

A number of approaches have been developed to incorporate the impact of credit risk on the value of derivatives. These approaches can be divided into two major categories, according to the way the default event is modeled, that is, either using structural or intensity models. In structural models, the default event for a given firm is related to the evolution of some of its structural variables, while in intensity models default is governed by an exogenous Poisson (or Cox) process (the hazard-rate process). The structural approach originated with Merton (1974), where a firm defaults if the value of its assets is below the value of its liabilities at the debt maturity. Although a structural framework is intuitive, its calibration for pricing needs is challenging (see for instance Brigo et al. (2011) for applications using structural models illustrating the calibration approach using credit default swap (CDS) rates). On the other hand, an intensity-based approach is more direct and calibration of intensity models is straightforward, since default probabilities can be easily extracted from the observed CDS premiums (see for instance Brigo and Masetti (2006) and Gregory (2012)). The literature on credit risk intensity models include Lando (1998), Duffie and Singleton (1999) and Brigo and Alfonsi (2005), among others.

CVA evaluation has been addressed under both frameworks and leads to analytical expressions for European options (e.g. Klein (1996) in the structural model case and Lando (1998) in the intensity model case). However, the issue of CVA evaluation is much more complicated for options with early-exercise opportunities. Simulation-regression approaches (see Tilley (1993), Carriere (1996), Tsitsiklis and Van Roy (2001) and Longstaff and Schwartz (2001)), commonly known as least-squares Monte-Carlo (LSMC) methods, are extensively used in the financial industry to approximate the exposure of an exotic derivative (see for instance Cesari et al. (2009) for a description of the use of LSMC to compute exposure profiles). While LSMC can be useful to approximate the optimal early-exercise strategy, it may introduce large statistical errors, as outlined for instance in Svenstrup (2005), and is generally recognized not to be very accurate for the estimation of the continuation value, which defines the exposure of the derivative contract.

Moreover, simulation-based approaches that are presently used involve two separate steps: the default-free derivative value is first evaluated independently from any counterparty default concern, and then used in a Monte-Carlo setting, involving the simulation of the default process along with the market risk factors, in order to estimate the expected loss (Brigo and Pallavicini (2007), Cesari et al. (2009) and Gregory (2012)). Such an approach can only work under the assumption that counterparty risk does not alter the exercise mechanism, which is an unrealistic simplification since the default driver is generally an observable market process (either a set of structural variables or a hazard-rate process). Klein and Yang (2013) show that the presence of counterparty risk can significantly affect the exercise boundary of an American option.

In this chapter, we introduce a new approach to price counterparty risk, possibly under WWR, based on a recursive formulation for the CVA of a derivative security with path-dependent features. We consider a general recovery function that may incorporate many counterparty risk features and we account for the relation between the CVA and the exercise strategy for contracts with early-exercise opportunities. In particular, we show that the CVA for early-exercise products can not be reduced to an expected loss, because of the change in the exercise strategy as a result of the presence of counterparty risk. Our formulation gives rise to a dynamic programming (DP) algorithm that may be used to evaluate counterparty risk corresponding to any exercise strategy or stochastic stopping time. When the dimension of the state space is low, this algorithm is much more efficient than the currently available methods, thereby providing an accurate evaluation without the need for costly simulation. Moreover, the algorithm provides more than a point estimate: it yields the value of a vulnerable derivative and its CVA for all possible values of the underlying variables and of time-to-maturity in a single execution. The CVA pricing model is implemented using an intensity model for counterparty default; however, it can be easily adapted to structural models. Numerical implementations are based on efficient DP interpolation techniques, as described in Breton and de Frutos (2012).

The chapter is organized as follows. Section 2.2 proposes a general model for the computation of the CVA in a default-intensity framework. Section 2.3 illustrates the application of the CVA model to various types of contracts. Section 2.4 provides details about the numerical implementation.

Section 2.5 reports on numerical experiments. Section 2.6 is a conclusion.

2.2 Credit Valuation Adjustment Model

In this section, we develop a general model and a recursive characterization of the CVA that can be used for defaultable derivative contracts, with or without early-exercise opportunities.

2.2.1 Notation

Consider a defaultable contract between an investor and a counterparty with inception date $t = 0$ and maturity T. Denote by $(Y_t)_{0\leq t\leq T}$ the (possibly multidimensional) process of the underlying factors, including the short interest rate, denoted by $(r_t)_{0\leq t\leq T}$. Let τ be the default time of the counterparty. τ is assumed to represent the first jump time of a Cox process with intensity process $(\lambda_t)_{0\leq t\leq T}$, also called the hazard-rate process. We assume that the process of all market quantities $(X_t)_{0\leq t\leq T} = (Y_t, \lambda_t)_{0\leq t\leq T}$ is Markovian and denote by $(\mathcal{F}_t)_{0\leq t\leq T}$ the filtration generated by the process $(X_t)_{0\leq t\leq T}$. In what follows, the notation $\mathbb{E}_t[\cdot]$ represents the expectation, under the risk-neutral measure, conditional on no prior default and on $\mathcal{F}_t$.

For a given $u \geq t$, denote by

$$\begin{aligned}
\Lambda_t(u) &\equiv \exp\left(-\int_t^u \lambda_s ds\right), \\
\Gamma_t(u) &\equiv \exp\left(-\int_t^u r_s ds\right).
\end{aligned}$$

The conditional risk-neutral default probability in $(t, u]$ is then given by

$$D_t(u) = 1 - \mathbb{E}_t[\Lambda_t(u)].$$

It will be useful to recall that

$$\int_t^u \lambda_s \Lambda_t(s) ds = 1 - \Lambda_t(u),$$

and that, for a given function f,

$$\mathbb{E}_t[\mathbb{1}_{(t,u]}(\tau)f(\tau)] = \mathbb{E}_t\left[\int_t^u f(s)\lambda_s\Lambda_t(s)ds\right], \tag{2.1}$$

where the function $\mathbb{1}_I(\cdot)$ is defined by

$$\mathbb{1}_I(x) = \begin{cases} 1 & \text{if } x \in I \\ 0 & \text{otherwise.} \end{cases}$$

We consider contracts with an exercise feature; the exercise event may lead for instance to immediate cash-flows (e.g. the payoff of an option) or to a physical contract (e.g. an interest-rate swap). In a general setting, the exercise event date can be exogenous (deterministic or stochastic, e.g. as in the case of respectively European options or barrier options), or it can be at the discretion of one of the parties (e.g. as in the case of Bermudan or American options). In the sequel, we assume that the investor has a terminating option that leads to a final cash-flow and revokes the contract, but all developments can easily be adapted to the case where the exercise date is exogenous or where the exercise event leads to a subsequent contract.

For three given dates $u \in [0,T]$, $s \in [0,T]$ and $t \in [0,u]$, we denote by $F^u(t,s)$ the random variable representing the sum of the cash-flows promised by the contract to the investor in the time interval $[t,s]$, discounted back at t, if the terminating option is exercised at date u. The amount that is recovered (or paid) by the investor in case of default is often expressed as a fixed proportion of the claim; for the moment however we do not assume any particular form and simply define a general recovery process, denoted $R_t(x)$, where $R_\tau(x)$ is the (possibly negative) amount recovered at $t=\tau$ if the default event happens at $\tau \leq u$ when $X_\tau = x$.

We then define

$$\begin{aligned} V_t(x;u) &= \mathbb{E}_t\left[F^u(t,T)\right], \\ V_t^D(x;u) &= \mathbb{E}_t\left[\mathbb{1}_{(T,\infty]}(\tau)F^u(t,T)\right] \\ &\quad + \mathbb{E}_t\left[\mathbb{1}_{(t,T]}(\tau)\left(F^u(t,\tau)+\Gamma_t(\tau)R_\tau(X_\tau)\right)\right]. \end{aligned} \tag{2.2}$$

$V_t(x; u)$ represents, at a given date $t \in [0, T]$ where $X_t = x$, the expected sum, under the risk-neutral measure, of discounted net cash-flows to the investor if the terminating option is exercised at date $u \in [t, T]$ for a counterparty-risk-free claim with the same characteristics as the defaultable claim. Similarly, conditional on no prior default at $(t,\, X_t = x)$, $V_t^D(x; u)$ represents the expected sum of discounted cash-flows of the defaultable claim if the terminating option is exercised at date u. If default happens after maturity T, then all the promised cash-flows are earned (first term); but in case of early default, only cash-flows between t and τ are received, along with the amount recovered at the time of the default event.

The notation $V_t(x; \kappa)$ and $V_t^D(x; \kappa)$ will be used to represent the expected cash-flows corresponding to a given κ, where κ is a stopping time with respect to $\mathcal{F}_t$. According to the risk-neutral pricing principle, conditional on no prior default, the value of a defaultable claim and that of the corresponding risk-free claim, denoted by $V_t^D(x)$ and $V_t(x)$ respectively, are then given by

$$
\begin{aligned}
V_t^D(x) &= \sup_{t \le \kappa \le T} \left\{ V_t^D(x; \kappa) \right\}, && (2.3) \\
V_t(x) &= \sup_{t \le \kappa \le T} \left\{ V_t(x; \kappa) \right\}. && (2.4)
\end{aligned}
$$

At a given date $t \in [0, T]$, conditional on no prior default or exercise, and assuming an optimal exercise strategy exists for each contract, we denote by κ_t^* the stopping time corresponding to the optimal exercise strategy of the defaultable claim and by $\widehat{\kappa}_t$ the stopping time corresponding to the optimal exercise strategy of the corresponding counterparty-risk-free claim.

2.2.2 General pricing formula

The CVA is defined as the difference between the value of a risk-free claim and the value of the corresponding defaultable claim. Conditional on no prior default at a given date $t \in [0, T]$ where $X_t = x$, we then have

$$
\mathrm{CVA}_t(x) \equiv V_t(x) - V_t^D(x). \tag{2.5}
$$

On the other hand, we define the expected potential loss from a derivative contract at $(t, X_t = x)$ as the difference between the expected discounted cash-flows for the default-free and the defaultable claims when the same exercise strategy is used for both contracts, resulting in the same stopping time κ:

$$C_t(x;\kappa) \equiv V_t(x;\kappa) - V_t^D(x;\kappa). \tag{2.6}$$

We then have, using (2.3)-(2.4) and (2.6),

$$\mathrm{CVA}_t(x) = V_t(x;\widehat{\kappa}_t) - V_t(x;\kappa_t^*) + C_t(x;\kappa_t^*).$$

When the contract has an early-exercise feature, the CVA can be decomposed into two parts; the first part, $V_t(x;\widehat{\kappa}_t) - V_t(x;\kappa_t^*)$, is due to the change in the optimal exercise strategy when a contract is subject to counterparty risk, while the second part, $C_t(x;\kappa_t^*)$, is the expected loss under the exercise strategy that is optimal for the defaultable claim.

Notice that for contracts with no early-exercise feature ($u = T$), the CVA pricing formula (2.5) reduces to

$$\begin{aligned}\mathrm{CVA}_t(x) &= \mathbb{E}_t\left[\mathbb{1}_{(t,T]}(\tau)\left(F^T(t,T) - F^T(t,\tau) - \Gamma_t(\tau)R_\tau(X_\tau)\right)\right] \\ &= \mathbb{E}_t\left[\mathbb{1}_{(t,T]}(\tau)\Gamma_t(\tau)\left(V_\tau(X_\tau) - R_\tau(X_\tau)\right)\right]. \end{aligned} \tag{2.7}$$

When $R_t(x) = R\max\{V_t(x);0\} + \min\{V_t(x);0\}$, where $R \in [0,1]$ is a constant recovery factor, we recover the CVA pricing formula of Brigo and Masetti (2006):

$$\mathrm{CVA}_t(x) = (1-R)\,\mathbb{E}_t[\mathbb{1}_{(t,T]}(\tau)\Gamma_t(\tau)\max\{V_\tau(X_\tau);0\}].$$

In the following section, we propose a recursive characterization of the CVA that can be used for contracts with a finite number of early terminating opportunities.

2.2.3 Recursive pricing formula

To this end, we define the set $\mathcal{T} = \{t_m, m = 0, ..., M\}$ of discrete evaluation dates, where $t_M \equiv T$. The set $\mathcal{T}$ includes all the dates where a cash-flow is promised in the contract, all possible exercise dates for the terminating option, which we assume to be finite in number, and any other date where the CVA needs to be evaluated. In this setting, the characterization of an exercise strategy reduces to a discrete collection of stopping sets $\mathcal{H} = \{H_m, m = 1, ..., M\}$, such that the investor should exercise the terminating option at the first time t_m such that $X_{t_m} \in H_m$. An exercise strategy characterized by a collection $\mathcal{H} = \{H_m, m = 1, ..., M\}$ generates an increasing discrete sequence of stopping times defined by

$$\kappa_i = \min \{t_m \in \mathcal{T} : t_m \geq t_i \text{ and } X_{t_m} \in H_m\}, \ i = 1, ..., M.$$

We denote by $C_{t_m}^{\mathcal{H}}(x) \equiv C_{t_m}(x; \kappa_m)$ the expected potential loss at t_m for a given exercise strategy characterized by $\mathcal{H}$. To simplify notation, we also denote by $V_{t_m}(x; \mathcal{H})$ (resp. $V_{t_m}^D(x; \mathcal{H})$) the expected sum at $(t_m, X_{t_m} = x)$ of discounted cash-flows corresponding to a given strategy characterized by $\mathcal{H}$, conditional on no prior default and given no prior exercise.

The set $\mathcal{T}$ of evaluation dates coincides with the set of early-exercise opportunities without loss of generality, since it suffices to set $H_m = \varnothing$ when terminating the contract is not allowed at t_m. Define

$$\begin{aligned}
\delta_m &\equiv \exp\left(-\int_{t_m}^{t_{m+1}} \lambda_s ds\right) = \Lambda_{t_m}(t_{m+1}), \ m = 0, ..., M-1, \\
\beta_m &\equiv \exp\left(-\int_{t_m}^{t_{m+1}} r_s ds\right) = \Gamma_{t_m}(t_{m+1}), \ m = 0, ..., M-1.
\end{aligned}$$

Conditional on no prior default and given no prior exercise at date t_m, we now compute the expected loss corresponding to a given exercise strategy characterized by $\mathcal{H} = \{H_m, m = 1, ..., M\}$.

For $x \notin H_m$ (i.e., $\kappa_m = \kappa_{m+1} \geq t_{m+1}$), we have using (2.1)

$$
\begin{aligned}
C^{\mathcal{H}}_{t_m}(x) &= V_{t_m}(x;\mathcal{H}) - V^{D}_{t_m}(x;\mathcal{H}) \\
&= \mathbb{E}_{t_m}\left[\mathbb{1}_{(t_m,\kappa_{m+1}]}(\tau)\Gamma_{t_m}(\tau)\left(V_\tau(X_\tau;\mathcal{H}) - R_\tau(X_\tau)\right)\right] \\
&= \mathbb{E}_{t_m}\left[\int_{t_m}^{t_{m+1}} \Gamma_{t_m}(s)\left(V_s(X_s;\mathcal{H}) - R_s(X_s)\right)\lambda_s\Lambda_{t_m}(s)ds\right] \\
&\quad + \mathbb{E}_{t_m}\left[\int_{t_{m+1}}^{\kappa_{m+1}} \Gamma_{t_m}(s)\left(V_s(X_s;\mathcal{H}) - R_s(X_s)\right)\lambda_s\Lambda_{t_m}(s)ds\right] \\
&= \mathbb{E}_{t_m}\left[\int_{t_m}^{t_{m+1}} \Gamma_{t_m}(s)\left(V_s(X_s;\mathcal{H}) - R_s(X_s)\right)\lambda_s\Lambda_{t_m}(s)ds\right] \\
&\quad + \mathbb{E}_{t_m}\left[\beta_m\delta_m\int_{t_{m+1}}^{\kappa_{m+1}} \Gamma_{t_{m+1}}(s)\left(V_s(X_s;\mathcal{H}) - R_s(X_s)\right)\lambda_s\Lambda_{t_{m+1}}(s)ds\right] \\
&= B^{\mathcal{H}}_m(x) + \mathbb{E}_{t_m}\left[\beta_m\delta_m C^{\mathcal{H}}_{t_{m+1}}\left(X_{t_{m+1}}\right)\right],
\end{aligned}
$$

where

$$
B^{\mathcal{H}}_m(x) \equiv \mathbb{E}_{t_m}\left[\int_{t_m}^{t_{m+1}} \Gamma_{t_m}(s)\left(V_s(X_s;\mathcal{H}) - R_s(X_s)\right)\lambda_s\Lambda_{t_m}(s)ds\right]. \tag{2.8}
$$

On the other hand, for $x \in H_m$ (i.e., $\kappa_m = t_m$), we have $C^{\mathcal{H}}_{t_m}(x) = 0$.

We therefore obtain a recursive definition of the expected loss corresponding to a given exercise strategy characterized by $\mathcal{H}$, conditional on no prior default and given no prior terminating at date t_m:

$$
C^{\mathcal{H}}_{t_m}(x) = \mathbb{1}_{\overline{H_m}}(x)\left(B^{\mathcal{H}}_m(x) + \mathbb{E}_{t_m}\left[\beta_m\delta_m C^{\mathcal{H}}_{t_{m+1}}\left(X_{t_{m+1}}\right)\right]\right), \; m = 0, ..., M-1, \tag{2.9}
$$

$$
C^{\mathcal{H}}_{T}(x) = 0. \tag{2.10}
$$

Equations (2.9)-(2.10) apply to any exercise strategy, as long as there is a finite number of possible terminating dates. The limiting case where the terminating option can be exercised at any time is obtained by letting $M \to \infty$. In practice, the number of possible terminating dates is constrained by the observation frequency.

When the contract offers no early-exercise opportunities, the superscript $\mathcal{H}$ can be dropped and $\text{CVA}_{t_m}(x) = C_{t_m}(x)$. We then obtain a recursive characterization of the CVA that can be interesting in many cases, for instance, when the CVA of a contract maturing at a near deterministic date (the term $B_m(x)$) is relatively easy to evaluate—as illustrated for instance in Section 2.3.3. This recursive formulation can also be used for contracts with stochastic maturities, for example involving deactivating barriers; in that case, the direct valuation used in (2.7) infeasible, but it is straightforward to adapt the recursive formulation (2.9)-(2.10) by identifying H_m with the set of states, specified in the contract, that trigger a terminating event at date t_m. Besides, the recursive formulation can be easily adapted to first-passage structural models (see Appendix 1 for details).

2.2.4 Optimal exercise strategy

We now characterize the optimal exercise strategy of a defaultable claim with a finite number of exercise opportunities. Denote by $q_m^e(x)$ the exercise payoff at t_m when $X_{t_m} = x$, $m = 0, ..., M$ and by $q_m^c(x)$ the contractual payoff at $(t_m, X_{t_m} = x)$ when the option is not exercised. Without loss of generality, we can assume that the set of exercise opportunities coincides with $\mathcal{T}$ by setting $q_m^e(x) = -\infty$ when exercise is not allowed at t_m.

Let $\mathcal{H}^* = \{H_m^*, m = 1, ..., M\}$ represent the collection of stopping sets characterizing the optimal exercise strategy of the defaultable claim. Accordingly, $V_{t_m}^D(x) = V_{t_m}^D(x; \mathcal{H}^*)$ denotes the value of the defaultable claim at t_m when $X_{t_m} = x$, obtained by using the optimal exercise strategy for this defaultable claim, and $V_{t_m}(x; \mathcal{H}^*)$ denotes the expected payoff of the corresponding risk-free claim under the same exercise strategy.

At a given exercise date $t_m \in \mathcal{T}$, $m = 0, ..., M-1$, define an auxiliary strategy, indexed by $\mathcal{C}$, that consists of holding the claim until the next exercise date and of using the optimal exercise strategy of the defaultable claim from then on. From (2.9) and (2.6), the expected loss due to counterparty risk resulting from using this strategy is given by

$$
\begin{aligned}
C_{t_m}^{\mathcal{C}}(x) &= B_m^{\mathcal{C}}(x) + \mathbb{E}_{t_m}\left[\beta_m \delta_m C_{t_{m+1}}^{\mathcal{H}^*}\left(X_{t_{m+1}}\right)\right] \\
&\equiv V_{t_m}(x; \mathcal{C}) - V_{t_m}^D(x; \mathcal{C}).
\end{aligned}
$$

Recall that $\mathcal{T}$ contains all the dates where contractual cash-flows are possible; we then have using the property of iterated expectations and (2.8)

$$
\begin{aligned}
V_{t_m}(x;\mathcal{C}) &= \mathbb{E}_{t_m}\left[\beta_m V_{t_{m+1}}\left(X_{t_{m+1}};\mathcal{H}^*\right)\right] + q_m^c(x), \\
B_m^{\mathcal{C}}(x) &= \mathbb{E}_{t_m}\left[(1-\delta_m)\beta_m V_{t_{m+1}}\left(X_{t_{m+1}};\mathcal{H}^*\right)\right] - \mathbb{E}_{t_m}\left[\int_{t_m}^{t_{m+1}} \Gamma_{t_m}(s)R_s(X_s)\lambda_s\Lambda_{t_m}(s)ds\right].
\end{aligned}
$$

As a consequence, given that $C_{t_{m+1}}^{\mathcal{H}^*}(x) = V_{t_{m+1}}(x;\mathcal{H}^*) - V_{t_{m+1}}^D(x;\mathcal{H}^*)$, we obtain

$$
\begin{aligned}
V_{t_m}^D(x;\mathcal{C}) &= \mathbb{E}_{t_m}\left[\beta_m V_{t_{m+1}}\left(X_{t_{m+1}};\mathcal{H}^*\right)\right] + q_m^c(x) - B_m^{\mathcal{C}}(x) - \mathbb{E}_{t_m}\left[\beta_m\delta_m C_{t_{m+1}}^{\mathcal{H}^*}\left(X_{t_{m+1}}\right)\right] \\
&= \mathbb{E}_{t_m}\left[\int_{t_m}^{t_{m+1}} \Gamma_{t_m}(s)R_s(X_s)\lambda_s\Lambda_{t_m}(s)ds\right] + q_m^c(x) + \mathbb{E}_{t_m}\left[\beta_m\delta_m V_{t_{m+1}}^D(X_{t_{m+1}})\right].
\end{aligned}
$$

Now consider an alternative strategy, indexed by $\mathcal{E}$, which consists of exercising at date t_m. The expected loss at t_m resulting from using this strategy is zero, yielding

$$
V_{t_m}^D(x;\mathcal{E}) = q_m^e(x).
$$

We then have at t_m, conditional on no prior default and given no prior exercise,

$$
\begin{aligned}
V_{t_m}^D(x) &= \max\left\{V_{t_m}^D(x;\mathcal{E}); V_{t_m}^D(x;\mathcal{C})\right\} && (2.11)\\
&= \max\Bigg\{ q_m^e(x); \\
&\qquad \mathbb{E}_{t_m}\left[\int_{t_m}^{t_{m+1}} \Gamma_{t_m}(s)R_s(X_s)\lambda_s\Lambda_{t_m}(s)ds\right] + q_m^c(x) + \mathbb{E}_{t_m}\left[\beta_m\delta_m V_{t_{m+1}}^D(X_{t_{m+1}})\right]\Bigg\} && (2.12)\\
H_m^* &= \{x : V_{t_m}^D(x) = q_m^e(x)\}. && (2.13)
\end{aligned}
$$

Since Equations (2.11)-(2.13) are valid for any $m = 1, ..., M-1$, we obtain a characterisation of the optimal exercise of a vulnerable claim. Equation (2.12) for $m = 1, ..., M-1$ along with the terminal condition

$$
V_T^D(x) = q_T^e(x) \tag{2.14}
$$

yield a recursive expression for the (optimal) value of a defaultable claim. It is important to notice that the function $V_{t_m}^D(x)$ is continuous in x, which is not the case for the expected payoff under a stopping strategy that is suboptimal at t_m.

2.2.5 Naive strategy

Denote by $\mathcal{N} = \{N_m, m = 1, ..., M\}$ the collection of stopping sets characterizing the strategy that maximizes the default-free value of the contract, so that $V_{t_m}(x;\mathcal{N}) = V_{t_m}(x)$. This strategy, which we call the naive strategy, is characterized by the following dynamic program:

$$\begin{aligned}
V_{t_m}(x) &= \max\{q_m^e(x); \mathbb{E}_{t_m}\left[\beta_m V_{t_{m+1}}\left(X_{t_{m+1}}\right)\right] + q_c^m(x)\}, \quad m = 0, ..., M-1, && (2.15)\\
V_T(x) &= q_T^e(x); && (2.16)\\
N_m &= \{x : V_{t_m}(x) \ = q_m^e(x)\}. && (2.17)
\end{aligned}$$

Using similar calculations as in the previous section, the expected payoff of a defaultable claim under the naive strategy is, for $m = 0, ..., M-1$,

$$\begin{aligned}
V_{t_m}^D(x;\mathcal{N}) &= \mathbb{1}_{N_m}(x) q_m^e(x)\\
&+\mathbb{1}_{\overline{N_m}}(x)\Bigg(\mathbb{E}_{t_m}\left[\int_{t_m}^{t_{m+1}} \Gamma_{t_m}(s) R_s(X_s)\lambda_s \Lambda_{t_m}(s) ds\right]\\
&+q_c^m(x) + \mathbb{E}_{t_m}\left[\beta_m \delta_m V_{t_{m+1}}^D(X_{t_{m+1}};\mathcal{N})\right]\Bigg).
\end{aligned}$$

It is clear therefore that, in general, the naive strategy is not optimal, that is, $V_t^D(x;\mathcal{N}) \leq V_t^D(x)$. Hence, we have the following result:

$$\mathrm{CVA}_t(x) = V_t(x) - V_t^D(x) \leq V_t(x) - V_t^D(x;\mathcal{N}) = C_t^{\mathcal{N}}(x)\,,$$

where it is clear that the CVA is not necessarily equal to the expected loss associated with the naive strategy. It is interesting to note that approximating the CVA by the expected loss associated with the naive strategy is a common practice. However, the CVA cannot be expressed as a simple expected loss for early-exercise products, because of the change in the exercise strategy. In this sense, the computation of the CVA for early-exercise instruments cannot be done directly and involves the computation of the (optimal) value of the defaultable contract and the associated exercise strategy, as provided by the DP recursion (2.12)-(2.14). Note also that when the naive strategy is suboptimal, the value of a vulnerable claim under the naive strategy is discontinuous at the exercise barrier, which results in arbitrage opportunities. This will be illustrated through a numerical example.

2.3 Application Examples

In this section, we illustrate the application of Equations (2.7), (2.9)-(2.10) and (2.12)-(2.14) for the computation of the CVA and the evaluation of vulnerable contracts, for various types of contracts and loss functions, and we show how to account for WWR in this general framework.

2.3.1 European options

Consider a European option paying $q^e(Y_T)$ at maturity T, so that $V_t(x) = \mathbb{E}_t\left[\Gamma_t(T)q^e(Y_T)\right]$ and suppose that $R_t(x) = RV_t(x)$ where $R \in [0,1]$ is a constant recovery factor. Because there is no stopping feature in this case, we have $\mathrm{CVA}_t(x) = C_t(x)$. From (2.7), we then have, at $(t, X_t = x)$,

$$
\begin{aligned}
\mathrm{CVA}_t(x) &= \int_t^T \mathbb{E}_t\left[\Gamma_t(s)\left(1-R\right)V_s(X_s)\lambda_s\Lambda_t(s)\right]ds \\
&= (1-R)\mathbb{E}_t\left[\Gamma_t(T)q^e(Y_T)\left(1-\Lambda_t\left(T\right)\right)\right] \qquad (2.18)
\end{aligned}
$$

and

$$
V_t^D(x) = \mathbb{E}_t\left[\Gamma_t(T)q^e(Y_T)\left(1-\left(1-R\right)\left(1-\Lambda_t\left(T\right)\right)\right)\right]. \qquad (2.19)
$$

Notice that in order to compute the expectation $\mathbb{E}_t[\cdot]$ in (2.18) and (2.19), we need to specify the correlation between the hazard rate and the market factors. If such a correlation exists, we are in the presence of the right-way/wrong-way risk. If, however, we assume that the default intensity is independent from the other market factors, we obtain

$$\begin{aligned}\mathrm{CVA}_t(x) &= (1-R)\mathbb{E}_t\left[\Gamma_t(T)q^e(Y_T)\right]\mathbb{E}_t\left[(1-\Lambda_t(T))\right]\\ &= (1-R)D_t(T)V_t(x).\end{aligned}$$

If default probabilities $D_t(T)$ can be expressed in closed form (for instance if we adopt an affine term-structure model for the hazard rate), then the CVA of a defaultable European option is easily obtained as a fraction of the value of an equivalent risk-free option.

2.3.2 Bermudan options

Consider a Bermudan option that can be exercised at any date $t_m \in \mathcal{T}$ where the exercise payoff is $q_m^e(X_{t_m})$. As in the European option case, we assume that $R_t(x) = RV_t(x)$, where R is a constant recovery factor and where $V_t(x)$ is the default-free value of the option at $(t, X_t = x)$ under the optimal exercise strategy for the default-free option (the naive strategy).

We then have

$$\mathbb{E}_{t_m}\left[\int_{t_m}^{t_{m+1}}\Gamma_{t_m}(s)R_s(X_s)\lambda_s\Lambda_{t_m}(s)ds\right] = \mathbb{E}_{t_m}\left[\beta_m\left(1-\delta_m\right)RV_{t_{m+1}}(X_{t_{m+1}})\right],$$

so that Equation (2.12) yields

$$V_{t_m}^D(x) = \max\left\{q_m^e(x); \mathbb{E}_{t_m}\left[\beta_m\left(\left(1-\delta_m\right)RV_{t_{m+1}}(X_{t_{m+1}}) + \delta_m V_{t_{m+1}}^D(X_{t_{m+1}})\right)\right]\right\},$$

where $V_{t_m}^D(x)$ is the value of the defaultable option (i.e., under the optimal exercise strategy characterized by $\mathcal{H}^*$). If the option is not exercised, the first term involves the amount recovered if default happens before t_{m+1}, while the second term involves the value of the defaultable option conditional on no prior default and given no prior exercise at t_{m+1}. If $R = 0$, this reduces to

$$V_{t_m}^D(x) = \max\left\{q_m^e(x); \mathbb{E}_{t_m}\left[\beta_m\delta_m V_{t_{m+1}}^D(X_{t_{m+1}})\right]\right\}.$$

The CVA of a Bermudan option at (t,x) is obtained by computing the difference between $V_t(x)$ and $V_t^D(x)$; it therefore requires the determination of both value functions and associated strategies.

2.3.3 Interest-rate swaps

Consider an interest-rate payer swap, where the principal is normalized to 1 and the swap rate is γ. Assume that the fixed and floating payments are exchanged on the same dates, denoted by t_m, $m = 1, ..., M$, where $\Delta_m = t_m - t_{m-1}$ is the length of period m. In that case, $X_t = (r_t, \lambda_t)$ and $V_t(x)$ denotes the default-free market value of the swap at $(t, X_t = x)$. Assume that $R_t(x) = R \max\{V_t(x); 0\} + \min\{V_t(x); 0\}$, where $R \in [0,1]$ is a constant recovery factor.
If the exchange of payments starts at t_i, then the value of the swap at some date $t \leq t_i$ is

$$V_t(x) = \mathbb{E}_t[\Gamma_t(t_i)] - \gamma \sum_{m=i+1}^{M} \Delta_m \mathbb{E}_t[\Gamma_t(t_m)] - \mathbb{E}_t[\Gamma_t(T)].$$

If zero-coupon bond prices $P_t(x,T) = \mathbb{E}_t[\Gamma_t(T)]$ at $(t, r_t = r)$ can be obtained in closed form, which is the case for most popular interest-rate models, then the swap value V_t can also be expressed in closed form:

$$V_t(x) = P_t(x, t_i) - \gamma \sum_{m=i+1}^{M} \Delta_m P_t(x, t_m) - P_t(x,T). \tag{2.20}$$

The CVA of an interest-rate swap with constant recovery factor is defined by

$$\mathrm{CVA}_t(x) = (1-R) \int_t^T \mathbb{E}_t[\Gamma_t(s) \max\{V_s(x); 0\} \lambda_s \Lambda_t(s)]\, ds.$$

Equivalently, since there is no stopping feature in this case, $\mathrm{CVA}_t(x) = C_t(x)$, and using the recursive expression (2.9), we get

$$\begin{aligned}
B_m(x) &= (1-R)\mathbb{E}_{t_m}\left[\int_{t_m}^{t_{m+1}} \Gamma_{t_m}(s) \max\{V_s(x); 0\} \lambda_s \Lambda_{t_m}(s) ds\right] &(2.21)\\
\mathrm{CVA}_{t_m}(x) &= B_m(x) + \mathbb{E}_{t_m}\left[\beta_m \delta_m \mathrm{CVA}_{t_{m+1}}\left(X_{t_{m+1}}\right)\right],\ m = 0, ..., M-1 &(2.22)\\
\mathrm{CVA}_T(x) &= 0. &(2.23)
\end{aligned}$$

Clearly, the recursive formulation is much easier to evaluate. If the Δ_i are sufficiently small, one can make either one of the commonly used approximations (see, for instance, Brigo and Masetti (2006)):

$$\begin{aligned} B_m(x) &\simeq (1-R)D_{t_m}(t_{m+1})\max\{V_{t_m}(x);0\} \text{ (anticipated default);} \\ B_m(x) &\simeq (1-R)\mathbb{E}_{t_m}\left[\beta_m\delta_m \max\left\{V_{t_{m+1}}\left(X_{t_{m+1}}\right);0\right\}\right] \text{ (postponed default).} \end{aligned}$$

The value of a defaultable swap is then given by

$$V^D_{t_m}(x) = V_{t_m}(x) - \mathrm{CVA}_{t_m}(x). \tag{2.24}$$

2.3.4 Interest-rate Bermudan swaptions

A swaption is an option to enter into a swap contract. We consider a Bermudan swaption with a set $\mathcal{T} = \{t_m, m = 0, ..., M\}$ of discrete dates at which the option holder has the right to enter a payer swap resetting at the same date, and with the remaining subsequent dates as payment dates. Denote by $V_{t_m}(x)$ the (default-free) value of this swap at $(t_m, x = X_{t_m})$. The default-free value of the swaption at $(t_m, x = X_{t_m})$, denoted by $U_{t_m}(x)$, is given by the following dynamic program:

$$U_{t_m}(x) = \max\{V_{t_m}(x); \mathbb{E}_{t_m}\left[\beta_m U_{t_{m+1}}(X_{t_{m+1}})\right]\},\ m = 0, ..., M-1, \tag{2.25}$$

$$U_T(x) = 0. \tag{2.26}$$

To compute the swaption value under counterparty risk, the CVA of the swap itself should be taken into account because, when the swaption is exercised, the investor enters into a new contract that promises future cash flows. Accordingly, we define two recovery processes, where $R^b_\tau(x)$ is the (possibly negative) amount recovered at $t = \tau$ if the default event happens before or at exercise, and $R^a_\tau(x)$ is the (possibly negative) amount recovered at $t = \tau$ if the default event happens after exercise, when $X_\tau = x$. Equation (2.2) then becomes

$$\begin{aligned} V_t^D(x;u) &= \mathbb{E}_t\left[\mathbb{1}_{(T,\infty]}(\tau)F^u(t,T)\right] + \mathbb{E}_t\left[\mathbb{1}_{(t,T]}(\tau)F^u(t,\tau)\right] \\ &\quad + \mathbb{E}_t\left[\mathbb{1}_{(t,u]}(\tau)\Gamma_t(\tau)R_\tau^b(X_\tau) + \mathbb{1}_{(u,T]}(\tau)\Gamma_t(\tau)R_\tau^a(X_\tau)\right]. \end{aligned}$$

When exercise does not terminate the contract, the recursive definition of the expected loss corresponding to a given exercise strategy characterized by $\mathcal{H}$, the optimal exercise strategy, and the value of the defaultable claim are obtained similarly as in Sections 2.2.3 and 2.2.4 (see Appendix 2 for details).

Assume that the recovery value of the swaption if default occurs before exercise is $R_t^b(x) = R_u U_t(x)$, while the recovery value for the underlying swap, that is, if default happens after exercise, is $R_t^a(x) = R\max\{V_t(x);0\} + \min\{V_t(x);0\}$, where R_u and R are the recovery rates of the swaption and the swap respectively, and where $V_t(x)$ is the default-free market value of the swap at $(t, X_t = x)$.

The value of a defaultable swaption, conditional on no prior default and given no prior exercise, is then given by

$$\begin{aligned} U_{t_m}^D(x) &= \max\Big\{V_{t_m}^D(x); \\ &\qquad \mathbb{E}_{t_m}\left[\beta_m\left((1-\delta_m)R_u U_{t_{m+1}}(X_{t_{m+1}}) + \delta_m U_{t_{m+1}}^D(X_{t_{m+1}})\right)\right]\Big\}, \qquad (2.27) \\ &\qquad m = 0, ..., M-1, \\ U_T^D(x) &= 0, \qquad (2.28) \end{aligned}$$

where $V_{t_m}^D(x)$ is the value of the defaultable swap at $(t_m, X_{t_m} = x)$. To compute the CVA of a swaption, the DP recursion (2.21)-(2.23) is first used, yielding the value of the defaultable swap for all dates as a function of $x = (r,\lambda)$ using (2.24). The recursion (2.25)-(2.28) is then used to compute the default-free and defaultable values of the swaption. The CVA of the swaption is the difference $\mathrm{CVA}_{t_m}^U(x) = U_{t_m}(x) - U_{t_m}^D(x)$.

2.3.5 Wrong-way risk

Wrong-way risk (WWR) is the additional risk implied by a dependence between counterparty credit quality and market factors. The general formulations (2.7) and (2.9)-(2.10) in the present paper allow for the existence of a correlation between market risk factors and default intensity.
One simple way to model WWR is to specify a relationship between default-free risk variables and the hazard rate. For instance, one may assume that

$$\lambda_t = f(t, Y_t), \tag{2.29}$$

where f is some deterministic positive function of time and risk factors, and where the dependence upon time is helpful for calibration purposes. This encompasses prevailing models where the hazard rate is a function of the exposure. For instance, Hull and White (2012) propose the following model:

$$\lambda_t = \exp(g(t) + hV_t(Y_t)),$$

where h is a constant and g is a deterministic function of time that can be calibrated to the observed term structure of credit spreads.
In any case, under (2.29), the hazard rate is fully specified by the process Y_t so that the computation of the CVA does not require an additional state variable, and the computational burden of evaluating the CVA is the same as that of evaluating a default-free contract. This makes the choice of the above model interesting in a DP context; moreover, it allows for the incorporation of WWR into the pricing procedure without increasing its numerical complexity.

2.4 Implementation

In this section, we describe the numerical implementation of the dynamic program used for the numerical experiments. We also explain the implementation of the classic simulation method whose performance will be compared to the performance of the DP approach in these experiments.

2.4.1 Dynamic program

The recursive approach to CVA valuation can be equated to solving the following general dynamic program:

$$v_m(x) = f_m\left(\mathbb{E}\left[G_m v_{m+1}\left(X_{t_{m+1}}\right)|X_{t_m}=x\right]\right), \ m=0,...,M-1, \tag{2.30}$$

$$v_M(x) = 0, \tag{2.31}$$

where f_m is a known function and G_m is a random variable, and where we assume that the joint density of $\left(G_m, X_{t_{m+1}}\right)$ under the risk-neutral measure, conditional on $X_{t_m}=x$, is known. To simplify the exposition, we describe the implementation when the state space is unidimensional, where $x \in [0,\infty)$. Suppose that the function v_{m+1} is known analytically on $[0,\infty)$. At a given x, since both the joint density and the function v_{m+1} are analytical, computation of $\mathbb{E}\left[G_m v_{m+1}\left(X_{t_{m+1}}\right)|X_{t_m}=x\right]$ amounts to evaluating the integral of an analytically known function.

In order to solve the dynamic program (2.30)-(2.31), we compute v_m on a finite grid and use a spectral interpolation scheme to obtain an analytical interpolation function $\hat{v}_m$ approximating v_m. Starting from the known function v_M, this process yields, by backward induction, analytical interpolation functions $\hat{v}_m(x)$ for all evaluation dates t_m.

More precisely, define a set $\mathcal{G} = \{x_j, j=1,...,n\}$ of n grid points, such that

$$0 < x_1 < x_2 < ... < x_n < \infty,$$

and a family of n basis functions, denoted by $(\psi_j)_{j=1,\dots,n}$. An interpolation function $\hat{v}_m(x)$ is defined by

$$\hat{v}_m(x) = \begin{cases} \sum_{j=1}^{n} c_j^m \psi_j(x) \text{ if } x \in [x_1, x_n] \\ o(x) \text{ if } x \notin [x_1, x_n], \end{cases}$$

where o is an extrapolation function characterizing the behavior of v outside the localization interval, and where the coefficients c_j satisfy the linear system

$$v_m\left(x_i\right)=\sum_{j=1}^{n}c_j^m\psi_j(x_i),\ i=1,...,n.$$

We use a spectral interpolation scheme with Chebyshev polynomials as basis functions. The use of these interpolating functions is known to be efficient when combined with Chebyshev interpolation nodes (Breton and de Frutos (2012)), and is often characterized by an exponential convergence. The computation of the interpolating coefficients c_j can be performed using a fast Fourier transform (FFT) algorithm.

Moreover, we evaluate the integrand for the computation of the expected value

$$\mathbb{E}\left[G_m v_{m+1}\left(X_{t_{m+1}}\right)|X_{t_m}=x\right]$$

on $\mathcal{G}$ and interpolate it using the same spectral interpolation scheme. The integration over the interval $[x_1, x_n]$ of the resulting interpolation function is analytic, and corresponds to the Clenshaw-Curtis quadrature (Clenshaw and Curtis (1960)). Quadrature methods are well known in the option pricing literature for their efficiency. They were adopted by several authors, including Sullivan (2000), Andricopoulos et al. (2003), Andricopoulos et al. (2007) and Chen et al. (2014). The extension of this approach to cases where the state space is multidimensional (corresponding to, e.g., asset prices, stochastic volatilities, stochastic interest rates) is straightforward and involves a multidimensional grid and multidimensional Chebyshev interpolation. However, the computational burden of the recursive approach increases significantly with the dimension of the state space.

The recursive approach to CVA valuation yields M analytical functions, which can be used to evaluate the CVA at any date $t_m \in \mathcal{T}$, and for any possible value of the market factors and hazard rate. Each function is completely characterized by the n coefficients c_j^m, $j=1,...,n$.

To conclude, it is worth mentioning that, for contracts with early-exercise opportunities, an exercise barrier divides the state space into two regions (H_m and $\overline{H_m}$) at t_m. Along this exercise barrier, the value function may present discontinuities (if the exercise strategy is not optimal) or changes in its curvature. As a consequence, the interpolation of the value function by a polynomial may be less precise near the exercise barrier. In our implementation, we adjusted the localization interval, at each evaluation date, so that its boundary would coincide with the exercise barrier. We found that setting a boundary of the localization interval to coincide with the exercise barrier can significantly improve the accuracy and the convergence of the algorithm.

2.4.2 Simulation

Our simulation experiments are performed assuming that the default-free value and the exercise strategy of the contracts have already been computed and are available for all exercise dates as a function of the underlying market variables. For instance, we obtain the default-free value and the naive strategy by solving the DP (2.15)-(2.17) using spectral interpolation, as described in the preceding section. We then simulate the default time τ and the underlying variable trajectory. For each sample path, we record the default time τ, the corresponding time index j such that $\tau \in (t_{j-1}, t_j]$, and the first date t_k at which the underlying variable is in the exercise region. On a given sample path, if $j > k$, default occurs after the exercise of the contract and the exposure is set to the non-recovered fraction of the discounted exercise value (for Bermudan options, the post-exercise exposure is simply 0; while for interest-rate swaptions, it is equal to the underlying swap residual value). If, however, $j \leq k$, default occurs during the time interval $(t_{j-1}, t_j]$ while the option is still alive, and the exposure is set to the non-recovered fraction of the discounted default-free value. The expected loss of the vulnerable contract is obtained by averaging the exposures on all sample paths.

It is important to stress that such a simulation scheme needs the exercise strategy as an input, and therefore cannot solely be used to compute the CVA of contracts with optional early-exercise features. We use simulation results as benchmarks to corroborate the accuracy of CVA evaluation for a given exercise strategy and to illustrate the relative computational burden of both computational approaches.

2.5 Numerical experiments

In this section, we report on various numerical experiments that illustrate the efficiency of the DP approach to CVA valuation. A first set of experiments compares the results obtained using the recursive pricing formula to those obtained using a standard Monte-Carlo approach for a given exercise strategy. A second set of experiments illustrates features of the CVA for various application examples and market models. All experiments were done using an AMD A6-6310 APU processor with 1.8 GHz of power and 8 GB of RAM.

2.5.1 Bermudan options under GBM: Comparative results

This first experiment is used to assess the efficiency of the DP approach and to compare the CVA evaluation to simulation results. Recall that in all simulation experiments, the CPU computing time does not include the computations required to obtain the exercise strategy and risk-free value of the contract, whereas DP does provide these results directly.

We assume a geometric Brownian motion (GBM) model for the asset price dynamics and a constant hazard rate λ, $X_t = S_t$, where the price dynamics under the risk-neutral measure are described by

$$S_t = S_0 \exp\left(\left(r - \frac{\sigma^2}{2}\right)t + \sigma\sqrt{t}Z_t\right), \tag{2.32}$$

where Z_t is a standard Brownian motion, r is the risk-free rate and σ is the volatility.

We compute the CVA at date t_0 of a Bermudan put option with a strike K and a maturity T of one year offering $M = 100$ exercise opportunities, with a zero recovery rate (R= 0), under both the optimal strategy and the naive strategy, as defined in (2.3)-(2.4).

We first compare the results obtained for the naive strategy in terms of values and computational burden, using DP and Monte Carlo simulation. Simulation is performed using a sample of 1,000,000 scenarios, requiring around 60 CPU seconds. Table 2.1 reports on the required CPU times and on the precision reached according to the number of grid points, while using the DP procedure.

n	50	100	150
CPU time (seconds)	0.187	0.343	0.578
Precision	10^{-5}	10^{-8}	10^{-9}

Table 2.1: Precision and CPU time according to the grid size, DP approach, geometric Brownian motion model.

Table 2.2 compares the value of the defaultable claim under the naive strategy obtained using DP to the 95% confidence intervals obtained by simulation for various parameter values. The length of these confidence intervals is of the order of 10^{-3}; all DP prices are inside the intervals. One can observe the efficiency of our proposed approach in precision, computation time and memory requirements: while 60 seconds are required to reach a precision of 10^{-3} by simulation using 10^6 samples, the DP approach reaches a precision of 10^{-5} in less than 0.2 seconds using 50 grid points.

λ	σ	**DP**	**Simulation**
0.1	0.2	2.8792	$[2.8777, 2.8807]$
0.1	0.15	2.0091	$[2.0083, 2.0102]$
0.1	0.25	3.7595	$[3.7576, 3.7615]$
0.05	0.2	2.9594	$[2.9587, 2.9608]$
0.05	0.15	2.0605	$[2.0599, 2.0613]$
0.05	0.25	3.8699	$[3.8682, 3.8711]$
0.15	0.2	2.8017	$[2.7996, 2.8031]$
0.15	0.15	1.9592	$[1.9576, 1.9599]$
0.15	0.25	3.6528	$[3.6501, 3.6547]$

Table 2.2: Value of a vulnerable Bermudan put option in the geometric Brownian motion model under the naive strategy. Parameters are $S_0 = K = 50$, $r = 0.05$, $T = 1$, $M = 100$.

Figure 2.1 compares the CVA in value and in percentage of the default-free value, according to the exercise strategy and to the moneyness of the option. One can observe that using the optimal exercise strategy results in a smaller CVA than the one resulting from the naive strategy, and that the difference is larger near the exercise barrier. Besides, the CVA is highest when the option is at the money. When the option is in the money, counterparty risk is not very significant since the investor will generally exercise early. On the other hand, when the option is deep out of the money, the option value becomes so small that the adjustment eventually vanishes – even if it still represents a relatively sizeable percentage of the option value.

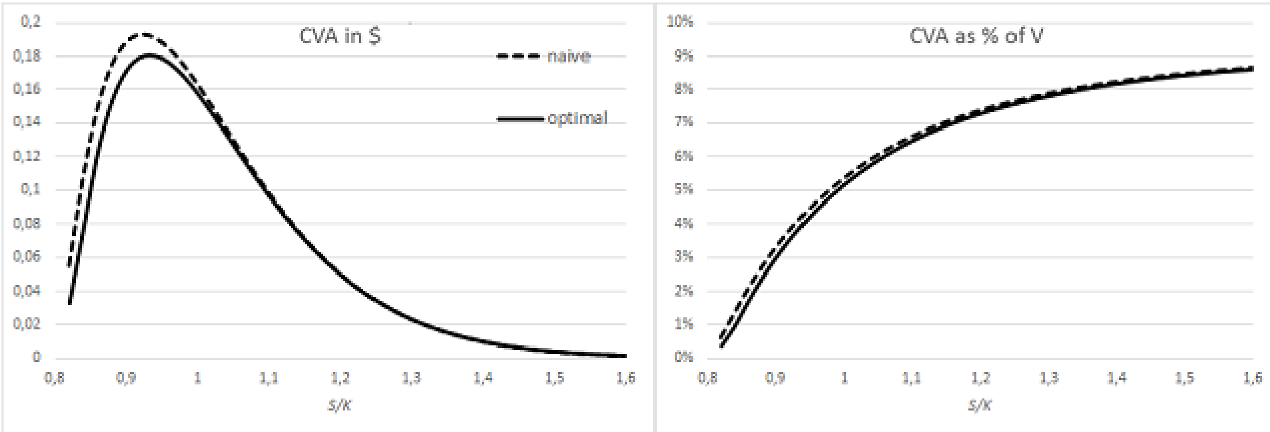

Figure 2.1: CVA of a Bermudan option at inception for the optimal and naive strategies, as a function of moneyness. Lognormal model with constant hazard rate; parameters are $r = 0.05$, $\sigma = 0.2,\ \lambda = 0.1,\ T = 1,\ M = 100$.

Although the difference between the value of the vulnerable option under the naive or the optimal strategy is generally not very large, the use of the naive strategy results in potential arbitrage opportunities due to the discontinuity of the value function at the exercise barrier when this strategy is used, as illustrated in Figure 2.2. When the asset price is sufficiently near the naive exercise barrier, but still in the detention region, an informed party could borrow to buy the option from its holder at a price equal to its value adjusted for counterparty risk, and then immediately exercise it to lock in a strictly positive profit.

2.5.2 Impact of WWR

Our second experiment introduces WWR for the Bermudan put option in the GBM model (2.32) considered in the previous section. We assume that the dependence between the hazard rate and the asset value is described by two parameters denoted $\overline{\lambda}$ and h, such that, during the time interval $[t_m, t_{m+1})$,

$$\lambda_t = \overline{\lambda} \exp(h S_{t_m}), \tag{2.33}$$

where h measures the amount of right-way/wrong-way risk ($h < 0$ indicates WWR[2]). Clearly, the introduction of such a dependence does not modify the numerical complexity of either the DP or

[2]For a put option, a decrease in the price of the underlying asset increases both the exposure and the probability of default.

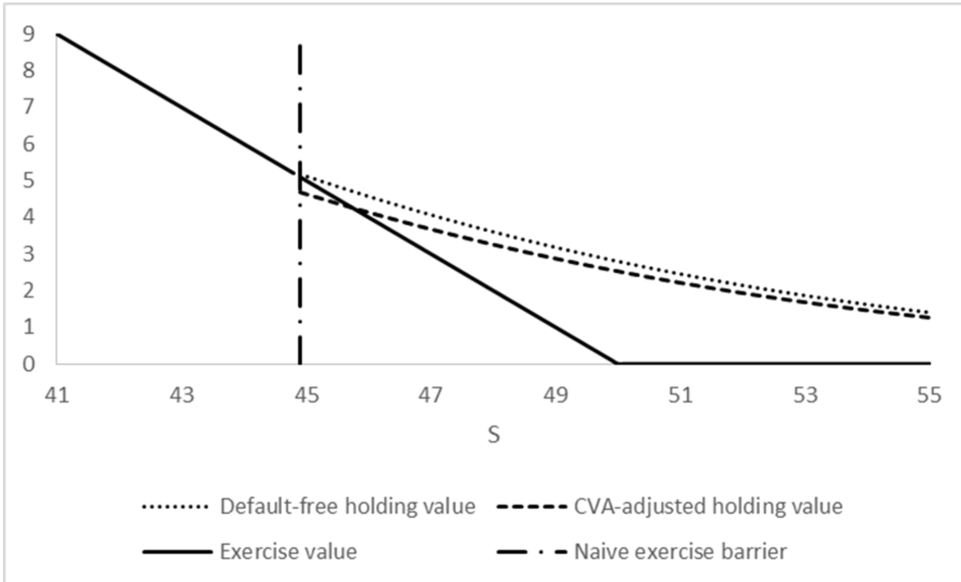

Figure 2.2: Discontinuity of the value function at the level of the exercise barrier when the naive strategy is used. Parameters are: $K = 50$, $r = 0.05$, $\sigma = 0.2$, $\lambda = 0.1$, $T = 1$, $M = 1$.

simulation approaches.

In order to assess the impact of WWR, we compare the CVA at date 0, obtained using the default model (2.33), with the one obtained when assuming a constant hazard rate equal to λ_0. The left panel of Figure 2.3 shows, as a function of S_0, the hazard rate $\lambda_0 = \overline{\lambda}\exp(hS_0)$ and the additional CVA when $\overline{\lambda} = 2$ and $h = -0.06$. The right panel of Figure 2.3 shows, as a function of S_0, the factor h satisfying $\lambda_0 = 0.1$ and the additional CVA when $\overline{\lambda} = 2$. Finally, Figure 2.4 shows, as a function of $\overline{\lambda}$, the value of h such that $\lambda_0 = 0.1$ at $S_0 = K$, and the additional CVA.

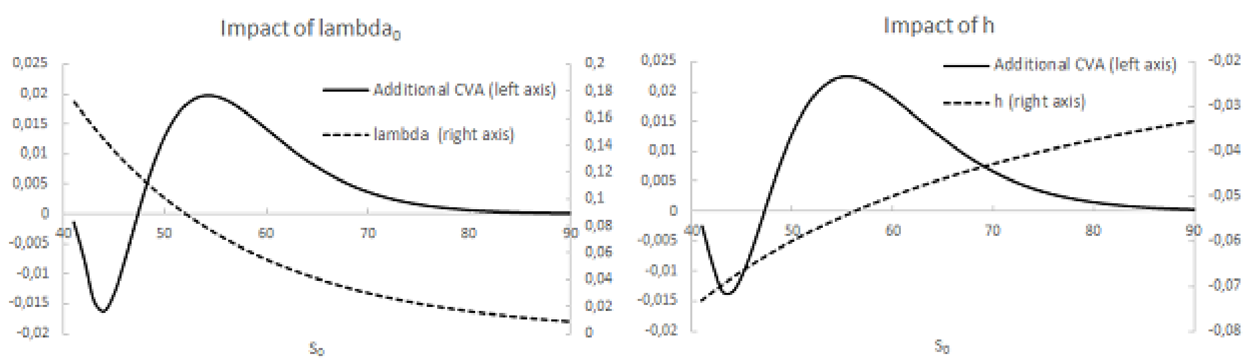

Figure 2.3: Impact of WWR, Bermudan put option. Parameters are $K = 50$, $r = 0.05$, $\sigma = 0.2$, $T = 1$, $M = 100$.

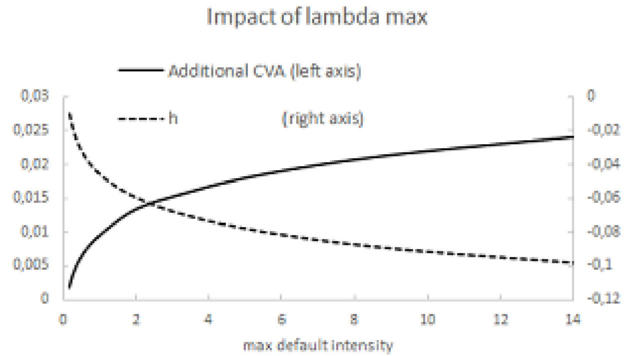

Figure 2.4: Impact of WWR, Bermudan put option. Parameters are $S_0 = K = 50$, $r = 0.05$, $\sigma = 0.2$, $T = 1$, $M = 100$.

It is interesting to note that the presence of WWR may imply a decrease in the CVA for Bermudan put options. Indeed, when the price of the underlying asset is low, a negative correlation between the hazard rate and the price of the underlying asset increases the probability of early exercise, and consequently decreases counterparty risk. This is not the case for European options, as illustrated in Figure 2.5.

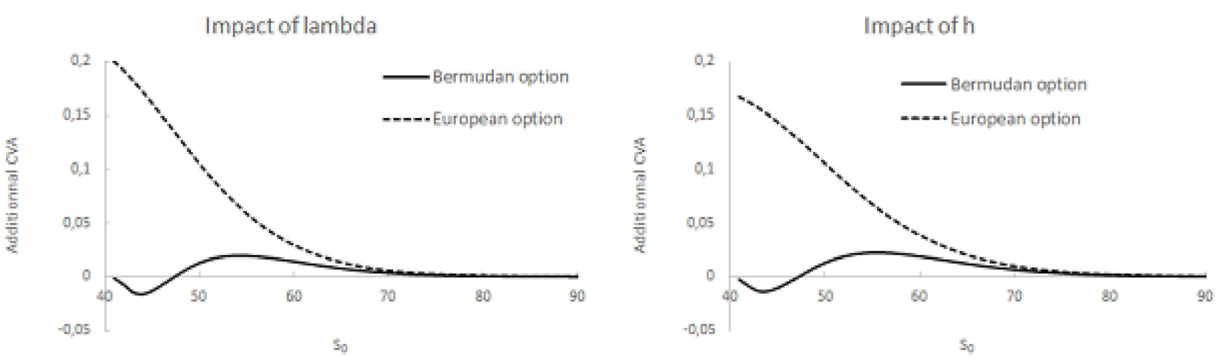

Figure 2.5: Impact of WWR on European and Bermudan put options. Parameters are $K = 50$, $r = 0.05$, $T = 1$, $M = 100$, $\sigma = 0.2$.

2.5.3 Jump-diffusion model

Our third set of results is obtained by specifying a different market model, namely, Merton's (1976) jump-diffusion model (the hazard rate remains constant). Accordingly, the price dynamics under the risk-neutral measure are described by

$$S_t = S_0 \exp\left(\left(r - \left(e^{\eta+\frac{\phi^2}{2}} - 1\right)\alpha - \frac{1}{2}\sigma^2\right)t + \sigma Z_t\right)\prod_{i=1}^{N_t}(J_i+1) \tag{2.34}$$

where the jump size $\log(J_i + 1)$ is a Gaussian random variable of mean η and standard deviation ϕ, and where N_t is a Poisson process with intensity α. In turbulent times, when counterparty risk is present, jumps in the asset price may well be a better assumption than the constant volatility of the lognormal model. As pointed out previously, the DP algorithm can accommodate any market model. However, a more complex model and added volatility may require additional processing time and number of grid points to attain a given level of precision. To assess the accuracy of the DP procedure, Figure 2.6 shows the convergence of the DP price to the analytical Merton formula for a European risk-free option, as the number of grid points increases.

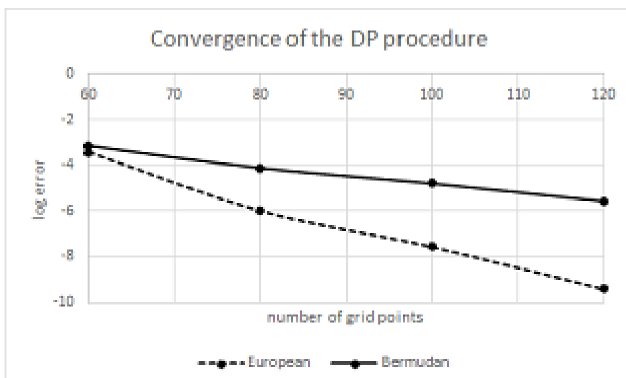

Figure 2.6: Log error as a function of the number of grid points in the DP procedure, vulnerable European put option under Merton's jump-diffusion model. Parameters are $S_0 = K = 50$, $r = 0.05$, $\sigma = 0.2$, $\alpha = 0.25$, $\eta = 0$, $\phi = 0.1$, $\lambda = 0.1$, $T = 1$, $M = 100$. Benchmark for the European case is the Merton analytical formula. Benchmark for the Bermudan case ($M = 100$) is computed with 600 grid points.

Figure 2.6 and Table 2.3 also illustrate the results obtained for the corresponding vulnerable Bermudan option with a zero recovery rate (optimal exercise strategy) for various grid sizes, using the DP approach (the benchmark is the value at $n = 600$). It shows that a precision of 10^{-4} is attained with 60 grid points in around 3 seconds.

n	60	80	100	120	Benchmark
Value	2.9860857	2.9854265	2.9853331	2.9853466	2.9853493
Error	7.3637E-04	7.7167E-05	1.6179E-05	2.7581E-06	
CPU seconds	3.125	4	4.8438	5.8281	

Table 2.3: Precision and computing time as a function of the number of grid points, vulnerable Bermudan option under the jump-diffusion model. Parameters are $S_0 = K = 50$, $r = 0.05$, $\sigma = 0.2$, $\alpha = 0.25$, $\eta = 0$, $\phi = 0.1$, $\lambda = 0.1$, $T = 1$, $M = 100$.

Finally, Table 2.4 presents the results obtained using simulation and DP for various parameter values. Simulation results are presented for both the naive and optimal strategies for comparison purposes; however, it is important to recall that exercise strategies cannot be obtained by simulation, and must be previously computed using DP. Simulations were performed using 10^6 samples and required 78 CPU seconds, with a precision of the order of 10^{-2}. All DP results are within the confidence interval and required 3 seconds and 60 grid points to attain a precision of 10^{-4}.

λ	σ	**DP (optimal)**	**Simulation (optimal)**	**DP (naive)**	**Simulation (naive)**
0.1	0.2	2.9853	$[2.9832, 2.9860]$	2.9796	$[2.9776, 2.9806]$
0.1	0.15	2.1373	$[2.1361, 2.1381]$	2.1341	$[2.1336, 2.1356]$
0.1	0.25	3.8513	$[3.8484, 3.8522]$	3.8427	$[3.8419, 3.8459]$
0.05	0.2	3.0646	$[3.0634, 3.0655]$	3.0631	$[3.0619, 3.0641]$
0.05	0.15	2.1902	$[2.1893, 2.1907]$	2.1894	$[2.1886, 2.1901]$
0.05	0.25	3.9583	$[3.9575, 3.9602]$	3.9561	$[3.9559, 3.9587]$
0.15	0.2	2.9109	$[2.9097, 2.9130]$	2.8989	$[2.8959, 2.8995]$
0.15	0.15	2.0873	$[2.0857, 2.0880]$	2.0804	$[2.0799, 2.0823]$
0.15	0.25	3.7512	$[3.7504, 3.7548]$	3.7333	$[3.7295, 3.7343]$

Table 2.4: CVA-adjusted price of a Bermudan put option in the jump-diffusion model. Parameters are $S_0 = K = 50$, $r = 0.05$, $\alpha = 0.25$, $\eta = 0$, $\phi = 0.1$, $T = 1$, $M = 100$.

2.5.4 Stochastic hazard rate

We now consider a stochastic hazard rate following a Cox-Ingersoll-Ross (CIR) process (Cox et al. (1985); Schönbucher (2003)):

$$d\lambda_t = \xi(\theta - \lambda_t)dt + \nu\sqrt{\lambda_t}dW_t,$$

where W_t is a Brownian motion. We assume that S_t follows a geometric Brownian motion, independent from λ_t, and that R =0. Here, the state vector $X_t = (S_t, \lambda_t)$ is bidimensional, requiring a two-dimensional discretization grid, where n_S and n_λ are the number of discretization points for the underlying asset price and the hazard rate respectively.

In the European case, the value of a vulnerable option can be obtained analytically since the default intensity is independent from the asset price, and Figure 2.7 illustrates the convergence of the DP price to the analytical value as the grid size and configuration change. A precision of 10^{-4} can be reached in 3 seconds with 60 grid points for the underlying asset and 80 grid points for the hazard rate.

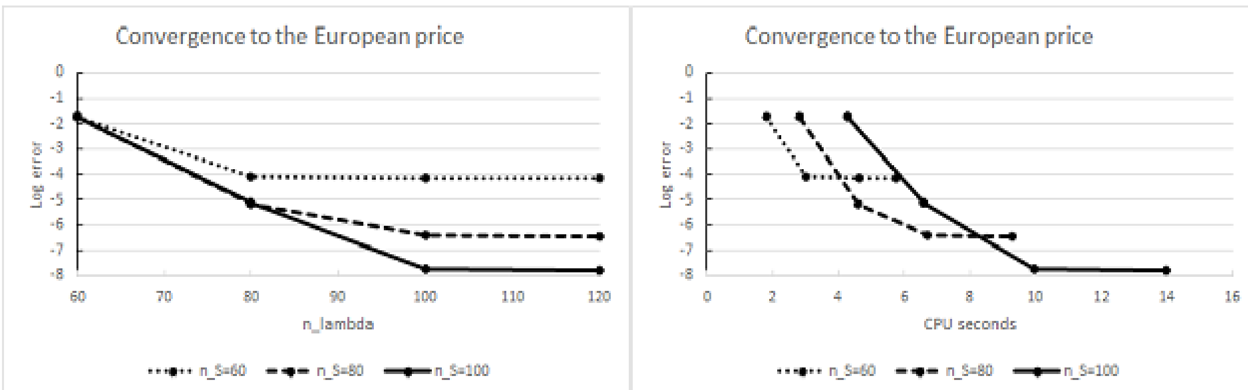

Figure 2.7: Precision (log error) as a function of grid size and computation time (CPU seconds), vulnerable European option with stochastic hazard rate. Parameter values are $S_0 = K = 50$, $\lambda_0 = 0.1$, $r = 0.05$, $\sigma = 0.2$, $\theta = 0.1$, $\xi = 0.5$, $\nu = 0.2$, $T = 1$, $M = 12$.

Figure 2.8 provides the convergence information for a corresponding Bermudan option with 12 exercise opportunities. In this case, the benchmark is approximated by the value obtained by DP with $n_S = 300$ and $n_\lambda = 300$. A precision of 10^{-5} is reached in 10 seconds with a 100×100 grid.

2.5.5 Swaps and swaptions with stochastic hazard rate and WWR

In our last set of results, we consider interest-rate swaps and swaptions, assuming that the evolution of the interest and hazard rates is described by CIR processes, that is,

$$dr_t = \xi_r(\theta_r - r_t)dt + \nu_r\sqrt{r_t}dW_t^1, \quad (2.35)$$

$$d\lambda_t = \xi_\lambda(\theta_\lambda - \lambda_t)dt + \nu_\lambda\sqrt{\lambda_t}dW_t^2. \quad (2.36)$$

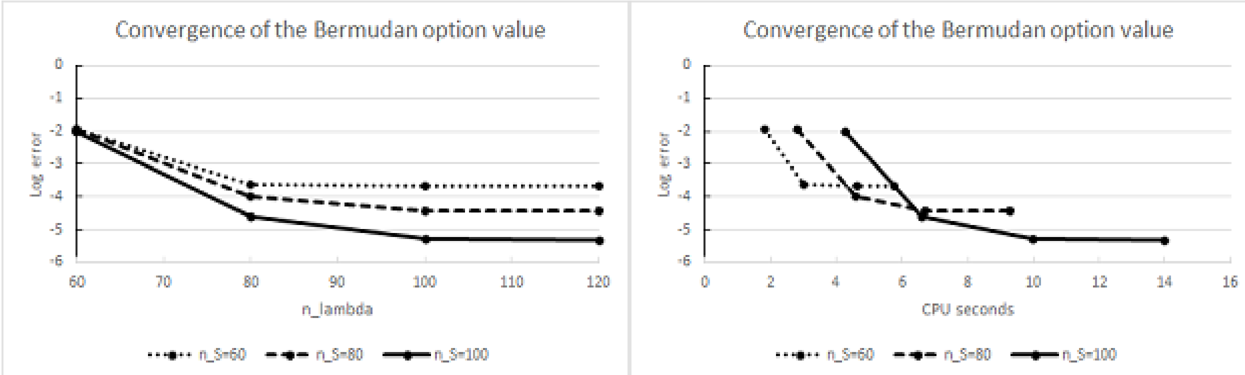

Figure 2.8: Precision (log error) as a function of grid size and computation time (CPU seconds), vulnerable Bermudan option with stochastic hazard rate. Parameter values are $S_0 = K = 50$, $\lambda_0 = 0.1$, $r = 0.05$, $\sigma = 0.2$, $\theta = 0.1$, $\xi = 0.5$, $\nu = 0.2$, $T = 1$, $M = 12$.

WWR is present when the two processes are correlated, where ρ denotes the correlation coefficient between the Brownian motions W_t^1 and W_t^2:

$$dW_t^1 dW_t^2 = \rho dt.$$

In practice, Equations (2.35) and (2.36) could be shifted by deterministic functions in order to match the observed term structure of interest rates and credit spreads (see for instance Brigo and Mercurio (2001)).

Under (2.35)-(2.36), when $\rho = 0$, the joint density of the state variable $\left(r_{t_{m+1}}, \lambda_{t_{m+1}}\right)$ can be expressed analytically. When the correlation is not null, no closed-form densities are available. In this case, the CIR processes can be approximated by Vasicek processes (see for instance Brigo and Alfonsi (2005) for a similar Gaussian mapping technique):

$$\begin{aligned} dr_t &= \xi_r(\theta_r - r_t)dt + \nu_r\sqrt{r_{t_m}}dW_t^1 \text{ for } t \in [t_m, t_{m+1}], \\ d\lambda_t &= \xi_\lambda(\theta_\lambda - \lambda_t)dt + \nu_\lambda\sqrt{\lambda_{t_m}}dW_t^2 \text{ for } t \in [t_m, t_{m+1}]. \end{aligned}$$

Tables 2.5 and 2.6 compare the CVAs (in basis points) of a swap and a Bermudan swaption, obtained by Monte-Carlo simulation (where the optimal strategy for the swaption is previously computed using DP) and by the DP recursions (2.21)-(2.23) and (2.27)-(2.28), for various values of

ρ, at $(t = 0, r_0, \lambda_0)$. The DP procedure uses $128 \times 128 = 16,384$ grid points, while the simulation uses $500,000$ samples and 180 time-discretization nodes. All DP results are within the simulation confidence intervals. The DP procedure requires less memory and computation time to produce the optimal strategy and the CVA, at all payment dates and for all possible values of the state vector, than simulation requires to produce a single estimate at $(t = 0, r_0, \lambda_0)$ for a specified exercise strategy. The correlation impact is illustrated in Figure 2.9.

ρ	**DP**	**Simulation**
0	1.6566	[1.6278, 1.6883]
0.25	1.8411	[1.8301, 1.8952]
0.50	2.0315	[2.0163, 2.0855]
0.75	2.2279	[2.2169, 2.2905]
CPU seconds	48	92

Table 2.5: CVA of a swap, CIR model with correlation. Parameters are $R = 0$, $r_0 = 0.05$, $\lambda_0 = 0.1$, $\theta_r = 0.05$, $\zeta_r = 0.5$, $\nu_r = 0.1$, $\theta_\lambda = 0.1$, $\zeta_\lambda = 0.5$, $\nu_\lambda = 0.2$, $T = 1$, $M = 12$.

ρ	**DP**	**Simulation (optimal)**
0	2.4214	[2.3737, 2.4383]
0.25	2.6117	[2.5578, 2.6258]
0.50	2.8078	[2.7479, 2.8199]
0.75	3.0097	[2.9423, 3.0179]
CPU seconds	80	100

Table 2.6: CVA of a Bermudan swaption, CIR model with correlation. Parameters are $R = R_w = 0$, $r_0 = 0.05$, $\lambda_0 = 0.1$, $\theta_r = 0.05$, $\zeta_r = 0.5$, $\nu_r = 0.1$, $\theta_\lambda = 0.1$, $\zeta_\lambda = 0.5$, $\nu_\lambda = 0.2$, $T = 1$, $M = 12$.

2.6 Conclusion

This chapter proposes a recursive formulation of the CVA that allows its evaluation using a DP approach. The contribution of the chapter is twofold. First, the DP algorithm can be used to evaluate the CVA of contracts with optional or exogenous stopping times, and can accommodate a wide range of market and default models. Illustrative examples are provided to show the flexibility of the proposed approach, and numerical experiments for various contracts and models illustrate

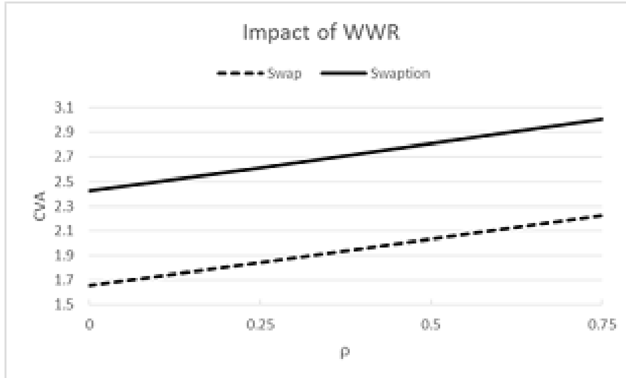

Figure 2.9: Impact of ρ on the CVAs of a swap and a Bermudan swaption. Parameters are as in Tables 2.5 and 2.6.

its precision and efficiency. For low state-space dimensions, the DP approach is computationally much more efficient than Monte-Carlo simulation, providing a complete characterization of the CVA at all possible stopping dates and for all possible states of the world, and doing so in less time and using less memory than simulation requires for a single evaluation. This characterization of the CVA as an analytical function of time and risk factors can be very useful for hedging and risk management purposes, as it allows the computation of the CVA sensitivities (the Greeks) and helps assessing the distribution of the future CVA. Second, for contracts with optional exercise features, the DP approach allows for the computation of the optimal exercise strategy and provides the corresponding CVA, which is not possible using solely Monte Carlo simulation. The use of the naive strategy is shown to be theoretically inconsistent and to result in arbitrage opportunities.
The computational burden of the recursive approach increases significantly with the dimension of the state space, which may be the only drawback of this procedure. Indeed, the CVA is in general computed for portfolios of derivative products rather than individual instruments. For large portfolios depending on several risk factors, it may not be possible to use our numerical approach, which can be seen as a quasi-analytical method, due to the curse of dimensionality. Yet, parallel computing and other technological solutions can be used to reduce the dimensionality problem. Moreover, it is important to note that our theoretical formulation is robust and can be used as a benchmark for heuristic methods based on the partial exploration of the state space, such as the LSMC algorithm (Longstaff and Schwartz (2001)).

A number of extensions can be made to our dynamic model, such as collateral modelling and the inclusion of funding costs. It can be also easily be extended to situations where bilateral counterparty risk is present, or where multiple exercise opportunities exist (e.g. in portfolio of Bermudan options). We leave these extensions for future research.

Appendix 1

In this appendix, we show how we can adapt the recursive equation to the case of first-passage structural models.

For a given firm value process F_t, assume that the default time is defined as

$$\tau = \inf \left\{ t \geq 0 : F_t \leq \overline{f}(t) \right\},$$

where $\overline{f}(t)$ is a deterministic time-dependent default barrier. Depending on the observation frequency and for ease of computations, we assume that default can be only observed at the set of discrete evaluation dates $\mathcal{T} = \{t_m, m = 0, ..., M\}$. Following this view, the definition of τ becomes

$$\tau = \min \left\{ t_m \in \mathcal{T} : F_{t_m} \leq \overline{f}(t_m) \equiv f_m \right\}.$$

In this context, the state vector is $X_t = (Y_t, F_t)$. Supposing that $\tau > t_m$, We can expand $C_{t_m}^{\mathcal{H}}(x)$ for $x \notin H_m$ in the following way:

$$\begin{aligned}
C_{t_m}^{\mathcal{H}}(x) &= \mathbb{E}_{t_m}[\mathbb{1}_{(t_m, \kappa_{m+1}]}(\tau)\Gamma_{t_m}(\tau)\left(V_\tau(X_\tau; \mathcal{H}) - R_\tau(X_\tau)\right)] \\
&= \mathbb{E}_{t_m}\left[\beta_m \mathbb{1}_{(0, f_{m+1}]}(F_{t_{m+1}})\left(V_{t_{m+1}}(X_{t_{m+1}}; \mathcal{H}) - R_{t_{m+1}}(X_{t_{m+1}})\right)\right] \\
&\quad + \mathbb{E}_{t_m}\left[\beta_m \mathbb{1}_{(f_{m+1}, +\infty]}(F_{t_{m+1}})\mathbb{1}_{(t_{m+1}, \kappa_{m+1}]}(\tau)\Gamma_{t_{m+1}}(\tau)\left(V_\tau(X_\tau; \mathcal{H}) - R_\tau(X_\tau)\right)\right] \\
&= B_m^{\mathcal{H}}(x) + \mathbb{E}_{t_m}\left[\beta_m \mathbb{1}_{(f_{m+1}, +\infty]}(F_{t_{m+1}})C_{t_{m+1}}^{\mathcal{H}}\left(X_{t_{m+1}}\right)\right],
\end{aligned}$$

If the joint density of $X_t = (Y_t, F_t)$ is known, then the above expectations can be computed recursively using Chebyshev interpolation and Clenshaw-Curtis quadrature.

Appendix 2

In the case where exercise does not terminate the contract, define

$$
\begin{aligned}
B_m^{\mathcal{H}}(x) &\equiv \mathbb{E}_{t_m}\left[\int_{t_m}^{t_{m+1}} \Gamma_{t_m}(s)\left(V_s(X_s;\mathcal{H}) - R_s^b(X_s)\right)\lambda_s\Lambda_{t_m}(s)ds\right], \\
A_m^{\mathcal{H}}(x) &\equiv \mathbb{E}_{t_m}\left[\int_{t_m}^{T} \Gamma_{t_m}(s)\left(V_s(X_s;\mathcal{H}) - R_s^a(X_s)\right)\lambda_s\Lambda_{t_m}(s)ds\right].
\end{aligned}
$$

For $x \notin H_m$ (i.e., $\kappa_m = \kappa_{m+1} \geq t_{m+1}$), we have

$$
\begin{aligned}
C_{t_m}^{\mathcal{H}}(x) &= V_{t_m}(x;\mathcal{H}) - V_{t_m}^D(x;\mathcal{H}) \\
&= \mathbb{E}_{t_m}[\mathbb{1}_{(t_m,\kappa_{m+1}]}(\tau)\Gamma_{t_m}(\tau)\left(V_\tau(X_\tau;\mathcal{H}) - R_\tau^b(X_\tau)\right)] \\
&\quad +\mathbb{E}_{t_m}[\mathbb{1}_{(\kappa_{m+1},T]}(\tau)\Gamma_{t_m}(\tau)\left(V_\tau(X_\tau;\mathcal{H}) - R_\tau^a(X_\tau)\right)] \\
&= \mathbb{E}_{t_m}\left[\int_{t_m}^{t_{m+1}} \Gamma_{t_m}(s)\left(V_s(X_s;\mathcal{H}) - R_s^b(X_s)\right)\lambda_s\Lambda_{t_m}(s)ds\right] \\
&\quad +\mathbb{E}_{t_m}\left[\int_{t_{m+1}}^{\kappa_{m+1}} \Gamma_{t_m}(s)\left(V_s(X_s;\mathcal{H}) - R_s^b(X_s)\right)\lambda_s\Lambda_{t_m}(s)ds\right] \\
&\quad +\mathbb{E}_{t_m}\left[\int_{\kappa_{m+1}}^{T} \Gamma_{t_m}(s)\left(V_s(X_s;\mathcal{H}) - R_s^a(X_s)\right)\lambda_s\Lambda_{t_m}(s)ds\right] \\
&= B_m^{\mathcal{H}}(x) + \mathbb{E}_{t_m}\left[\beta_m\delta_m C_{t_{m+1}}^{\mathcal{H}}\left(X_{t_{m+1}}\right)\right].
\end{aligned}
$$

On the other hand, for $x \in H_m$ (i.e., $\kappa_m = t_m$), we have

$$
\begin{aligned}
C_{t_m}^{\mathcal{H}}(x) &= \mathbb{E}_{t_m}[\mathbb{1}_{(t_m,T]}(\tau)\Gamma_{t_m}(\tau)\left(V_\tau(X_\tau;\mathcal{H}) - R_\tau^a(X_\tau)\right)] \\
&= A_m^{\mathcal{H}}(x).
\end{aligned}
$$

The expected loss corresponding to a given exercise strategy characterized by $\mathcal{H}$, conditional on no prior default and given no prior exercise at date t_m is then given by the recursion:

$$
\begin{aligned}
C_{t_m}^{\mathcal{H}}(x) &= \left(B_m^{\mathcal{H}}(x) + \mathbb{E}_{t_m}\left[\beta_m\delta_m C_{t_{m+1}}^{\mathcal{H}}\left(X_{t_{m+1}}\right)\right]\right)\mathbb{1}_{\overline{H_m}}(x) \\
&+ A_m^{\mathcal{H}}(x)\mathbb{1}_{H_m}(x),\ m = 0, ..., M-1, \\
C_T^{\mathcal{H}}(x) &= 0.
\end{aligned}
$$

The value of a defaultable claim at $(t_m, X_{t_m} = x)$ under the exercise strategies $\mathcal{C}$ (do not exercise at t_m and then use the optimal strategy) and $\mathcal{E}$ (exercise at t_m), conditional on no prior default and given no prior exercise, are then given respectively by

$$\begin{aligned} V^D_{t_m}(x;\mathcal{C}) &= \mathbb{E}_{t_m}\left[\beta_m V_{t_{m+1}}\left(X_{t_{m+1}};\mathcal{H}^*\right)\right] + q^c_m(x) - B^{\mathcal{C}}_m(x) - \mathbb{E}_{t_m}\left[\beta_m \delta_m C^{\mathcal{H}^*}_{t_{m+1}}\left(X_{t_{m+1}}\right)\right] \\ &= \mathbb{E}_{t_m}\left[\int_{t_m}^{t_{m+1}} \Gamma_{t_m}(s) R^b_s(X_s)\lambda_s \Lambda_{t_{m+1}}(s)ds\right] + q^c_m(x) + \mathbb{E}_{t_m}\left[\beta_m \delta_m V^D_{t_{m+1}}(X_{t_{m+1}})\right], \end{aligned}$$

$$\begin{aligned} V^D_{t_m}(x;\mathcal{E}) &= V_{t_m}(x;\mathcal{E}) - C^{\mathcal{E}}_{t_m}(x) \\ &= q^e_m(x) - A^{\mathcal{E}}_m(x). \end{aligned}$$

We then have, for $m = 0, ..., M-1$, conditional on no prior default and given no prior exercise at t_m

$$\begin{aligned} V^D_{t_m}(x) &= \max\Big\{ q^e_m(x) - A^{\mathcal{E}}_m(x); \\ &\quad \mathbb{E}_{t_m}\left[\int_{t_m}^{t_{m+1}} \Gamma_{t_m}(s) R^b_s(X_s)\lambda_s \Lambda_{t_{m+1}}(s)ds\right] + q^c_m(x) + \mathbb{E}_{t_m}\left[\beta_m \delta_m V^D_{t_{m+1}}(X_{t_{m+1}})\right]\Big\}, \\ H^*_m &= \{x : V^D_{t_m}(x) = q^e_m(x) - A^{\mathcal{E}}_m(x)\}, \end{aligned}$$

with the terminal condition

$$V^D_T(x) = q^e_T(x).$$

Chapter 3

An efficient method to estimate the CVA VaR

3.1 Introduction

In the first chapter, we adressed the problem of computing the CVA which quantifies the market risk of a counterparty default. However, during the financial crisis, the major losses were caused by CVA movements rather than actual defaults. Most institutions were hit by accounting mark-to-market losses rather than real ones. Regulators reported that roughly two thirds of the losses attributed to counterparty risk resulted from CVA volatility. In more colloquial terms, the volatility of the price of counterparty risk, as described by a CVA process, was much more harmful than the risk itself. To respond to such a shortcoming in the regulation, the third installment of the Basel Accords (Basel III) advocated a capital charge against CVA variability. This implies the computation of a risk measure for the CVA process, and in this way the Value at Risk of the CVA (CVA VaR) is introduced.

Generally speaking, the CVA VaR corresponds to a quantile of the distribution of the CVA changes at a given risk horizon. Hence, we need to assess the probability distribution of the future CVA movements. This poses both technological and conceptual issues. First, as outlined in the previous chapter, the valuation of the CVA is done generally with Monte-Carlo methods, especially for exotic derivatives for which direct calculations are not possible. Because Monte-Carlo simulation produces a single estimate for just one point in space and time, sampling the future CVA changes would require nested simulations that naturally exceed standard computational capacities. In practice, the number of scenarios that are generated in order to assess the distribution of the CVA changes is generally very low, which makes the credibility of the CVA VaR estimate very questionable (Brigo et al. (2013)). Alternatively, practitioners would use ad-hoc assumptions to simplify calculations, for instance the simplifying assumption of a constant credit exposure that eliminates the impact of the underlying factors changes. Second, the CVA is by nature a pricing component, while risk measurement concerns real-world profit-and-loss. This is why the distribution of the CVA movements should be assessed under the real (or historical) probability measure denoted by $\mathbb{P}$, while the CVA itself should be priced under the risk-neutral (or pricing) measure denoted by $\mathbb{Q}$. The bridge between $\mathbb{P}$ and $\mathbb{Q}$ then may be considered to some extent, or ignored for practical reasons, since the estimation of the $\mathbb{P}$-parameters is generally problematic.

In this chapter, we suggest an alternative method for the computation of the CVA VaR, whose advantage holds when the number of risk factors is not large. In the previous chapter, we have shown the backward nature of the CVA and suggested an efficient DP procedure to evaluate it. The proposed pricing algorithm provides more than a point estimate: it yields the CVA for all states and all dates in just one execution. In other terms, the algorithm yields the CVA as a known function of the market risk factors for different future dates. Such powerful property allows to avoid nested simulations and makes it possible to estimate the CVA VaR in just one simulation. This chapter is organized as follows. Section 3.2 sets the procedure for estimating the CVA VaR. Section 3.3 reports on illustrative numerical experiments. Section 3.4 is a conclusion.

3.2 Estimating the distribution of CVA changes

In order to assess adverse changes in mark-to-market CVA, one needs to simulate the risk factors affecting the derivative portfolio under the real probability measure $\mathbb{P}$ and then valuate the CVA at the risk horizon for each scenario. A sample of the CVA changes is therefore obtained and the CVA VaR can be estimated. Because the pricing engine is traditionnally a Monte-Carlo simulation, the naive procedure that consists in performing nested simulations becomes computationally prohibitve, resulting in non-precise estimates of the CVA VaR. The pricing approach introduced in the previous chapter clearly overcomes this problem, since one execution of the recursive algorithm yields the CVA for all states and all dates. The following steps would allow to build a robust sample of the future CVA movements:

1. Run the dynamic programming algorithm, and obtain the current CVA and the CVA function at the risk horizon. The computation of expectations should be done under the pricing measure $\mathbb{Q}$.

2. Simulate the risk factors to the risk horizon, under the real measure $\mathbb{P}$.

3. For each scenario, compute the projected future CVA using the approximate function obtained in the first step.

4. A sample of simulated CVA changes is therefore obtained. The CVA change is simply $\Delta\mathrm{CVA}_t = \mathrm{CVA}_t - \mathrm{CVA}_0$, where CVA_0 is the current CVA computed as for today and CVA_t is the projected CVA at the risk horizon t. The CVA VaR for the specified risk horizon can be estimated as a quantile of this sample.

The DP algorithm generally runs fast, unless the dimension of the state space is high, so that generating a high number of scenarios would not exceed standard computational capacities. This would result in much better estimates than the naive approach would handle.

It is worth noting that Basel III suggested two methods to compute the CVA VaR. The first method is a standardized formula that can be equated to a standard variance-covariance method. The second approach (called advanced approach) consists in simulating only the hazard rates of the counterparties with the strong assumption of a constant exposure over the risk period, in order to keep tractability of the CVA computations at the risk horizon. As outlined in Pykhtin (2012), both approaches do not take into account the sensitivity of the CVA to the underlying market variables movements. In particular, right-way/wrong-way risk can not be taken into account using a direct modeling approach. It is accounted for by the use of ad-hoc multipliers with little significance. As discussed in Gregory (2012), the constant exposure assumption can be justified by the fact that default-risk volatility was the main source of CVA volatility during the financial crisis. However, it is important to not forget that counterparty risk is a complex combination of default risk and market risk. Following this view, eliminating the volatility of market risk may dramatically underestimate the probability of extreme CVA losses. It seems therefore that the constant exposure assumption can be justified only by tractability and operational concerns.

An important problem that arises is the need to know the dynamics of the risk factors under both $\mathbb{P}$ and $\mathbb{Q}$. Estimating the $\mathbb{Q}$-dynamics is much easier; it can be done by calibrating the models to the observed current derivative prices. The only assumption underlying the calibration procedure is that markets are efficient, so that all available information is embedded in the current prices. However, estimating the $\mathbb{P}$-dynamics is more difficult and generally goes through historical estimation. The implicit assumption underlying the historical estimation is that the past predicts the future. However, it is not clear how such stationarity assumption can hold. In practice, there is a tradeoff concerning the length of the period used for statistical inference. Short periods put more weight on the most recent observations and stationarity is likely to hold over such short periods, but statistical inference is less accurate simply because fewer observations are included. In contrast, long periods produce more accurate estimates if stationarity holds over long horizons, which is not likely to be true.

In the next section, we present illustrative numerical experiments in which we apply the suggested procedure to estimate the CVA VaR. In particular, we show that the constant exposure assumption can strongly underestimate the CVA VaR. Moreover, we analyze the non-linearity effects that arise as a consequence of the nature of the CVA function, and we link these effects to the CVA sensitivities (the CVA greeks). We also examine to which extent a distortion between $\mathbb{P}$ and $\mathbb{Q}$ can affect the CVA VaR. Finally, we investigate the impact of right-way/wrong-way risk on the CVA VaR.

3.3 Numerical experiments

In this section, we illustrate the CVA VaR methodology with two fundamental examples. In the first example we focus on Bermudan put options, while in the second we consider interest-rate swaps. In both examples, the recovery value is assumed to be null.

3.3.1 Independent CVA of Bermudan put options

In this section, we run numerical experiments on the CVA VaR of Bermudan put options. We consider monthly-exercisable put options with various maturities and moneynesses. Assume that the underlying asset price S_t follows a geometric Brownian motion and that the counterparty hazard rate λ_t follows an independent CIR process. Under the risk-neutral probability measure $\mathbb{Q}$, the dynamics of S_t and λ_t are given by

$$
\begin{aligned}
dS_t &= rS_t dt + \sigma S_t dW_{1t}^{\mathbb{Q}}, \\
d\lambda_t &= \xi(\theta - \lambda_t)dt + \nu\sqrt{\lambda_t}dW_{2t}^{Q},
\end{aligned}
$$

where $W_{1t}^{\mathbb{Q}}$ and $W_{2t}^{\mathbb{Q}}$ are two independent Brownian motions under $\mathbb{Q}$, r is the risk-free interest rate (assumed to be a constant), σ is the underlying asset volatility, θ is the long-run mean of the counterparty hazard rate, ξ is the speed of adjustment to the long-run mean and ν is the hazard-rate volatility. Because switching from the risk neutral measure $\mathbb{Q}$ to the physical probability measure $\mathbb{P}$ affects the drifts of the underlying processes but not their volatility components (Girsanov's theorem), we also assume that S_t and λ_t follow under $\mathbb{P}$

$$
\begin{aligned}
dS_t &= \mu S_t dt + \sigma S_t dW_{1t}^{\mathbb{P}}, \\
d\lambda_t &= \xi^{\mathbb{P}}(\theta^{\mathbb{P}} - \lambda_t)dt + \nu\sqrt{\lambda_t}dW_{2t}^{\mathbb{P}},
\end{aligned}
$$

where $W_{1t}^{\mathbb{P}}$ and $W_{2t}^{\mathbb{P}}$ are two independent Brownian motions under $\mathbb{P}$, μ is the physical rate of return of the underlying asset, $\theta^{\mathbb{P}}$ is the physical long-run mean of λ_t and $\xi^{\mathbb{P}}$ is the physical speed of adjustment to the long-run mean.

The benchmark values of the parameters are reported in Table 3.1.

r, μ	0.05
σ	0.2
$\lambda_0, \theta, \theta^{\mathbb{P}}$	0.1
$\xi, \xi^{\mathbb{P}}$	1
ν	0.1

Table 3.1: Benchmark values for Bermudan put options

In Table 3.5, we report the current CVA and the CVA VaR at the 99% confidence level over short horizons of 10 days and 1 month for different maturities ($T = 2, 3, 4, 5$) and moneynesses ($S_0/K = 0.5, 1, 1.5$ where K is the strike price). Through Table 3.5 and Figure 3.1 in which we plot the distribution of the 10-day CVA changes, we can analyze the effect of maturity on the tail of the distribution. For in-the-money options, the maturity has no effect on the CVA estimates. This is clearly an early-exercise effect. Whatever the maturity is, in-the money-options will be exercised early, so that concern about losses resulting from a default of the counterparty will be just over a short period of time. For out-of-the-money options, we can see that the CVA VaR increases with maturity. This effect can be related to the shape of the CVA function. The slope of the option exposure in the out-of-the-money region increases with maturity. An increasing slope enhances the sensitivity of the CVA to the underlying asset movements.

A common practice in the industry is to assume a constant exposure over the risk period in order to avoid nested simulations. In this way, the CVA VaR is related only to the movements of the hazard rate and excludes the impact of changes in the underlying market variables. In Table 3.6 and Figure 3.2, we examine the impact of the constant exposure assumption. It is quite obvious that such assumption affects the tail of the distribution of the CVA movements for all maturities and all moneynesses, resulting in a lower estimate of the CVA VaR. The effect of neglecting the volatility of the underlying asset is particularly strong for out-of-the-money options, but much less pronounced for in-the-money options.

We analyze the sensitivity of the CVA VaR to λ_0 (the initial guess of the counterparty hazard rate) in Table 3.7 and Figure 3.3. We compare the benchmark case for which $\lambda_0 = 0.1$ to the cases where $\lambda_0 = 0.05$ and $\lambda_0 = 0.15$. It is clear that higher values of λ_0 make the tail of the distribution slightly heavier, and thus increase the CVA VaR estimates for all maturities and all moneynesses. This can be explained by two effects. The first is related to the nature of the model considered for the hazard rate. The volatility of the hazard-rate process is proportional to the square root of the actual level of the hazard rate. Hence, higher values of λ_0 are more likely to lead to higher movements of the hazard rate, and that naturally results in more pronounced CVA movements. The second effect is related to the CVA function. Given that the CVA can be generally assimilated as the contract exposure multiplied by the counterparty default probability, the sensitivity of the CVA to the underlying asset price movements increases with the hazard-rate level. Mathematically, this effect is related to the greek $\dfrac{\partial \text{CVA}}{\partial S}$ which increases in absolute value with the default probability, as reported in Table 3.2. Note that the constant exposure assumption does not capture this behavior, since it excludes the potential changes in the underlying risk factors.

	In-the-money	At-the-money	Out-of-the-money
$\lambda_0 = 0.05$	0.0043	0.0089	0.0031
$\lambda_0 = 0.1$	0.0083	0.0144	0.0041
$\lambda_0 = 0.15$	0.0123	0.0192	0.0051

Table 3.2: $\dfrac{\partial \text{CVA}}{\partial S}$ in absolute value for different values of λ_0 (Maturity is 2 years)

In Table 3.8 and Figure 3.4, we examine the sensitivity of the CVA VaR to the volatility of the hazard rate. We compare the benchmark case for which $\nu = 0.1$ to the cases where $\nu = 0.2$ and $\nu = 0.3$. Higher values of ν result in heavier tails of the CVA movements distribution. The effect is quite pronounced for in-the-money and at-the-money options. This is because the exposure level in in-the-money and at-the-money regions of the state space is relatively high, thus enhancing the impact of higher hazard-rate movements that are allowed by a higher hazard-rate volatility. Technically, this effect is related to the greek $\dfrac{\partial \text{CVA}}{\partial \lambda}$ which increases with the exposure level, as reported in Table 3.3. Indeed, for out-of-the-money options the effect of the hazard rate volatility is negligible, simply because the exposure level in the out-of-money region is relatively low.

In-the-money	At-the-money	Out-of-the-money
1.9657	1.8640	0.1722

Table 3.3: $\dfrac{\partial \text{CVA}}{\partial \lambda}$ for different moneynesses (Maturity is 2 years)

We now turn to analyze the sensitivity to the underlying asset volatility σ. In Table 3.9 and Figure 3.5, we compare the benchmark results for which $\sigma = 0.2$ to higher volatility cases implied by $\sigma = 0.25$ and $\sigma = 0.3$. As expected, higher asset volatilities increase the likelihood of higher movements in the exposure profile, thus producing heavier tails of the CVA changes distribution. The effect is obvious for at-the-money and out-of-the-money options. However, it is relatively small for in-the-money options. This is again a consequence of early-exercise. Due to early-exercise, the shape of the option exposure in the in-the-money region is not too sensitive to the volatility parameter, in contrast to the out-of-the-money region where the volatility affects the slope of the option value as does the maturity. Intuitively, because in-the-money options will be exercised very early, concern about market risk is of little relevance in this case. What matters instead is default risk over the short waiting period. This is why the CVA VaR of in-the-money options is sensitive to the hazard-rate volatility, but not that sensitive to the underlying asset volatility.

Until here, we have assumed that the risk-neutral and the physical parameters are the same. We now examine the effect of a distortion between $\mathbb{P}$ and $\mathbb{Q}$ on the tail of the distribution of CVA movements. In Table 3.10 and Figure 3.6, we compare the benchmark results for which $\mu = 0.05$ to alternative results implied by $\mu = 0.075$ and $\mu = 0.1$. It is clear that changing μ has practically no impact on the CVA VaR estimates, and this is true for all maturities and all moneynesses. In Table 3.11 and Figure 3.7, we compare the benchmark results for which $\theta^{\mathbb{P}} = 0.1$ to cases associated with $\theta^{\mathbb{P}} = 0.05$ and $\theta^{\mathbb{P}} = 0.15$. The center of the distribution is slightly translated as a consequence of the mean effect resulting from changing the physical long-run mean of the hazard rate, but the tail and the CVA VaR are not seriously affected, and this holds for all maturities and all moneynesses. In Table 3.12 and Figure 3.8, we compare the benchmark results for which $\xi^{\mathbb{P}} = 1$ to results implied by $\xi^{\mathbb{P}} = 0.25$ and $\xi^{\mathbb{P}} = 1.75$. We can see that changing $\xi^{\mathbb{P}}$ has no effect at all on the distribution of CVA movements for all maturities and all moneynesses. Summing up, we can say that increasing the distortion between the risk-neutral measure and the physical measure does not seem to significantly affect the tail of the distribution, at least for this example. Because the horizon at which the CVA VaR is computed is short, as it is the practice for standard market VaR, the role of the drift terms to generate extreme values of the risk factors is not expected to be relevant with comparison to the role of the volatility components. As discussed in Gregory (2012), the importance of drift terms arises when dealing with risk measures associated with relatively long risk horizons, such as the potential future exposure for credit limits concerns.

To conclude, the CVA VaR patterns can be complex mainly due to the non-linearity of the CVA function and the exotic characteristics of financial contracts like early-exercise. Moreover, the distributional properties of the hazard rate and the underlying factors can be of relevant importance. The $\mathbb{P}$-Versus-$\mathbb{Q}$ problem does not seem to be an important issue from a quantitative point of view, since the discrepancy between the two measures is driven by drift terms that are of secondary importance when dealing with short-horizon risk measures. Besides, simplifying assumptions often made in industry practices such as assuming a constant exposure over the risk period may misestimate the CVA VaR. Note that the aim of such simplifying assumption is to avoid the computational burden associated with nested simulations. The suggested approach is an alternative computational methodology that captures all the properties of the CVA VaR without making any simplifying assumptions.

3.3.2 Right-way/wrong-way CVA of interest-rate swaps

In this section, we report numerical experiments on the CVA VaR of interest-rate swaps. We consider payer interest-rate swap positions where fixed and floating payments are exchanged at each month. Assume that under $\mathbb{P}$ and $\mathbb{Q}$, the spot interest rate r_t and the counterparty hazard rate λ_t follow two correlated CIR processes

$$\begin{aligned} dr_t &= \xi_r(\theta_r - r_t)dt + \nu_r\sqrt{r_t}dW_{1t}, \\ d\lambda_t &= \xi_\lambda(\theta_\lambda - \lambda_t)dt + \nu_\lambda\sqrt{\lambda_t}dW_{2t}, \end{aligned}$$

where W_{1t} and W_{2t} are two correlated Brownian motions with correlation coefficient ρ

$$dW_{1t}dW_{2t} = \rho dt.$$

Wrong-way risk (respectively right-way risk) is present when $\rho > 0$ (respectively when $\rho < 0$). In fact, the payer swap value is an increasing function of the spot interest rate. If the interest rate increases, this would increase the value of the payer position, but also the likelihood of a counterparty default in case of a positive correlation with the counterparty hazard rate.
The benchmark values of the parameters are reported in Table 3.4.

r_0, θ_r	0.05
ξ_r	0.5
$\lambda_0, \theta_\lambda$	0.1
ξ_λ	1
ν_r, ν_λ	0.1

Table 3.4: Benchmark values for interest rate swaps

In Table 3.13, we report the current CVA and the CVA VaR at the 99 % confidence level over horizons of 10 days and 1 month for different swap maturities ($T = 2, 3, 4, 5$) and correlations ($\rho = -0.5, 0, 0.5$). The CVA estimates are reported in basis points. In Figure 3.9, we compare the distributions of the 10-day CVA movements implied by the three correlation levels. Even if the effects are not very material, it is clear that wrong-way risk (respectively right-way risk) increases (respectively decreases) the CVA VaR estimate for all considered maturities. In case of a positive correlation, scenarios in which the swap exposure is high imply higher levels of the hazard rate (with comparison to the zero-correlation case) which results in more pronounced upward movements of the CVA. The reverse effect happens in the case of right-way risk.
We now investigate the role of the hazard-rate volatility in increasing the right-way/wrong-way effect. In Table 3.14 and Figure 3.10, we compare the benchmark results to results implied by increased hazard-rate volatilities ($\nu_\lambda = 0.2$ and $\nu_\lambda = 0.3$). We notice that a higher hazard-rate volatility enhances both the right-way and the wrong-way effects. Particularly, in the case

of a negative correlation, a higher hazard-rate volatility decreases the CVA VaR estimate. At first glance, this would seem counter-intuitive, since an increased volatility would naturally lead to more extreme CVA upward movements. However, it is important to note that the CVA is essentially driven by the contract exposure. This means that high exposure scenarios are the ones that contribute most to the tail of the distribution, independently from hazard-rate levels. In the presence of a negative correlation, a higher hazard-rate volatility leads to lower hazard-rate levels in high exposure scenarios, which decreases the CVA VaR estimate. The reverse effect happens in the case of wrong-way risk, resulting in a higher CVA VaR. Note that the right-way effect would not be observed in the case of a higher interest-rate volatility, since the interest-rate volatility affects the exposure profile. In this sense, an increased interest-rate volatility would increase the CVA VaR whatever the correlation is. The assymetric roles of the interest-rate volatility and the hazard-rate volatility are a result of the complementary statuses of the exposure and the default probability. The default probability defines the likelihood of a market loss while the exposure measures the severity of a loss if it occurs.

Summarizing the reported results and interpretations, right-way/wrong-way risk affects not only the CVA level but also the CVA VaR. The role of the hazard-rate volatility is to increase both the right-way and the wrong-way effects. In particular, in case of right-way risk, a higher hazard-rate volatility is beneficial in that it decreases the CVA VaR.

3.4 Conclusion

This chapter is a straightforward risk management application of the CVA pricing model developed in the first chapter. An interesting property of the dynamic pricing model is that it yields approximate CVA functions at different horizons rather than a single CVA estimate as does Monte-Carlo simulation. This allows to build a robust methodology for estimating the CVA VaR and overcoming the computational issue associated with nested simulations. We have analyzed the complex patterns of the CVA VaR through two numerical examples in which we applied the suggested methodology, and we have shown that the ad-hoc assumptions used in industry practices may result in a substantial misestimation of extreme CVA losses.

	In-the-money			At-the-money			Out-of-the-money		
	Current	10 days	1 month	Current	10 days	1 month	Current	10 days	1 month
$T = 2$	0.2058	0.0294	0.0508	0.3429	0.0418	0.0430	0.0386	0.0303	0.0539
$T = 3$	0.2058	0.0294	0.0508	0.5042	0.0421	0.0488	0.1006	0.0541	0.0952
$T = 4$	0.2058	0.0294	0.0508	0.6443	0.0395	0.0484	0.1762	0.0738	0.1289
$T = 5$	0.2058	0.0294	0.0508	0.7659	0.0377	0.0479	0.2559	0.0892	0.1551

Table 3.5: Current CVA and CVA VaR over horizons of 10 days and 1 month for Bermudan put options

		In-the-money			At-the-money			Out-of-the-money		
		Current	10 days	1 month	Current	10 days	1 month	Current	10 days	1 month
$T = 2$	Benchmark	0.2058	0.0294	0.0508	0.3429	0.0418	0.0430	0.0386	0.0303	0.0539
$T = 2$	Constant exposure	0.2058	0.0243	0.0418	0.3429	0.0226	0.0229	0.0386	0.0021	0.0036
$T = 3$	Benchmark	0.2058	0.0294	0.0508	0.5042	0.0421	0.0488	0.1006	0.0541	0.0952
$T = 3$	Constant exposure	0.2058	0.0243	0.0418	0.5042	0.0286	0.0358	0.1006	0.0043	0.0073
$T = 4$	Benchmark	0.2058	0.0294	0.0508	0.6443	0.0395	0.0484	0.1762	0.0738	0.1289
$T = 4$	Constant exposure	0.2058	0.0243	0.0418	0.6443	0.0315	0.0428	0.1762	0.0061	0.0104
$T = 5$	Benchmark	0.2058	0.0294	0.0508	0.7659	0.0377	0.0479	0.2559	0.0892	0.1551
$T = 5$	Constant exposure	0.2058	0.0243	0.0418	0.7659	0.0331	0.0469	0.2559	0.0075	0.0129

Table 3.6: Effect of the constant exposure assumption on the CVA VaR over horizons of 10 days and 1 month for Bermudan put options

		In-the-money			At-the-money			Out-of-the-money		
		Current	10 days	1 month	Current	10 days	1 month	Current	10 days	1 month
$T = 2$	$\lambda_0 = 0.1$	0.2058	0.0294	0.0508	0.3429	0.0418	0.0430	0.0386	0.0303	0.0539
$T = 2$	$\lambda_0 = 0.05$	0.1073	0.0223	0.0428	0.2475	0.0299	0.0360	0.0298	0.0232	0.0419
$T = 2$	$\lambda_0 = 0.15$	0.3038	0.0349	0.0564	0.4320	0.0491	0.0448	0.0470	0.0372	0.0647
$T = 3$	$\lambda_0 = 0.1$	0.2058	0.0294	0.0508	0.5042	0.0421	0.0488	0.1006	0.0541	0.0952
$T = 3$	$\lambda_0 = 0.05$	0.1073	0.0223	0.0428	0.3858	0.0308	0.0400	0.0829	0.0437	0.0782
$T = 3$	$\lambda_0 = 0.15$	0.3038	0.0349	0.0564	0.6177	0.0518	0.0536	0.1176	0.0639	0.1103
$T = 4$	$\lambda_0 = 0.1$	0.2058	0.0294	0.0508	0.6443	0.0395	0.0484	0.1762	0.0738	0.1289
$T = 4$	$\lambda_0 = 0.05$	0.1073	0.0223	0.0428	0.5144	0.0298	0.0414	0.1508	0.0616	0.1094
$T = 4$	$\lambda_0 = 0.15$	0.3038	0.0349	0.0564	0.7695	0.0476	0.0530	0.2004	0.0854	0.1462
$T = 5$	$\lambda_0 = 0.1$	0.2058	0.0294	0.0508	0.7659	0.0377	0.0479	0.2559	0.0892	0.1551
$T = 5$	$\lambda_0 = 0.05$	0.1073	0.0223	0.0428	0.6286	0.0292	0.0425	0.2247	0.0761	0.1344
$T = 5$	$\lambda_0 = 0.15$	0.3038	0.0349	0.0564	0.8976	0.0444	0.0508	0.2858	0.1017	0.1735

Table 3.7: Effect of λ_0 on the current CVA and the CVA VaR over horizons of 10 days and 1 month for Bermudan put options

		In-the-money			At-the-money			Out-of-the-money		
		Current	10 days	1 month	Current	10 days	1 month	Current	10 days	1 month
$T = 2$	$\nu = 0.1$	0.2058	0.0294	0.0508	0.3429	0.0418	0.0430	0.0386	0.0303	0.0539
$T = 2$	$\nu = 0.2$	0.2057	0.0531	0.0913	0.3408	0.0606	0.0768	0.0384	0.0308	0.0542
$T = 2$	$\nu = 0.3$	0.2057	0.0793	0.1401	0.3376	0.0821	0.1161	0.0380	0.0309	0.0554
$T = 3$	$\nu = 0.1$	0.2058	0.0294	0.0508	0.5042	0.0421	0.0488	0.1006	0.0541	0.0952
$T = 3$	$\nu = 0.2$	0.2057	0.0531	0.0913	0.5006	0.0680	0.0934	0.0999	0.0549	0.0958
$T = 3$	$\nu = 0.3$	0.2057	0.0793	0.1401	0.4951	0.0947	0.1420	0.0989	0.0550	0.0979
$T = 4$	$\nu = 0.1$	0.2058	0.0294	0.0508	0.6443	0.0395	0.0484	0.1762	0.0738	0.1289
$T = 4$	$\nu = 0.2$	0.2057	0.0531	0.0913	0.6403	0.0691	0.0996	0.1748	0.0748	0.1297
$T = 4$	$\nu = 0.3$	0.2057	0.0793	0.1401	0.6333	0.0997	0.1541	0.1727	0.0749	0.1324
$T = 5$	$\nu = 0.1$	0.2058	0.0294	0.0508	0.7659	0.0377	0.0479	0.2559	0.0892	0.1551
$T = 5$	$\nu = 0.2$	0.2057	0.0531	0.0913	0.7611	0.0697	0.1022	0.2539	0.0905	0.1562
$T = 5$	$\nu = 0.3$	0.2057	0.0793	0.1401	0.7522	0.1026	0.1623	0.2507	0.0905	0.1592

Table 3.8: Effect of ν on the current CVA and the CVA VaR over horizons of 10 days and 1 month for Bermudan put options

		In-the-money			At-the-money			Out-of-the-money		
		Current	10 days	1 month	Current	10 days	1 month	Current	10 days	1 month
$T = 2$	$\sigma = 0.2$	0.2058	0.0294	0.0508	0.3429	0.0418	0.0430	0.0386	0.0303	0.0539
$T = 2$	$\sigma = 0.25$	0.2058	0.0320	0.0549	0.4814	0.0583	0.0597	0.1075	0.0669	0.1157
$T = 2$	$\sigma = 0.3$	0.2058	0.0345	0.0601	0.6261	0.0765	0.0796	0.2070	0.1090	0.1785
$T = 3$	$\sigma = 0.2$	0.2058	0.0294	0.0508	0.5042	0.0421	0.0488	0.1006	0.0541	0.0952
$T = 3$	$\sigma = 0.25$	0.2058	0.0320	0.0549	0.7240	0.0603	0.0682	0.2436	0.1039	0.1775
$T = 3$	$\sigma = 0.3$	0.2058	0.0345	0.0601	0.9511	0.0781	0.0883	0.4321	0.1549	0.2511
$T = 4$	$\sigma = 0.2$	0.2058	0.0294	0.0508	0.6443	0.0395	0.0484	0.1762	0.0738	0.1289
$T = 4$	$\sigma = 0.25$	0.2058	0.0320	0.0549	0.9400	0.0577	0.0694	0.3978	0.1312	0.2226
$T = 4$	$\sigma = 0.3$	0.2058	0.0345	0.0601	1.2463	0.0743	0.0886	0.6767	0.1858	0.2990
$T = 5$	$\sigma = 0.2$	0.2058	0.0294	0.0508	0.7659	0.0377	0.0479	0.2559	0.0892	0.1551
$T = 5$	$\sigma = 0.25$	0.2058	0.0320	0.0549	1.1319	0.0539	0.0681	0.5549	0.1510	0.2544
$T = 5$	$\sigma = 0.3$	0.2058	0.0345	0.0601	1.5116	0.0695	0.0865	0.9205	0.2061	0.3297

Table 3.9: Effect of σ on the current CVA and the CVA VaR over horizons of 10 days and 1 month for Bermudan put options

		In-the-money			At-the-money			Out-of-the-money		
		Current	10 days	1 month	Current	10 days	1 month	Current	10 days	1 month
$T = 2$	$\mu = 0.05$	0.2058	0.0294	0.0508	0.3429	0.0418	0.0430	0.0386	0.0303	0.0539
$T = 2$	$\mu = 0.075$	0.2058	0.0293	0.0504	0.3429	0.0418	0.0420	0.0386	0.0300	0.0524
$T = 2$	$\mu = 0.1$	0.2058	0.0289	0.0497	0.3429	0.0412	0.0420	0.0386	0.0297	0.0517
$T = 3$	$\mu = 0.05$	0.2058	0.0294	0.0508	0.5042	0.0421	0.0488	0.1006	0.0541	0.0952
$T = 3$	$\mu = 0.075$	0.2058	0.0293	0.0504	0.5042	0.0423	0.0477	0.1006	0.0536	0.0928
$T = 3$	$\mu = 0.1$	0.2058	0.0289	0.0497	0.5042	0.0416	0.0476	0.1006	0.0530	0.0917
$T = 4$	$\mu = 0.05$	0.2058	0.0294	0.0508	0.6443	0.0395	0.0484	0.1762	0.0738	0.1289
$T = 4$	$\mu = 0.075$	0.2058	0.0293	0.0504	0.6443	0.0398	0.0481	0.1762	0.0732	0.1260
$T = 4$	$\mu = 0.1$	0.2058	0.0289	0.0497	0.6443	0.0391	0.0478	0.1762	0.0723	0.1244
$T = 5$	$\mu = 0.05$	0.2058	0.0294	0.0508	0.7659	0.0377	0.0479	0.2559	0.0892	0.1551
$T = 5$	$\mu = 0.075$	0.2058	0.0293	0.0504	0.7659	0.0378	0.0476	0.2559	0.0885	0.1519
$T = 5$	$\mu = 0.1$	0.2058	0.0289	0.0497	0.7659	0.0373	0.0472	0.2559	0.0874	0.1499

Table 3.10: Effect of μ on the CVA VaR over horizons of 10 days and 1 month for Bermudan put options

		In-the-money			At-the-money			Out-of-the-money		
		Current	10 days	1 month	Current	10 days	1 month	Current	10 days	1 month
$T=2$	$\theta^{\mathbb{P}}=0.1$	0.2058	0.0294	0.0508	0.3429	0.0418	0.0430	0.0386	0.0303	0.0539
$T=2$	$\theta^{\mathbb{P}}=0.05$	0.2058	0.0263	0.0414	0.3429	0.0390	0.0345	0.0386	0.0298	0.0530
$T=2$	$\theta^{\mathbb{P}}=0.15$	0.2058	0.0320	0.0589	0.3429	0.0445	0.0503	0.0386	0.0309	0.0547
$T=3$	$\theta^{\mathbb{P}}=0.1$	0.2058	0.0294	0.0508	0.5042	0.0421	0.0488	0.1006	0.0541	0.0952
$T=3$	$\theta^{\mathbb{P}}=0.05$	0.2058	0.0263	0.0414	0.5042	0.0385	0.0376	0.1006	0.0531	0.0938
$T=3$	$\theta^{\mathbb{P}}=0.15$	0.2058	0.0320	0.0589	0.5042	0.0455	0.0586	0.1006	0.0551	0.0966
$T=4$	$\theta^{\mathbb{P}}=0.1$	0.2058	0.0294	0.0508	0.6443	0.0395	0.0484	0.1762	0.0738	0.1289
$T=4$	$\theta^{\mathbb{P}}=0.05$	0.2058	0.0263	0.0414	0.6443	0.0354	0.0367	0.1762	0.0725	0.1270
$T=4$	$\theta^{\mathbb{P}}=0.15$	0.2058	0.0320	0.0589	0.6443	0.0432	0.0594	0.1762	0.0751	0.1308
$T=5$	$\theta^{\mathbb{P}}=0.1$	0.2058	0.0294	0.0508	0.7659	0.0377	0.0479	0.2559	0.0892	0.1551
$T=5$	$\theta^{\mathbb{P}}=0.05$	0.2058	0.0263	0.0414	0.7659	0.0334	0.0354	0.2559	0.0877	0.1529
$T=5$	$\theta^{\mathbb{P}}=0.15$	0.2058	0.0320	0.0589	0.7659	0.0413	0.0590	0.2559	0.0907	0.1574

Table 3.11: Effect of $\theta^{\mathbb{P}}$ on the CVA VaR over horizons of 10 days and 1 month for Bermudan put options

		In-the-money			At-the-money			Out-of-the-money		
		Current	10 days	1 month	Current	10 days	1 month	Current	10 days	1 month
$T=2$	$\xi^{\mathbb{P}}=1$	0.2058	0.0294	0.0508	0.3429	0.0418	0.0430	0.0386	0.0303	0.0539
$T=2$	$\xi^{\mathbb{P}}=0.25$	0.2058	0.0297	0.0519	0.3429	0.0420	0.0439	0.0386	0.0301	0.0532
$T=2$	$\xi^{\mathbb{P}}=1.75$	0.2058	0.0292	0.0499	0.3429	0.0417	0.0421	0.0386	0.0305	0.0534
$T=3$	$\xi^{\mathbb{P}}=1$	0.2058	0.0294	0.0508	0.5042	0.0421	0.0488	0.1006	0.0541	0.0952
$T=3$	$\xi^{\mathbb{P}}=0.25$	0.2058	0.0297	0.0519	0.5042	0.0424	0.0505	0.1006	0.0537	0.0941
$T=3$	$\xi^{\mathbb{P}}=1.75$	0.2058	0.0292	0.0499	0.5042	0.0418	0.0477	0.1006	0.0543	0.0946
$T=4$	$\xi^{\mathbb{P}}=1$	0.2058	0.0294	0.0508	0.6443	0.0395	0.0484	0.1762	0.0738	0.1289
$T=4$	$\xi^{\mathbb{P}}=0.25$	0.2058	0.0297	0.0519	0.6443	0.0400	0.0503	0.1762	0.0732	0.1275
$T=4$	$\xi^{\mathbb{P}}=1.75$	0.2058	0.0292	0.0499	0.6443	0.0390	0.0476	0.1762	0.0740	0.1283
$T=5$	$\xi^{\mathbb{P}}=1$	0.2058	0.0294	0.0508	0.7659	0.0377	0.0479	0.2559	0.0892	0.1551
$T=5$	$\xi^{\mathbb{P}}=0.25$	0.2058	0.0297	0.0519	0.7659	0.0382	0.0499	0.2559	0.0886	0.1535
$T=5$	$\xi^{\mathbb{P}}=1.75$	0.2058	0.0292	0.0499	0.7659	0.0370	0.0467	0.2559	0.0895	0.1544

Table 3.12: Effect of $\xi^{\mathbb{P}}$ on the CVA VaR over horizons of 10 days and 1 month for Bermudan put options

	$T=2$			$T=3$			$T=4$			$T=5$		
	Current	10 days	1 month	Current	10 days	1 month	Current	10 days	Current	Current	10 days	1 month
$\rho=-0.5$	6.39	5.20	8.60	13.07	7.89	13.46	20.39	9.91	17.13	27.62	11.28	19.67
$\rho=0$	7.16	5.79	9.93	14.72	8.76	15.44	23.00	10.94	19.54	31.14	12.39	22.37
$\rho=0.5$	7.97	6.48	11.22	16.45	9.82	17.38	25.73	12.24	21.88	34.84	13.84	24.91

Table 3.13: Effect of ρ on the current CVA and the CVA VaR over horizons of 10 days and 1 month for interest rate swaps

		$T=2$			$T=3$			$T=4$			$T=5$		
		Current	10 days	1 month	Current	10 days	1 month	Current	10 days	1 month	Current	10 days	1 month
$\rho=-0.5$	$\nu_\lambda=0.1$	6.39	5.20	8.60	13.07	7.89	13.46	20.39	9.91	17.13	27.62	11.28	19.67
$\rho=-0.5$	$\nu_\lambda=0.2$	5.66	4.64	7.80	11.50	7.02	12.17	17.91	8.81	15.46	24.24	10.05	17.76
$\rho=-0.5$	$\nu_\lambda=0.3$	4.93	4.20	7.00	9.84	6.27	10.77	15.11	7.81	13.57	20.21	8.84	15.48
$\rho=0$	$\nu_\lambda=0.1$	7.16	5.79	9.93	14.72	8.76	15.44	23.00	10.94	19.54	31.14	12.39	22.37
$\rho=0$	$\nu_\lambda=0.2$	7.14	5.87	10.17	14.64	8.86	15.79	22.85	11.02	19.84	30.92	12.46	22.64
$\rho=0$	$\nu_\lambda=0.3$	7.05	6.02	10.57	14.36	9.03	16.19	22.22	11.18	20.21	29.81	12.57	22.88
$\rho=0.5$	$\nu_\lambda=0.1$	7.97	6.48	11.22	16.45	9.82	17.38	25.73	12.24	21.88	34.84	13.84	24.91
$\rho=0.5$	$\nu_\lambda=0.2$	8.74	7.33	12.81	18.08	11.04	19.72	28.27	13.66	24.67	38.24	15.38	27.91
$\rho=0.5$	$\nu_\lambda=0.3$	9.47	8.13	14.42	19.52	12.18	22.07	30.35	15.01	27.39	40.80	16.80	30.76

Table 3.14: Effect of ν_λ on the right/wrong-way CVA VaR over horizons of 10 days and 1 month for interest rate swaps

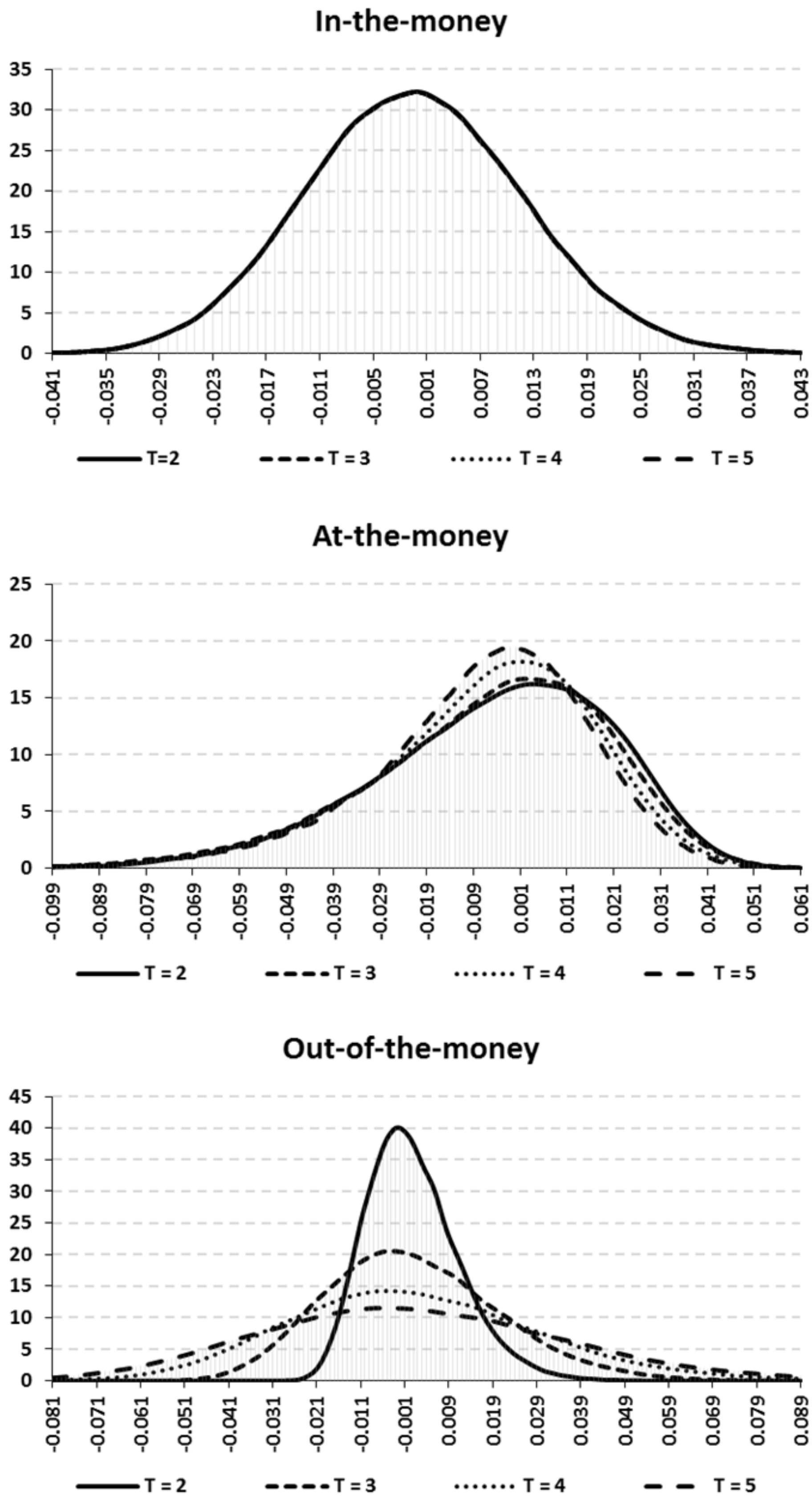

Figure 3.1: Effect of maturity on the distribution of the 10-day CVA movements for Bermudan put options

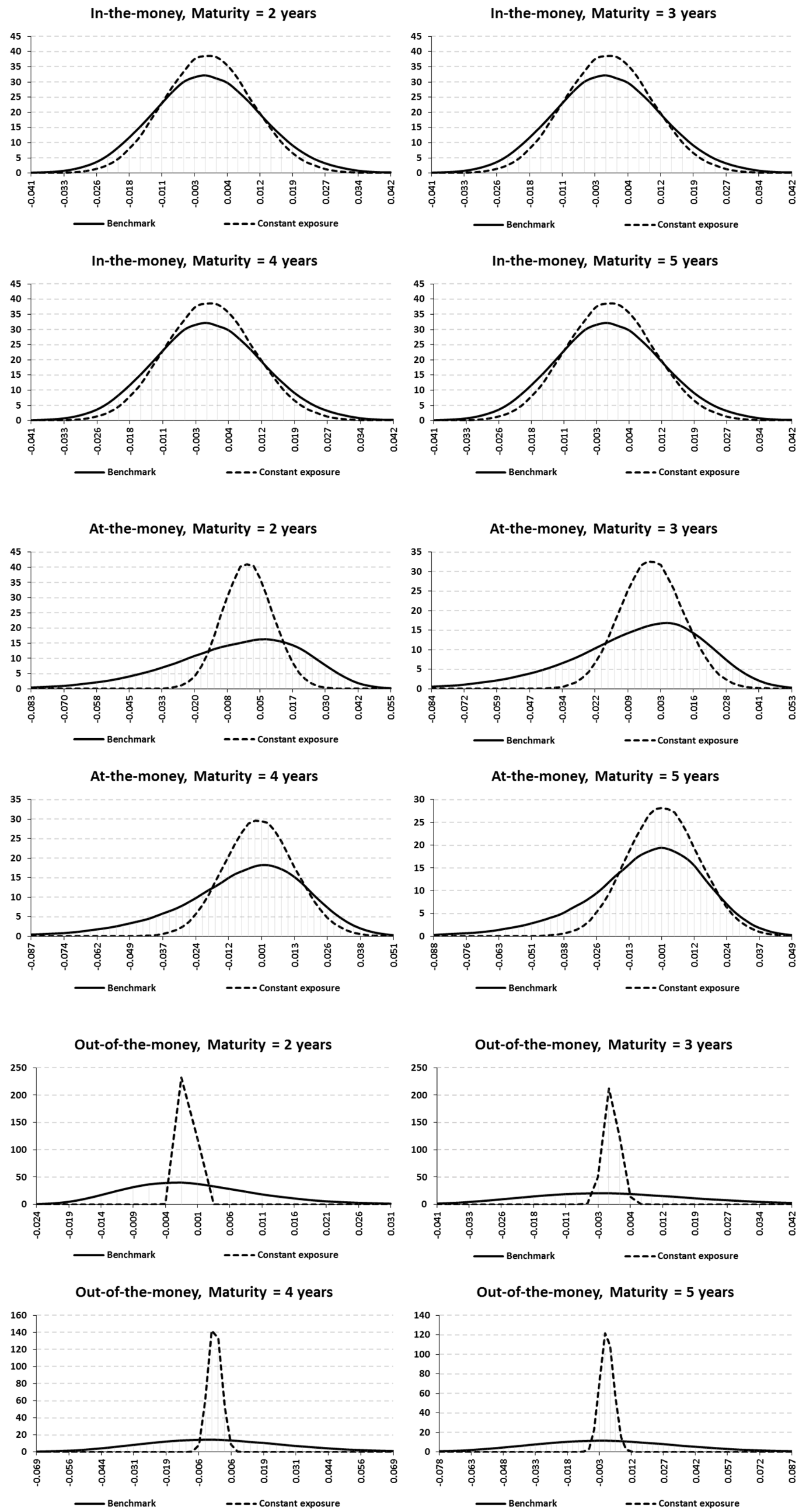

Figure 3.2: Effect of the constant exposure assumption on the distribution of the 10-day CVA movements for Bermudan put options

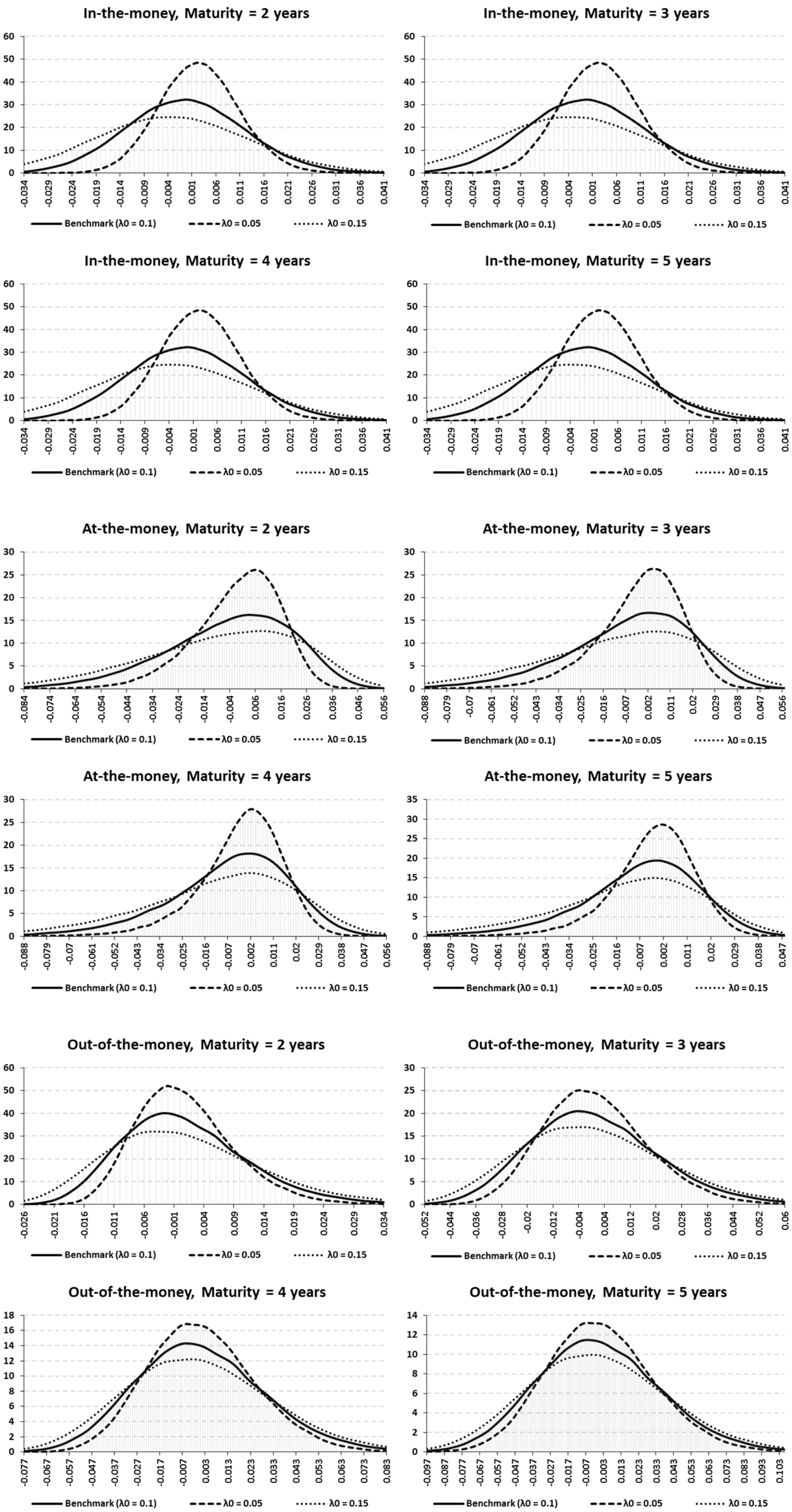

Figure 3.3: Effect of λ_0 on the distribution of the 10-day CVA movements for Bermudan put options

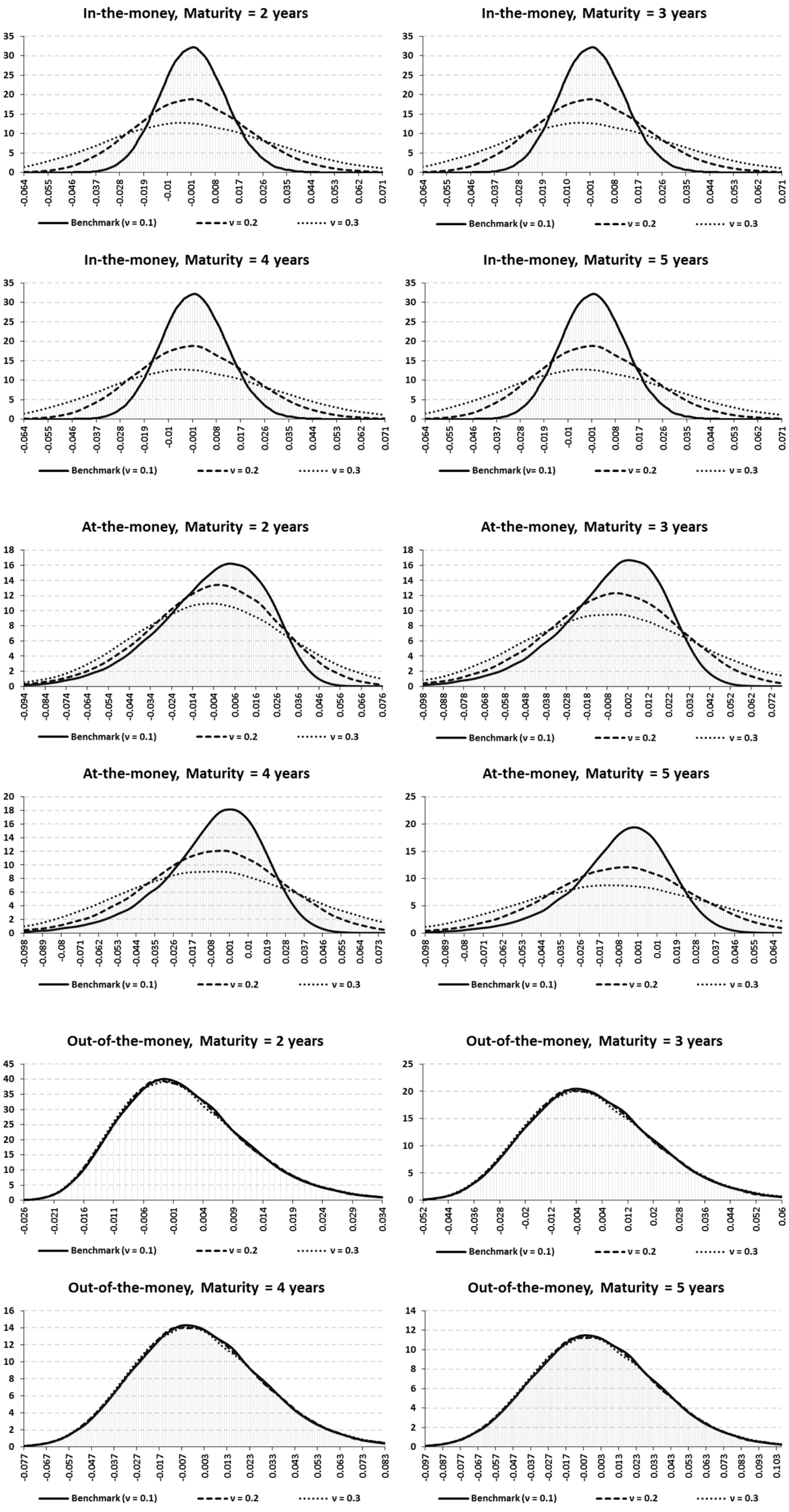

Figure 3.4: Effect of ν on the distribution of the 10-day CVA movements for Bermudan put options

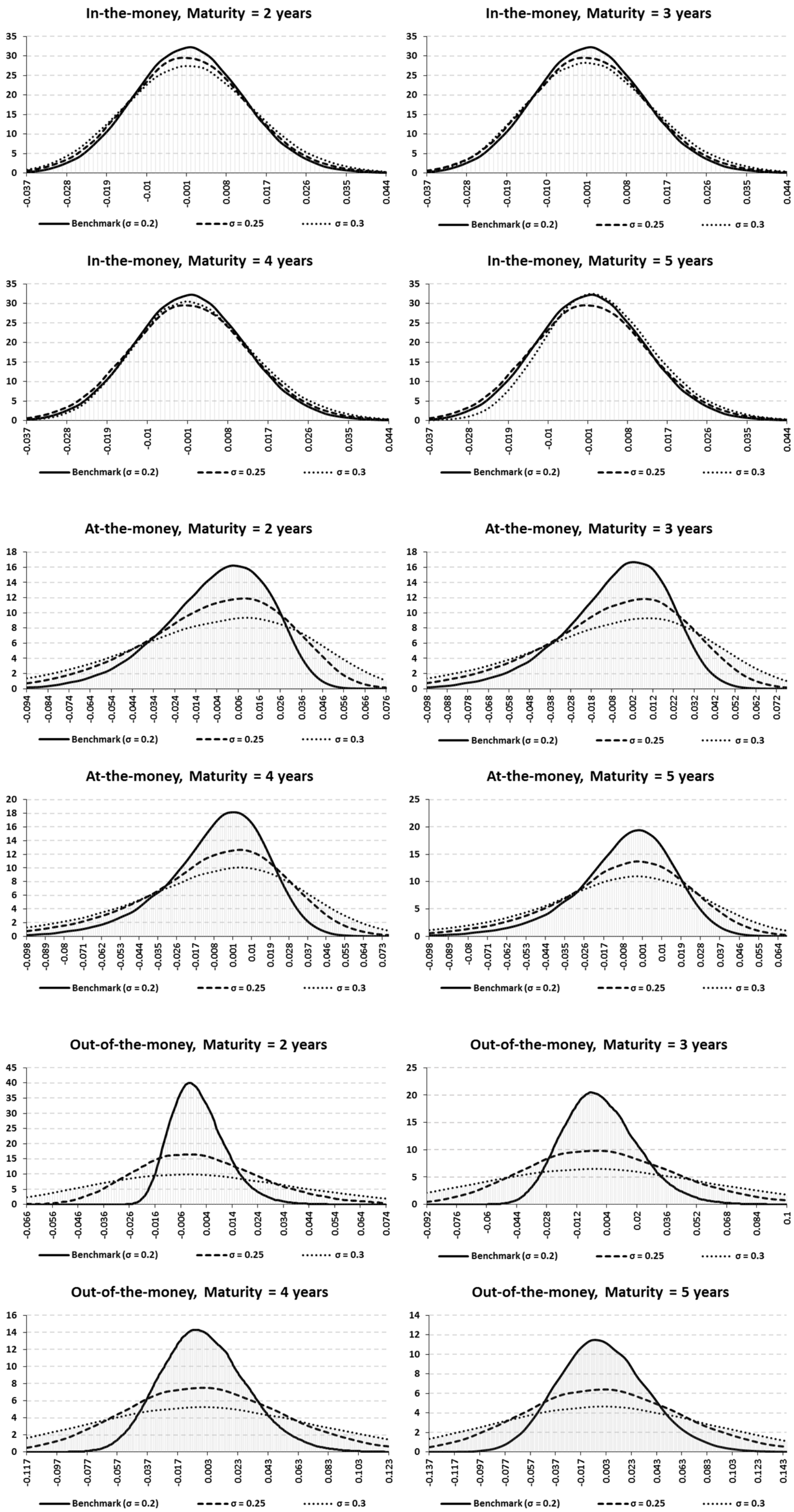

Figure 3.5: Effect of σ on the distribution of the 10-day CVA movements for Bermudan put options

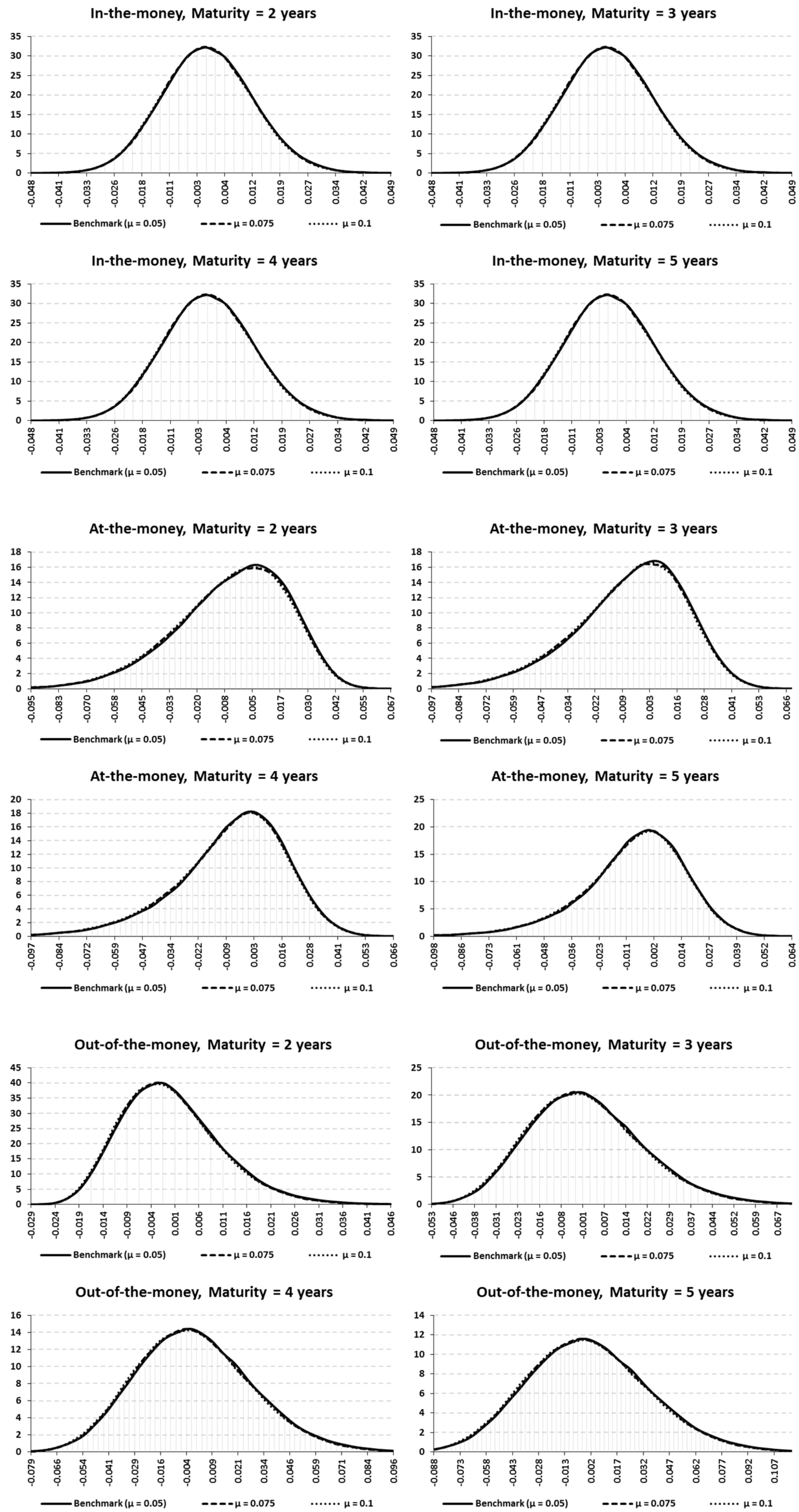

Figure 3.6: Effect of μ on the distribution of the 10-day CVA movements for Bermudan put options

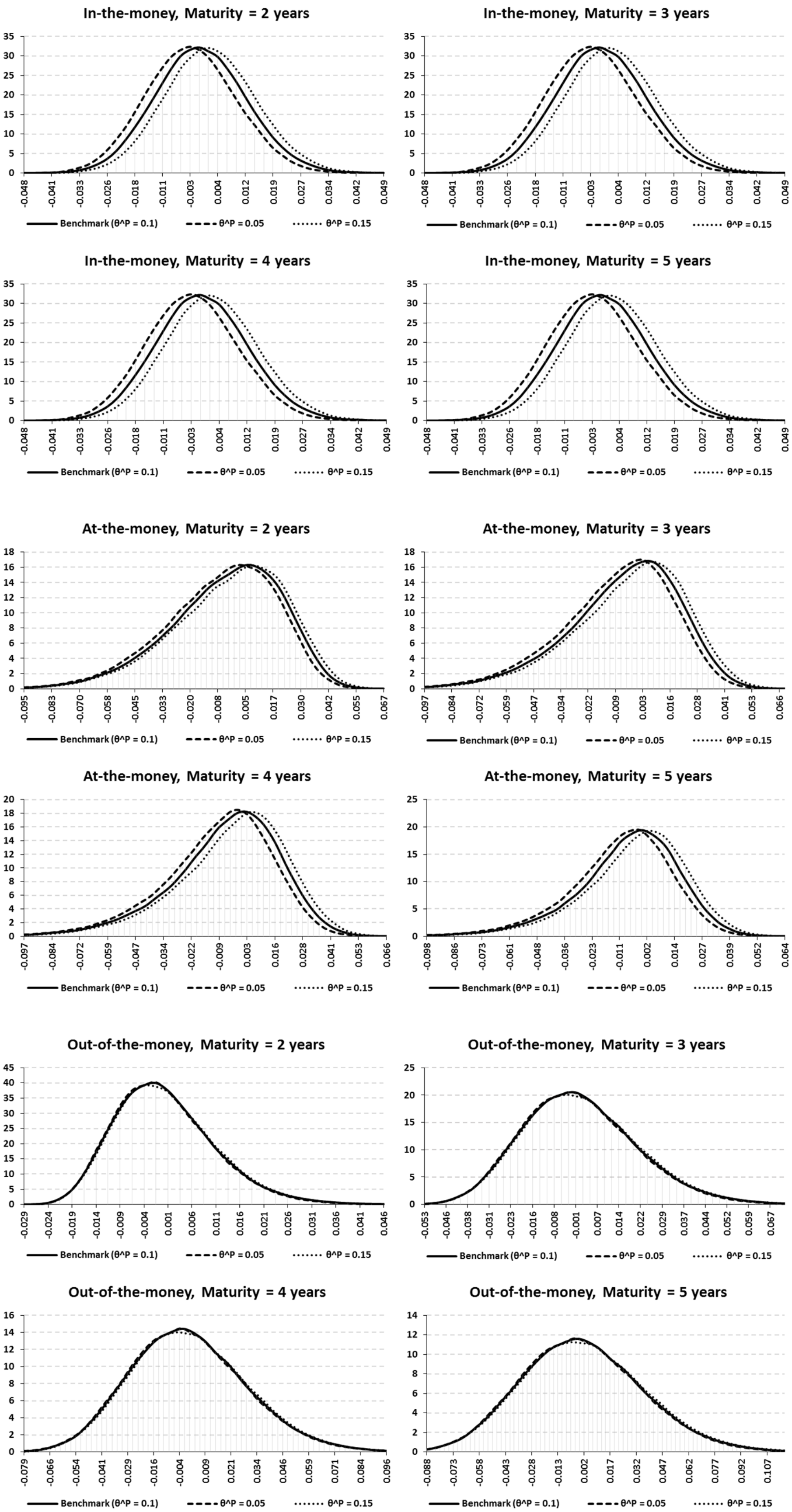

Figure 3.7: Effect of $\theta^{\mathbb{P}}$ on the distribution of the 10-day CVA movements for Bermudan put options

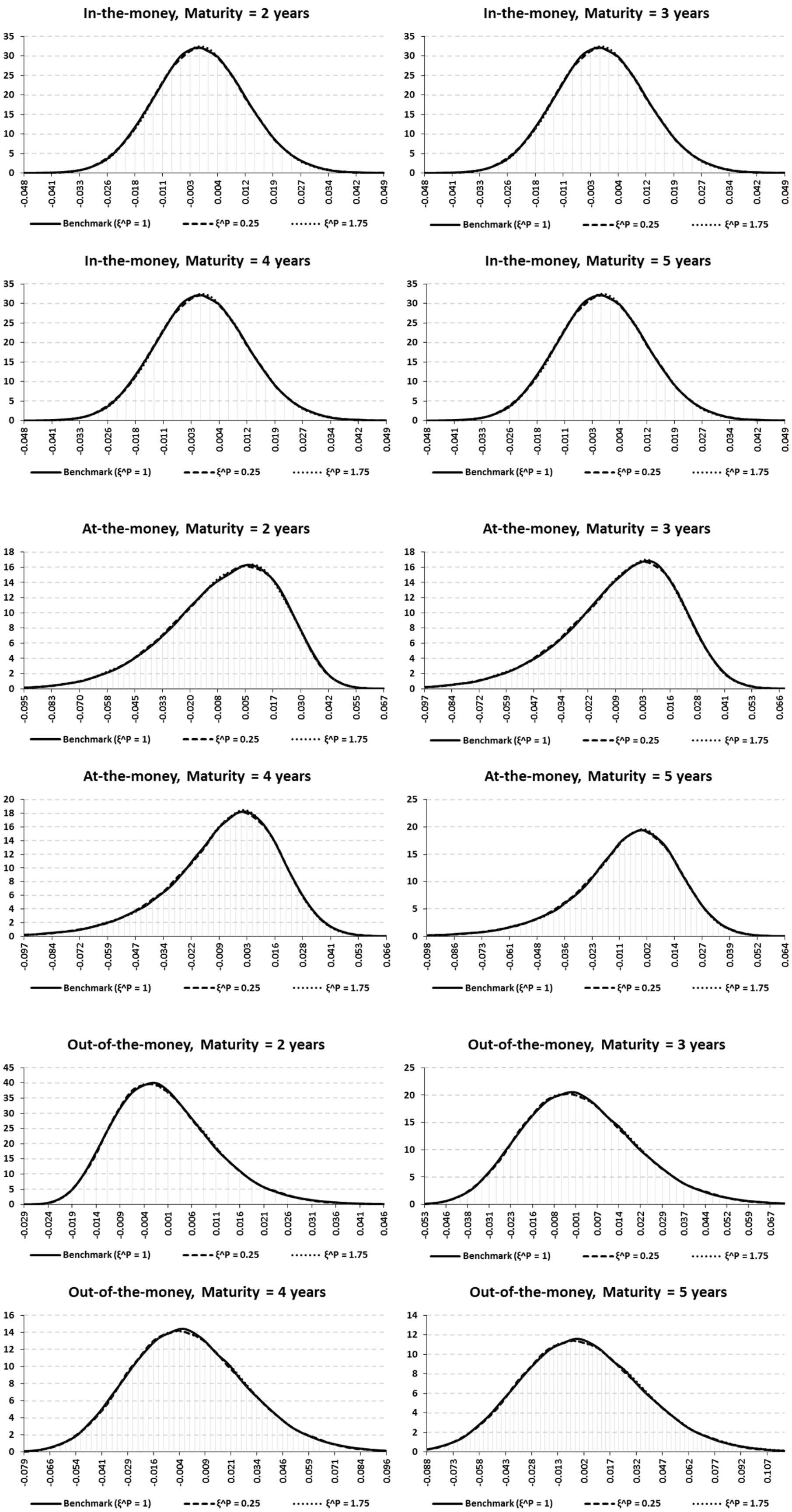

Figure 3.8: Effect of $\xi^{\mathbb{P}}$ on the distribution of the 10-day CVA movements for Bermudan put options

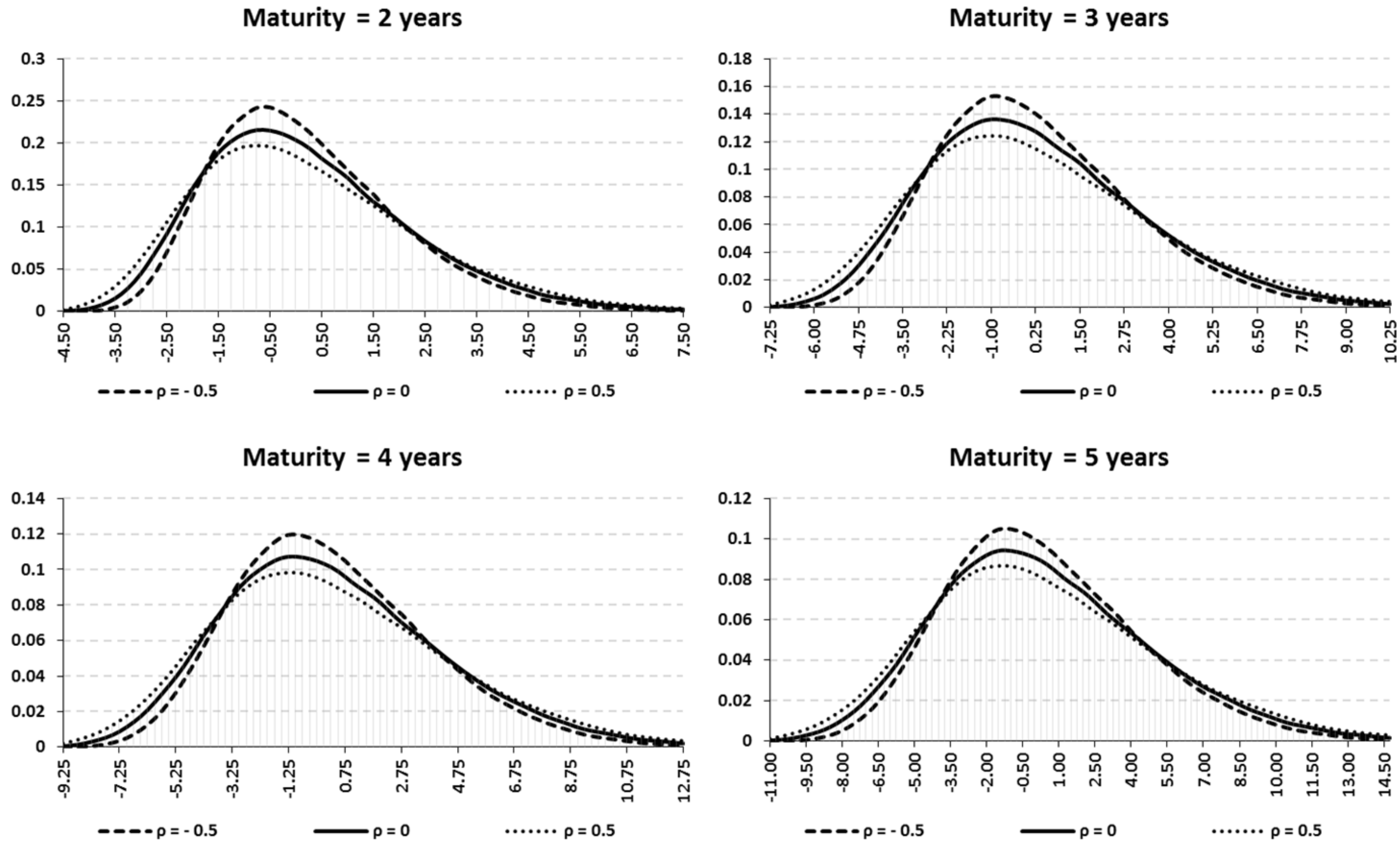

Figure 3.9: Effect of ρ on the distribution of the 10-day CVA movements for interest rate swaps

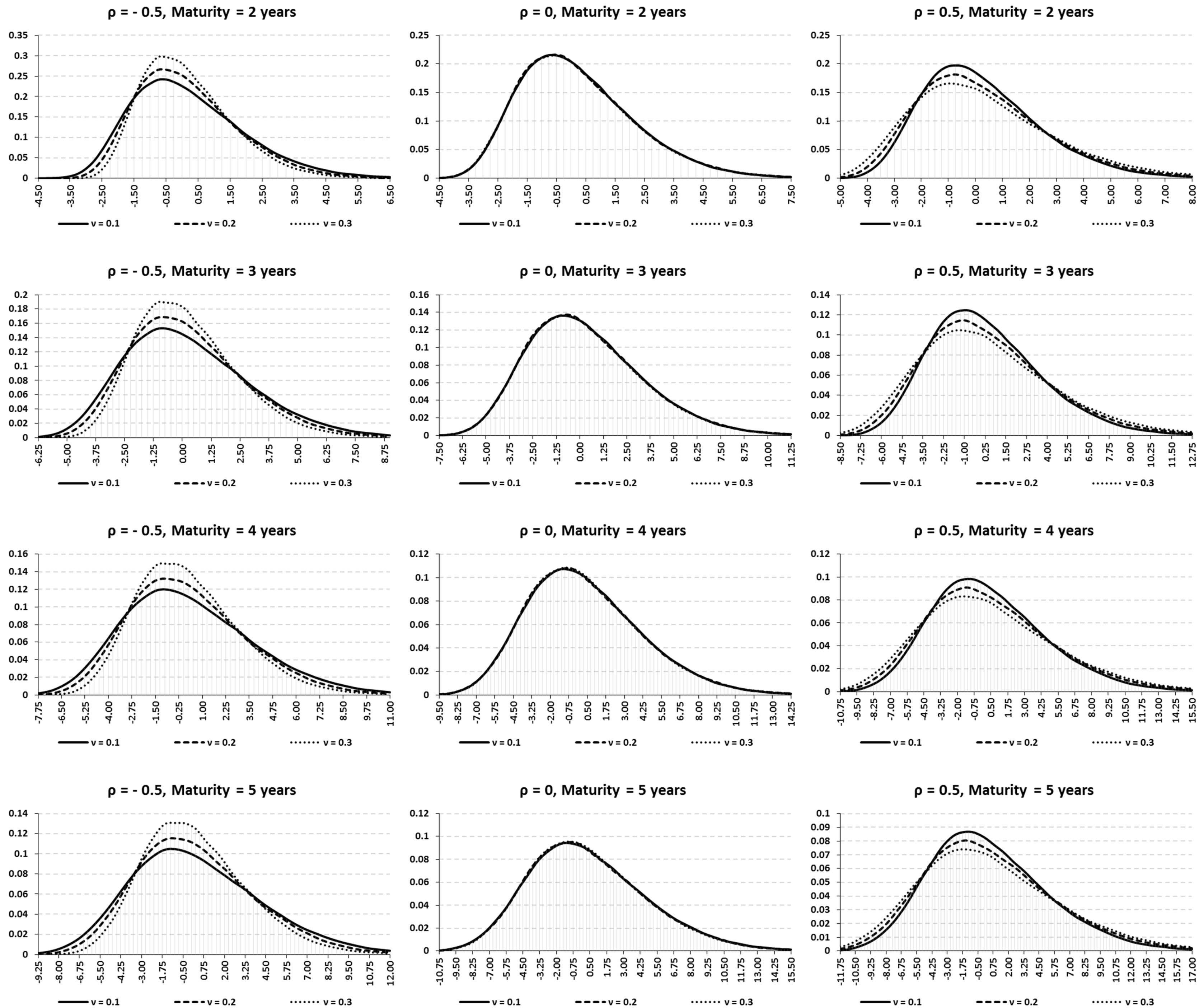

Figure 3.10: Effect of ν_λ on the distribution of the 10-day CVA movements for interest rate swaps

Chapter 4

An investigation of wrong-way risk in the interest-rate market

4.1 Introduction

Right-way/Wrong-way risk is defined as the decrease/increase in the quantification of counterparty risk caused by a correlation between default-free risk factors and the default probability. In the fixed-income market, the standard framework for the modeling of right-way/wrong-way risk has been generally relying on correlating the default probability with the level of interest rates (see, e.g., Brigo and Pallavacini (2007) and Brigo et al. (2009)). For instance, using such a framework to assess counterparty risk for interest-rate swaps would result in a wrong-way effect for payer positions and a right-way effect for receiver positions when the correlation between the level of interest rates and the default probability is positive. These effects are reversed under negative correlation, i.e., the effect is wrong-way for the receiver positions whilst it is right-way for the payer positions. Hence, a joint wrong-way behavior for interest-rate-swap positions that may be relevant during stress periods is precluded under such a standard correlation modeling. An interesting alternative is to correlate the default probability with the interest-rate volatility instead of the interest-rate level (Gregory (2012) and Harris et al. (2015)). Intuitively, a positive correlation between the interest-rate volatility and the default probability would result in a wrong-way effect whatever the swap position is.

Harris et al. (2015) studied the effect of a correlation between the interest-rate volatility and the default probability on the expected loss of collateralized interest-rate swaps. They considered an advanced interest-rate model with stochastic volatility (the model of Trolle and Schwartz (2009)) and they found that the correlation between the volatility factor and the default probability has a non-negligible wrong-way effect. However, in their study, Harris et al. (2015) have based their conclusions on the conditional expected loss, that is the average loss considering only defaulted scenarios, while the price of counterparty risk is defined as the unconditional expected loss taking into account all scenarios. From the numbers they reported, we can see that the correlation does not have a significant effect on the unconditional expected loss, resulting at maximum in a variation of only 1 basis point. Moreover, Harris et al. (2015) did not compare the contribution of the correlation between the interest-rate volatility and the default probability to the contribution of the correlation between the interest-rate level and the default probability, which is the standard choice in modeling right-way/wrong-way risk. Furthermore, Harris et al. (2015) did not analyze the expected loss of non-collateralized instruments, for which counterparty risk is the most relevant.
In this chapter, we investigate in details the role of the correlation between the interest-rate volatility and the default intensity. To this end, we consider an interest-rate model featuring stochastic volatility, which is similar to the model considered in Harris et al. (2015). We also consider a standard default-intensity model. We calibrate both models on December 5, 2008 and we analyze the effects of the correlations on the CVA of interest-rate instruments for eight counterparties which are the major American banks and financial companies. We finally perform a sensitivity analysis to validate our conclusions.
The rest of the chapter is organized as follows. Section 4.2 is dedicated to the description of the interest-rate and the default-intensity models. Section 4.3 reports the results of the calibration of the interest-rate and the default-intensity models. Section 4.4 presents the results of our empirical study examining the impact of correlation modeling on counterparty risk. Section 4.5 is devoted to the numerical results of the sensitivity analysis that we conduct. Section 4.6 is a conclusion.

4.2 Description of the models

In this section, we describe the interest-rate and the default-intensity models considered in this study. The first sub-section is dedicated to the interest-rate model, while the second one is dedicated to the default-intensity model.

4.2.1 The interest-rate model

We consider the model of Casassus et al. (2005) for the instantaneous spot interest rate, which can be seen as a stochastic-volatility extension of the well-known Hull-White (Hull and White (1990)) or the Vasicek (Vasicek (1977)) interest-rate models. This model is among the first frameworks that feature unspanned stochastic volatility (USV) behavior, i.e., it is designed in a way that the stochastic volatility factor does not affect bond prices but drives bond-option prices. In earlier versions of stochastic-volatility models of interest rates such as Fong and Vasicek (1991) and Longstaff and Schwartz (1992), bond prices are functions of both the interest-rate and the volatility variables, meaning that bonds can serve as building blocks of hedging strategies that span the universe of interest-rate derivatives. However, empirical evidence on USV was documented in a number of papers, for instance Collin-Dufresne and Goldstein (2002) show that there are volatility factors that influence interest-rate derivatives but do not affect the bond yield curve. We choose a model with this fundamental characteristic in order to analyze the effects of the correlation between the counterparty default and the interest-rate volatility on the CVA of both volatility-insensitive instruments (interest-rate swaps) and volatility-sensitive products (caps and floors). For interest-rate swaps, the volatility plays only a role of uncertainty on the future exposure, while for bond options, the exposure is directly affected by the volatility factor. This model is also a particular case of the more general Heath-Jarrow-Morton (HJM, Heath et al. (1992)) stochastic-volatility framework proposed in Trolle and Schwartz (2009).

The model in its short-rate form is written under the risk-neutral measure as

$$
\begin{aligned}
dr_t &= \xi_r(\theta_t - r_t)dt + \sqrt{V_t}dW_{1t}, \\
d\theta_t &= \left(\gamma(t) - 2\xi_r\theta_t + \frac{V_t}{\xi_r}\right) dt, \\
dV_t &= \xi_V(\theta_V - V_t)dt + \nu_V\sqrt{V_t}dW_{2t},
\end{aligned}
$$

where W_{1t} and W_{2t} are two independent Brownian motions and $\gamma(t)$ is a deterministic function of time. r_t is the spot interest-rate level, which is a mean-reverting process with the parameter ξ_r as the speed of adjustment and the stochastic process θ_t as the long-run interest-rate level. V_t is the volatility of the spot rate, which is a square-root process with the parameter ξ_V as the speed of adjustment, the parameter θ_V as the long-run volatility level and the parameter ν_V as the volatility of volatility. The specification of θ_t may seem a bit strange; however, it should be designed in this way, in order for the model to feature USV. Note that although there are two stochastic factors (the two Brownian processes), the model is Markovian in three state variables (r_t, θ_t, V_t). Collin-Dufresne and Goldstein (2002) show that in order to exhibit USV in an affine framework, at least three state variables are needed.

Through a fast application of Ito's lemma, zero-coupon bond prices are given by (see Proposition 1 in Casassus et al. (2005))

$$
P(t,T) = \exp(-B_r(T-t)r_t - B_\theta(T-t)\theta_t - A(t,T)),
$$

where

$$
\begin{aligned}
B_r(T-t) &= \frac{\left(1 - e^{-\xi_r(T-t)}\right)}{\xi_r}, \\
B_\theta(T-t) &= \frac{\left(1 - e^{-\xi_r(T-t)}\right)^2}{2\xi_r}, \\
A(t,T) &= \int_t^T \gamma(s)B_\theta(T-s)ds.
\end{aligned}
$$

We can see therefore that bond prices do not depend on the volatility factor V_t (the USV behavior). The deterministic function of time $\gamma(t)$ allows to perfectly calibrate the model-implied initial term structure to the one actually observed, which is therefore an input to the model. Given an observed initial curve of instantaneous forward rates $f(t)$, the deterministic function of time $\gamma(t)$ should be set to

$$\gamma(t) = \frac{1}{\xi_r} \frac{d^2 f(t)}{dt^2} + 3 \frac{df(t)}{dt} + 2\xi_r f(t), \tag{4.1}$$

so that the model-implied initial forward curve would exactly fit the market forward curve (see Proposition 2 in Casassus et al. (2005)).

The risk-neutral dynamics of bond prices are described by

$$\begin{aligned} dP(t,T) &= r_t P(t,T)dt - B_r(T-t)\sqrt{V_t}P(t,T)dW_{1t}, \\ dV_t &= \xi_V(\theta_V - V_t)dt + \nu_V \sqrt{V_t} dW_{2t}. \end{aligned}$$

In order to price interest-rate derivatives (i.e., caps and floors), we need to compute for $t < T_0 < T_1$ and a given strike K the quantities

$$\begin{aligned} Call(t,T_0,T_1,K) &= \mathbb{E}_t \left[\exp\left(-\int_t^{T_0} r_s ds \right) \left(P(T_0,T_1) - K \right) \mathbb{1}_{P(T_0,T_1)>K} \right], \\ Put(t,T_0,T_1,K) &= \mathbb{E}_t \left[\exp\left(-\int_t^{T_0} r_s ds \right) \left(K - P(T_0,T_1) \right) \mathbb{1}_{P(T_0,T_1)<K} \right], \end{aligned}$$

where $Call(t,T_0,T_1,K)$ (respectively $Put(t,T_0,T_1,K)$) is the price at date t of a call (respectively put) option written on the process $P(t,T_1)$, having strike K and maturing at T_0. To this end, the Fourier transform $\psi_{t,T_0,T_1}(u) = \mathbb{E}_t \left[\exp\left(-\int_t^{T_0} r_s ds \right) e^{uP(T_0,T_1)} \right]$ is introduced (u is a complex number). $\psi_{t,T_0,T_1}(u)$ has the following expression (see Proposition 7 in Casassus et al. (2005))

$$\psi_{t,T_0,T_1}(u) = \exp\left(M(T_0-t) + N(T_0-t)V_t + uP(t,T_1) + (1-u)P(t,T_0) \right),$$

where $M(T_0 - t)$ and $N(T_0 - t)$ are two deterministic functions that satisfy the system of ODEs $(\tau = T_0 - t)$

$$\begin{aligned}
\frac{dN(\tau)}{d\tau} &= \frac{\nu_V^2}{2} N(\tau)^2 - \xi_V N(\tau) \\
&+ \frac{1}{2}\left((uB_r(\tau + T_1 - T_0) + (1-u)B_r(\tau))^2 - uB_r(\tau + T_1 - T_0)^2 - (1-u)B_r(\tau)^2 \right), \\
\frac{dM(\tau)}{d\tau} &= \theta_V \xi_V N(\tau),
\end{aligned}$$

subject to the initial conditions $M(0) = N(0) = 0$. This system can be solved numerically using efficient standard techniques. Following the literature on the use of Fourier transform techniques to price options (Heston (1993) and Duffie et al. (2000)), the call and put prices are given by

$$\begin{aligned}
Call(t, T_0, T_1, K) &= \frac{\psi_{t,T_0,T_1}(1)}{2} + \frac{1}{\pi}\int_0^\infty \frac{Im\left(\psi_{t,T_0,T_1}(1+ix)e^{-ix\log(K)}\right)}{x} dx \qquad (4.2) \\
&\quad - K\left(\frac{\psi_{t,T_0,T_1}(0)}{2} + \frac{1}{\pi}\int_0^\infty \frac{Im\left(\psi_{t,T_0,T_1}(ix)e^{-ix\log(K)}\right)}{x} dx \right), \\
Put(t, T_0, T_1, K) &= K\left(\frac{\psi_{t,T_0,T_1}(0)}{2} - \frac{1}{\pi}\int_0^\infty \frac{Im\left(\psi_{t,T_0,T_1}(ix)e^{-ix\log(K)}\right)}{x} dx \right) \qquad (4.3) \\
&\quad - \left(\frac{\psi_{t,T_0,T_1}(1)}{2} - \frac{1}{\pi}\int_0^\infty \frac{Im\left(\psi_{t,T_0,T_1}(1+ix)e^{-ix\log(K)}\right)}{x} dx \right).
\end{aligned}$$

These formulas can be evaluated using direct numerical integration or efficient FFT techniques. The inputs for the model are $\gamma(t)$, ξ_r and the volatility process parameters V_0, ξ_V, θ_V and ν_V. For a given ξ_r, $\gamma(t)$ is calibrated using Equation (4.1) to fit the observed initial term structure, while ξ_r and the volatility process parameters are calibrated to the observed derivative prices (caps and floors) using Equations (4.2)-(4.3) .

4.2.2 The default-intensity model

To model the default intensity, we consider the following CIR representation (Cox et al. (1985)) under the risk-neutral measure:

$$d\lambda_t = \xi_\lambda(\theta_\lambda - \lambda_t)dt + \nu_\lambda\sqrt{\lambda_t}\left(\rho_{r\lambda}dW_{1t} + \rho_{V\lambda}dW_{2t} + \sqrt{1-\rho_{r\lambda}^2-\rho_{V\lambda}^2}dW_{3t}\right),$$

where W_{3t} is a third Brownian motion independent from W_{1t} and W_{2t}, and $\rho_{r\lambda}$ (respectively $\rho_{V\lambda}$) is the correlation between the Brownian components of λ_t and r_t (respectively λ_t and V_t). This model is the standard choice in modeling the default intensity, because it ensures the positivity of the process and has desirable mean-reverting properties. Moreover, this model is tractable and yields closed-form expressions for survival probabilities, which correspond to zero-coupon bond prices in the CIR model.

The information on the default intensity is embedded in the CDS quotes of the counterparty. In a CDS contract, the protection buyer pays fixed periodic fees (at discrete dates $0 < t_1 < t_2 < ... < t_m = T$) to the protection seller until the maturity of the contract or the default event. In return, if default happens, the contract seller agrees to pay back the buyer the amount of money lost due to the default of the reference entity. The standard price of a CDS with maturity T at date 0 is (as seen from the protection buyer point of view)

$$\text{CDS} = \mathbb{E}\left[\text{LGD}\mathbb{1}_{0<\tau\leq T}\Gamma_0(\tau) - \sum_{i=1}^{m}\Gamma_0(t_i)\alpha_i R\mathbb{1}_{\tau>t_i} - \Gamma_0(\tau)(\tau - t_{\delta(\tau)})R\mathbb{1}_{0<\tau<T}\right],$$

where R is the premium rate, LGD is the loss given default (computed as one minus the recovery rate), $\Gamma_t(u)$ is the discount factor for $u > t$, τ is the default time of the reference credit, $\alpha_i = t_i - t_{i-1}$, $\delta(\tau)$ is the index of the payment date that precedes the default event, and where the expectation is taken under the risk-neutral measure. The fair premium rate is chosen as to make the CDS value nil at the beginning of the contract. Under the default-intensity and the interest-rate models considered in this study, we can write the value of the CDS as follows

$$\begin{aligned}\text{CDS} \quad = \quad & \text{LGD}\int_0^T \mathbb{E}\left[\exp\left(-\int_0^s (r_u+\lambda_u)du\right)\lambda_s\right]ds - \sum_{i=1}^{m}\alpha_i R\mathbb{E}\left[\exp\left(-\int_0^{t_i}(r_u+\lambda_u)du\right)\right] \\ & -R\int_0^T \mathbb{E}\left[\exp\left(-\int_0^s (r_u+\lambda_u)du\right)\lambda_s\right](s - t_{\delta(s)})ds,\end{aligned}$$

which does not allow for a closed-form solution because of the correlation between the spot interest rate and the default intensity. However, it has been shown in the financial literature that this correlation has a minor effect on the CDS value (see, e.g., Brigo and Alfonsi (2005)), so that the independence between interest-rate and credit risks has become a common assumption in CDS pricing models. Under independence, the CDS value becomes

$$\begin{aligned}
\text{CDS} &= \text{LGD}\int_0^T \mathbb{E}\left[\exp\left(-\int_0^s r_u du\right)\right]\left(-\frac{d}{ds}\mathbb{E}\left[\exp\left(-\int_0^s \lambda_u du\right)\right]\right)ds \\
&\quad -\sum_{i=1}^m \alpha_i R\mathbb{E}\left[\exp\left(-\int_0^{t_i} r_u du\right)\right]\mathbb{E}\left[\exp\left(-\int_0^{t_i} \lambda_u du\right)\right] \\
&\quad -R\int_0^T \mathbb{E}\left[\exp\left(-\int_0^s r_u du\right)\right]\left(-\frac{d}{ds}\mathbb{E}\left[\exp\left(-\int_0^s \lambda_u du\right)\right]\right)(s-t_{\delta(s)})ds.
\end{aligned}$$

The term $\mathbb{E}\left[\exp\left(-\int_0^s r_u du\right)\right] = P(0,s)$ is the price of a zero-coupon bond that is obtained in closed form as we explained in Section 4.2.1, while $\mathbb{E}\left[\exp\left(-\int_0^s \lambda_u du\right)\right] = P^{\text{CIR}}(0,s)$ is the price of a zero-coupon bond in the CIR model of the default intensity which is also obtained in closed form. The CDS value can therefore be written analytically as

$$\begin{aligned}
\text{CDS} &= \text{LGD}\int_0^T P(0,s)\left(-\frac{dP^{\text{CIR}}(0,s)}{ds}\right)ds - \sum_{i=1}^m \alpha_i R P(0,t_i)P^{\text{CIR}}(0,t_i) \\
&\quad -R\int_0^T P(0,s)\left(-\frac{dP^{\text{CIR}}(0,s)}{ds}\right)(s-t_{\delta(s)})ds,
\end{aligned}$$

and the fair premium rate satisfies

$$R = \frac{\text{LGD}\int_0^T P(0,s)\left(-\frac{dP^{\text{CIR}}(0,s)}{ds}\right)ds}{\sum_{i=1}^m \alpha_i P(0,t_i)P^{\text{CIR}}(0,t_i) + \int_0^T P(0,s)\left(-\frac{dP^{\text{CIR}}(0,s)}{ds}\right)(s-t_{\delta(s)})ds}. \tag{4.4}$$

The inputs for the model are $\lambda_0, \theta_\lambda, \xi_\lambda, \nu_\lambda$, and the correlations $\rho_{r\lambda}$ and $\rho_{V\lambda}$. The parameters $(\lambda_0, \theta_\lambda, \xi_\lambda, \nu_\lambda)$ can be calibrated to the observed term structure of CDS premia using Equation

(4.4). Note that these parameters could also be calibrated to the prices of CDS options. However, as discussed in Brigo and Alfonsi (2005), this is not empirically consistent because CDS options are not liquid enough and exhibit a large bid-ask spread. We thus calibrate the parameters using the observed term structure of CDS spreads. As for the correlations $\rho_{r\lambda}$ and $\rho_{V\lambda}$, it is hard to find an instrument that is critically dependent on these two parameters. Therefore, they have to be either estimated historically from the joint evolution of interest rates and CDS spreads, or set on an expert judgement basis.

4.3 Calibration

We calibrate the interest-rate and the default-intensity models using the observed market conditions on December 5, 2008. We choose this date because it belongs to a period of significant systemic credit risk that immediately followed Lehman's bankruptcy. First, we calibrate the initial term structure of interest rates using the Nelson-Siegel-Svensson (NSS) scheme (Nelson and Siegel (1987), Svensson (1994)). Under the NSS scheme, the curve of instantaneous forward rates is assumed to have the following parametric form:

$$f(t) = \beta_0 + \beta_1 \exp\left(-\frac{t}{\tau_1}\right) + \beta_2 \frac{t}{\tau_1} \exp\left(-\frac{t}{\tau_1}\right) + \beta_3 \frac{t}{\tau_2} \exp\left(-\frac{t}{\tau_2}\right).$$

The parameters $(\beta_0, \beta_1, \beta_2, \beta_3, \tau_1, \tau_2)$ are estimated by minimizing the sum of squared errors between the NSS model implied rates and the actual observed rates. Included rates are Libor rates with maturities 3, 6 and 9 months and swap rates with maturities 1, 2, 3, 4, 5, 7, 10, 15, 20 and 30 years. The data on interest rates is obtained from Bloomberg. In Table 4.1, we report the estimated NSS parameters.

Once the initial term structure is calibrated, we calibrate the remaining interest-rate model parameters $(V_0, \xi_r, \xi_V, \theta_V, \nu_V)$ by minimizing the sum of squared errors between the model-implied cap prices and the actual observed cap prices. Included cap prices have maturities of 1, 2, 3, 5, 7 and 10

β_0	0.0254
β_1	-0.0023
β_2	-0.0453
β_3	0.0483
τ_1	1.6366
τ_2	3.1673

Table 4.1: Estimated NSS parameters on December 5, 2008

years and strike rates of 0.01, 0.02, 0.03, 0.04, 0.05 and 0.06. Actual cap prices are computed from Bloomberg's Black log-normal implied-volatility matrix (Black (1976)). The calibrated parameters of the interest-rate model are reported in Table 4.2.

V_0	0.0006
ξ_r	0.0828
ξ_V	0.1152
θ_V	0.0008
ν_V	0.0080

Table 4.2: Calibrated parameters of the interest-rate model on December 5, 2008

In our analysis, we consider eight counterparties, which are the major American banks and financial companies. The considered counterparties and their tickers are reported in Table 4.3. We calibrate the default-intensity parameters $(\lambda_0, \theta_\lambda, \xi_\lambda, \nu_\lambda)$ by minimizing the sum of squared errors between the model implied CDS spreads and actual observed CDS spreads. We consider CDS spreads with maturities 1, 2, 3, 4, 5, 7 and 10 years. Data on CDS spreads is obtained from Bloomberg. In Table 4.4, we report the calibrated parameters for the different counterparties.

At this level, we are left only with the parameters $\rho_{r\lambda}$ and $\rho_{V\lambda}$. As we said before, these parameters need to be estimated statistically based on historical data. We use the values estimated by Harris et al. (2015) based on the joint historical evolution of interest rates and default intensities during the financial crisis. The values of $\rho_{r\lambda}$ and $\rho_{V\lambda}$ for the different counterparties are reported in Table 4.5. Note that $\rho_{r\lambda}$ is negative and $\rho_{V\lambda}$ is positive for all counterparties. This is in line with

Counterparty	Ticker
Bank of America	BAC
Citi Group Inc	C
Goldman Sachs Group Inc	GS
JP Morgan Chase & Co	JPM
American Express	AXP
American International Group Inc	AIG
Morgan Stanley	MS
Merrill Lynch	MER

Table 4.3: Considered counterparties and their tickers

Counterparty	λ_0	θ_λ	ξ_λ	ν_λ
BAC	0.0070	0.0341	1.4851	0.1249
C	0.0535	0.0337	0.2596	0.1973
GS	0.0696	0.0330	0.2495	0.1023
JPM	0.0152	0.0269	1.6085	0.1799
AXP	0.0876	0.0133	0.1517	0.1071
AIG	0.1213	0.0933	0.0506	0.1780
MS	0.1712	0.0464	1.4014	0.1023
MER	0.0839	0.0316	1.5976	0.1989

Table 4.4: Calibrated parameters of the default-intensity model for the different counterparties on December 5, 2008

the conditions observed during the financial crisis, where the increase in counterparty risk was accompanied by an increase in interest-rate volatility and a decrease in interest-rate level due to uncertainty and monetary policy.

Counterparty	$\rho_{r\lambda}$	$\rho_{V\lambda}$
BAC	-0.4619	0.3859
C	-0.5485	0.3247
GS	-0.6758	0.6491
JPM	-0.4044	0.5576
AXP	-0.4284	0.5769
AIG	-0.5352	0.6271
MS	-0.2751	0.3149
MER	-0.4851	0.6677

Table 4.5: Values of correlations for the different counterparties

4.4 Impact of correlations on counterparty risk

In this section, we investigate the impact of $\rho_{r\lambda}$ and $\rho_{V\lambda}$ on the value of counterparty risk. In all results, we consider four correlation schemes: In the first one, we set $\rho_{V\lambda} = 0$ and $\rho_{r\lambda} = 0$; in the second, we consider only $\rho_{V\lambda}$ and we set $\rho_{r\lambda} = 0$; in the third, we consider only $\rho_{r\lambda}$ and we set $\rho_{V\lambda} = 0$; and finally in the fourth scheme we consider both correlations. The recovery factor is assumed to be nil.

In the first sub-section, we analyze the CVA of non-collateralized interest-rate swaps, where the CVA is driven by an exposure that fully corresponds to the defaut-free value of the swap. In this case, due to the USV nature of the interest-rate model, the volatility plays only a role of uncertainty on the future exposure. The same exercise is performed for non-collateralized caps and floors in the second sub-section. However, interest-rate options are contingent on the volatility state, and this may make the effect of $\rho_{V\lambda}$ more relevant. Finally, in the third sub-section, we analyze the CVA of collateralized interest-rate swaps, where potential losses can result from the so-called gap risk. In more details, even if the swap is fully collateralized, we assume a replacement period upon default of two weeks during which the swap value may significantly move; and in such a case, the interest-rate volatility may play an important role.

For the valuation of the CVA, we use a standard simulation approach to compute the CVA (as described in the first chapter). The simulation results are based on 100000 scenarios and 260 discretization steps for the underlying processes. Moreover, we use the same sample of random shocks for all situations in order to ensure that comparative results are not affected by sampling errors.

4.4.1 Impact of correlations on the CVA of non-collateralized interest-rate swaps

In this sub-section, we compare the CVA of non-collateralized interest-rate swaps implied by the different correlation schemes. We consider both payer and receiver positions.

In Tables 4.6-4.10, we report results for maturities ranging from 1 to 5 years. In each table, we include the computed CVA for each correlation scheme and the CVA variation in % with comparison to the no-correlation scheme.

		$\rho_{V\lambda} = 0,\ \rho_{r\lambda} = 0$	$\rho_{V\lambda} \neq 0,\ \rho_{r\lambda} = 0$		$\rho_{V\lambda} = 0,\ \rho_{r\lambda} \neq 0$		$\rho_{V\lambda} \neq 0,\ \rho_{r\lambda} \neq 0$	
		CVA	CVA	Variation	CVA	Variation	CVA	Variation
BAC	Payer	0.54	0.56	+2.81%	0.44	−19.00%	0.45	−16.72%
BAC	Receiver	0.60	0.60	+0.17%	0.69	+15.78%	0.70	+16.28%
C	Payer	1.26	1.30	+3.12%	0.28	−77.84%	0.30	−76.52%
C	Receiver	1.39	1.42	+2.68%	3.25	+134.84%	3.37	+143.52%
GS	Payer	1.72	1.72	−0.10%	1.37	−20.30%	1.39	−19.42%
GS	Receiver	1.88	1.89	+0.73%	2.28	+21.32%	2.30	+22.30%
JPM	Payer	0.59	0.60	+2.37%	0.44	−25.71%	0.45	−22.73%
JPM	Receiver	0.61	0.60	−2.15%	0.76	+23.60%	0.75	+21.87%
AXP	Payer	1.94	2.06	+6.49%	0.74	−61.97%	0.77	−60.13%
AXP	Receiver	2.17	2.23	+2.78%	4.11	+89.65%	4.26	+96.38%
AIG	Payer	2.78	2.92	+4.80%	0.88	−68.43%	0.91	−67.38%
AIG	Receiver	3.10	3.20	+3.20%	6.21	+100.06%	6.47	+108.35%
MS	Payer	3.03	3.02	−0.11%	2.90	−4.35%	2.90	−4.35%
MS	Receiver	3.21	3.23	+0.53%	3.36	+4.59%	3.38	+5.27%
MER	Payer	1.49	1.50	+0.85%	1.17	−21.26%	1.18	−20.42%
MER	Receiver	1.65	1.69	+2.43%	2.05	+24.24%	2.10	+27.13%

Table 4.6: CVA of 1-year swaps for different correlation schemes. The CVA is reported in basis points and variations are computed compared to the no-correlation case.

		$\rho_{V\lambda} = 0,\ \rho_{r\lambda} = 0$	$\rho_{V\lambda} \neq 0,\ \rho_{r\lambda} = 0$		$\rho_{V\lambda} = 0,\ \rho_{r\lambda} \neq 0$		$\rho_{V\lambda} \neq 0,\ \rho_{r\lambda} \neq 0$	
		CVA	CVA	Variation	CVA	Variation	CVA	Variation
BAC	Payer	3.71	3.72	+0.30%	3.09	−16.71%	3.08	−16.90%
BAC	Receiver	3.44	3.45	+0.20%	4.13	+19.97%	4.16	+20.79%
C	Payer	5.58	5.71	+2.36%	1.08	−80.62%	1.28	−77.00%
C	Receiver	5.32	5.57	+4.62%	13.18	+147.46%	13.66	+156.54%
GS	Payer	9.00	9.11	+1.31%	6.76	−24.91%	6.82	−24.16%
GS	Receiver	8.52	8.66	+1.64%	10.93	+28.21%	11.04	+29.51%
JPM	Payer	3.45	3.45	+0.07%	2.74	−20.56%	2.67	−22.56%
JPM	Receiver	3.19	3.27	+2.36%	4.07	+27.44%	4.14	+29.55%
AXP	Payer	8.15	8.62	+5.84%	2.93	−64.08%	3.18	−60.98%
AXP	Receiver	7.92	8.41	+6.18%	15.79	+99.38%	16.95	+114.14%
AIG	Payer	11.77	12.64	+7.33%	3.38	−71.28%	3.63	−69.15%
AIG	Receiver	11.35	11.99	+5.61%	24.86	+118.92%	26.11	+129.92%
MS	Payer	12.45	12.50	+0.39%	11.71	−5.98%	11.76	−5.55%
MS	Receiver	11.93	11.99	+0.54%	12.69	+6.37%	12.73	+6.74%
MER	Payer	6.94	7.02	+1.06%	5.25	−24.41%	5.34	−23.14%
MER	Receiver	6.62	6.71	+1.36%	8.36	+26.27%	8.53	+28.78%

Table 4.7: CVA of 2-year swaps for different correlation schemes. The CVA is reported in basis points and variations are computed compared to the no-correlation case.

		$\rho_{V\lambda} = 0,\ \rho_{r\lambda} = 0$	$\rho_{V\lambda} \neq 0,\ \rho_{r\lambda} = 0$		$\rho_{V\lambda} = 0,\ \rho_{r\lambda} \neq 0$		$\rho_{V\lambda} \neq 0,\ \rho_{r\lambda} \neq 0$	
		CVA	CVA	Variation	CVA	Variation	CVA	Variation
BAC	Payer	10.97	10.92	−0.43%	9.34	−14.88%	9.29	−15.31%
BAC	Receiver	9.01	9.14	+1.38%	10.93	+21.24%	10.99	+21.98%
C	Payer	11.93	12.61	+5.68%	2.73	−77.16%	2.99	−74.93%
C	Receiver	10.11	10.84	+7.26%	26.33	+160.46%	27.57	+172.71%
GS	Payer	22.34	22.61	+1.19%	16.23	−27.37%	16.42	−26.50%
GS	Receiver	19.01	19.31	+1.54%	25.72	+35.26%	26.10	+37.27%
JPM	Payer	9.41	9.50	+0.97%	7.53	−19.97%	7.58	−19.43%
JPM	Receiver	8.02	8.01	−0.14%	10.19	+27.03%	10.31	+28.61%
AXP	Payer	16.68	17.89	+7.23%	5.96	−64.28%	6.37	−61.82%
AXP	Receiver	14.68	15.76	+7.33%	29.81	+103.10%	32.38	+120.56%
AIG	Payer	24.46	26.05	+6.48%	6.92	−71.72%	7.52	−69.26%
AIG	Receiver	20.98	23.25	+10.79%	47.83	+127.95%	50.35	+139.97%
MS	Payer	27.68	27.69	+0.05%	26.09	−5.74%	26.08	−5.76%
MS	Receiver	24.28	24.36	+0.33%	25.90	+6.68%	25.98	+7.02%
MER	Payer	16.24	16.51	+1.64%	12.48	−23.14%	12.45	−23.36%
MER	Receiver	13.94	14.07	+0.94%	18.04	+29.41%	18.45	+32.33%

Table 4.8: CVA of 3-year swaps for different correlation schemes. The CVA is reported in basis points and variations are computed compared to the no-correlation case.

		$\rho_{V\lambda} = 0,\ \rho_{r\lambda} = 0$	$\rho_{V\lambda} \neq 0,\ \rho_{r\lambda} = 0$		$\rho_{V\lambda} = 0,\ \rho_{r\lambda} \neq 0$		$\rho_{V\lambda} \neq 0,\ \rho_{r\lambda} \neq 0$	
		CVA	CVA	Variation	CVA	Variation	CVA	Variation
BAC	Payer	22.74	22.88	+0.62%	19.18	−15.65%	19.22	−15.48%
BAC	Receiver	17.37	17.60	+1.32%	20.82	+19.90%	21.07	+21.36%
C	Payer	20.19	21.30	+5.48%	5.17	−74.38%	5.27	−73.90%
C	Receiver	15.96	16.89	+5.81%	40.82	+155.80%	43.47	+172.35%
GS	Payer	41.31	42.10	+1.90%	29.21	−29.30%	29.92	−27.59%
GS	Receiver	32.31	33.18	+2.70%	45.30	+40.21%	46.48	+43.86%
JPM	Payer	19.28	19.25	−0.18%	15.52	−19.53%	15.48	−19.73%
JPM	Receiver	14.90	15.25	+2.38%	18.66	+25.24%	19.26	+29.26%
AXP	Payer	25.70	27.73	+7.91%	9.42	−63.33%	10.34	−59.76%
AXP	Receiver	21.34	23.54	+10.31%	43.96	+105.97%	48.07	+125.25%
AIG	Payer	38.10	40.68	+6.78%	10.95	−71.26%	12.19	−68.00%
AIG	Receiver	30.77	33.73	+9.63%	70.59	+129.41%	74.17	+141.07%
MS	Payer	47.98	48.11	+0.26%	44.98	−6.26%	45.25	−5.70%
MS	Receiver	39.13	39.24	+0.29%	41.79	+6.80%	41.90	+7.07%
MER	Payer	29.37	29.68	+1.04%	22.69	−22.74%	23.04	−21.56%
MER	Receiver	23.42	23.80	+1.65%	30.61	+30.72%	31.03	+32.53%

Table 4.9: CVA of 4-year swaps for different correlation schemes. The CVA is reported in basis points and variations are computed compared to the no-correlation case.

		$\rho_{V\lambda} = 0,\ \rho_{r\lambda} = 0$	$\rho_{V\lambda} \neq 0,\ \rho_{r\lambda} = 0$		$\rho_{V\lambda} = 0,\ \rho_{r\lambda} \neq 0$		$\rho_{V\lambda} \neq 0,\ \rho_{r\lambda} \neq 0$	
		CVA	CVA	Variation	CVA	Variation	CVA	Variation
BAC	Payer	39.36	39.34	−0.05%	33.82	−14.07%	33.90	−13.88%
BAC	Receiver	28.55	28.69	+0.49%	33.74	+18.18%	33.74	+18.18%
C	Payer	29.83	30.72	+2.99%	8.19	−72.55%	8.40	−71.85%
C	Receiver	22.59	23.66	+4.74%	57.42	+154.19%	60.03	+165.77%
GS	Payer	64.85	66.23	+2.14%	44.40	−31.53%	45.94	−29.15%
GS	Receiver	49.20	50.44	+2.51%	70.26	+42.80%	72.46	+47.27%
JPM	Payer	32.48	32.64	+0.50%	26.63	−17.99%	26.54	−18.27%
JPM	Receiver	23.85	24.34	+2.06%	30.17	+26.50%	30.25	+26.84%
AXP	Payer	34.97	37.63	+7.61%	12.87	−63.20%	14.34	−59.00%
AXP	Receiver	28.13	31.20	+10.88%	58.23	+106.97%	62.46	+122.00%
AIG	Payer	51.56	54.63	+5.96%	15.13	−70.65%	17.06	−66.91%
AIG	Receiver	40.23	45.27	+12.55%	93.09	+131.41%	98.96	+146.02%
MS	Payer	72.90	73.12	+0.30%	68.62	−5.88%	69.06	−5.26%
MS	Receiver	56.65	57.08	+0.75%	60.70	+7.14%	61.14	+7.91%
MER	Payer	46.14	46.50	+0.78%	36.04	−21.88%	36.59	−20.71%
MER	Receiver	34.67	35.34	+1.91%	45.42	+31.00%	46.52	+34.17%

Table 4.10: CVA of 5-year swaps for different correlation schemes. The CVA is reported in basis points and variations are computed compared to the no-correlation case.

It is clear from Tables 4.6-4.10 that $\rho_{r\lambda}$ has a right-way effect (a decrease in the CVA) on the payer position and a wrong-way effect (an increase in the CVA) on the receiver position. This is expected since $\rho_{r\lambda}$ is negative. This effect is relatively signifcant, yielding a large variation in the CVA for most of the cases. The relative variation exceeds 100% in some situations.

On the other hand, except for a few cases, $\rho_{V\lambda}$ has a wrong-way effect on both the payer and the receiver positions. This is intuitive since a positive correlation between the uncertainty on the interest-rate movements and the default probability would increase the CVA in both directions. However, the magnitude of this wrong-way effect is minor compared to the effect of $\rho_{r\lambda}$. The maximum observed variation of the CVA is only about 10%. When we consider both correlations, it is always the effect of $\rho_{r\lambda}$ that predominates the change in the CVA.

These results contrast with the findings of Harris et al. (2015), who argue that $\rho_{V\lambda}$ has a non-negligible wrong-way effect on the CVA of interest-rate swaps. Moreover, Gregory (2012) suggests to consider right-way/wrong-way risk by correlating the default intensity with the interest-rate volatility. In the scope of our results, such suggestion may not be of great practical importance for interest-rate swaps. First, the increase in the CVA induced by $\rho_{V\lambda}$ is relatively small to be taken into consideration. Second, the contribution of $\rho_{V\lambda}$ is dominated by that of $\rho_{r\lambda}$.

The non-critical role of $\rho_{V\lambda}$ can be explained by the fact that in a USV framework, swap exposures are not affected by the volatility variable. The latter plays only a role of uncertainty on the future exposure. In the next section, we examine the effect of $\rho_{V\lambda}$ on the CVA of interest-rate derivatives whose exposures depend on the volatility factor, that is, caps and floors.

4.4.2 Impact of correlations on the CVA of non-collateralized interest-rate caps and floors

In this sub-section, we examine the effects of $\rho_{V\lambda}$ and $\rho_{r\lambda}$ on the CVA of non-collateralized interest-rate caps and floors. CVA results are reported in Tables 4.11-4.15.

		$\rho_{V\lambda} = 0,\ \rho_{r\lambda} = 0$	$\rho_{V\lambda} \neq 0,\ \rho_{r\lambda} = 0$		$\rho_{V\lambda} = 0,\ \rho_{r\lambda} \neq 0$		$\rho_{V\lambda} \neq 0,\ \rho_{r\lambda} \neq 0$	
		CVA	CVA	Variation	CVA	Variation	CVA	Variation
BAC	Cap	0.69	0.69	+0.65%	0.59	−14.35%	0.59	−13.77%
BAC	Floor	0.73	0.73	+0.56%	0.85	+15.71%	0.85	+16.35%
C	Cap	1.79	1.86	+3.68%	0.72	−60.05%	0.75	−58.29%
C	Floor	1.85	1.89	+2.65%	3.69	+99.72%	3.78	+104.97%
GS	Cap	2.44	2.46	+0.80%	2.10	−14.18%	2.11	−13.46%
GS	Floor	2.57	2.59	+0.76%	2.96	+15.33%	2.98	+16.13%
JPM	Cap	0.76	0.77	+1.36%	0.63	−17.42%	0.64	−16.25%
JPM	Floor	0.81	0.82	+1.22%	0.97	+19.55%	0.98	+20.94%
AXP	Cap	2.82	2.96	+4.78%	1.52	−46.20%	1.61	−43.02%
AXP	Floor	2.92	3.05	+4.41%	4.84	+65.60%	5.03	+72.26%
AIG	Cap	4.01	4.20	+4.74%	1.95	−51.22%	2.07	−48.43%
AIG	Floor	4.16	4.35	+4.56%	7.27	+74.73%	7.55	+81.37%
MS	Cap	4.39	4.40	+0.21%	4.25	−3.26%	4.25	−3.05%
MS	Floor	4.59	4.60	+0.20%	4.74	+3.39%	4.75	+3.59%
MER	Cap	2.26	2.29	+1.16%	1.93	−14.64%	1.95	−13.61%
MER	Floor	2.37	2.39	+1.10%	2.75	+16.18%	2.78	+17.38%

Table 4.11: CVA of 1-year caps and floors for different correlation schemes. The CVA is reported in basis points and variations are computed compared to the no-correlation case.

		$\rho_{V\lambda} = 0,\ \rho_{r\lambda} = 0$	$\rho_{V\lambda} \neq 0,\ \rho_{r\lambda} = 0$		$\rho_{V\lambda} = 0,\ \rho_{r\lambda} \neq 0$		$\rho_{V\lambda} \neq 0,\ \rho_{r\lambda} \neq 0$	
		CVA	CVA	Variation	CVA	Variation	CVA	Variation
BAC	Cap	4.90	4.94	+0.87%	4.25	−13.27%	4.29	−12.49%
BAC	Floor	4.62	4.66	+0.86%	5.33	+15.34%	5.38	+16.30%
C	Cap	8.38	8.81	+5.08%	3.51	−58.10%	3.75	−55.26%
C	Floor	7.98	8.40	+5.30%	15.89	+99.13%	16.43	+105.82%
GS	Cap	13.04	13.23	+1.51%	10.79	−17.21%	10.97	−15.86%
GS	Floor	12.54	12.73	+1.53%	14.99	+19.56%	15.20	+21.22%
JPM	Cap	4.75	4.83	+1.87%	3.96	−16.55%	4.04	−14.92%
JPM	Floor	4.51	4.60	+1.85%	5.40	+19.53%	5.49	+21.67%
AXP	Cap	12.67	13.60	+7.38%	6.97	−45.00%	7.62	−39.87%
AXP	Floor	12.12	13.04	+7.57%	20.16	+66.35%	21.45	+76.95%
AIG	Cap	18.31	19.54	+6.72%	9.19	−49.83%	10.01	−45.34%
AIG	Floor	17.61	18.84	+6.96%	30.88	+75.34%	32.74	+85.84%
MS	Cap	19.92	19.98	+0.35%	19.21	−3.56%	19.27	−3.22%
MS	Floor	19.41	19.48	+0.35%	20.15	+3.82%	20.22	+4.18%
MER	Cap	10.74	10.93	+1.82%	9.09	−15.34%	9.26	−13.73%
MER	Floor	10.42	10.61	+1.84%	12.27	+17.74%	12.48	+19.79%

Table 4.12: CVA of 2-year caps and floors for different correlation schemes. The CVA is reported in basis points and variations are computed compared to the no-correlation case.

		$\rho_{V\lambda}=0,\ \rho_{r\lambda}=0$	$\rho_{V\lambda}\neq 0,\ \rho_{r\lambda}=0$		$\rho_{V\lambda}=0,\ \rho_{r\lambda}\neq 0$		$\rho_{V\lambda}\neq 0,\ \rho_{r\lambda}\neq 0$	
		CVA	CVA	Variation	CVA	Variation	CVA	Variation
BAC	Cap	14.80	14.93	+0.92%	13.05	−11.80%	13.18	−10.97%
BAC	Floor	12.74	12.87	+1.01%	14.59	+14.50%	14.73	+15.63%
C	Cap	18.76	20.00	+6.61%	8.61	−54.10%	9.26	−50.63%
C	Floor	17.03	18.04	+5.93%	33.02	+93.91%	34.53	+102.74%
GS	Cap	33.54	34.20	+1.97%	27.37	−18.40%	27.96	−16.65%
GS	Floor	30.00	30.66	+2.18%	36.67	+22.21%	37.39	+24.62%
JPM	Cap	13.48	13.75	+1.98%	11.48	−14.86%	11.71	−13.12%
JPM	Floor	11.77	12.02	+2.18%	13.96	+18.61%	14.25	+21.12%
AXP	Cap	27.02	29.30	+8.46%	15.72	−41.83%	17.41	−35.57%
AXP	Floor	24.81	27.16	+9.45%	40.50	+63.21%	43.80	+76.54%
AIG	Cap	39.77	42.85	+7.74%	21.42	−46.14%	23.70	−40.41%
AIG	Floor	36.51	39.75	+8.87%	62.98	+72.51%	67.22	+84.13%
MS	Cap	46.39	46.58	+0.40%	44.79	−3.45%	44.98	−3.05%
MS	Floor	42.70	42.89	+0.44%	44.36	+3.88%	44.55	+4.33%
MER	Cap	26.03	26.56	+2.05%	22.26	−14.47%	22.74	−12.65%
MER	Floor	23.69	24.22	+2.24%	27.87	+17.68%	28.47	+20.21%

Table 4.13: CVA of 3-year caps and floors for different correlation schemes. The CVA is reported in basis points and variations are computed compared to the no-correlation case.

		$\rho_{V\lambda}=0,\ \rho_{r\lambda}=0$	$\rho_{V\lambda}\neq 0,\ \rho_{r\lambda}=0$		$\rho_{V\lambda}=0,\ \rho_{r\lambda}\neq 0$		$\rho_{V\lambda}\neq 0,\ \rho_{r\lambda}\neq 0$	
		CVA	CVA	Variation	CVA	Variation	CVA	Variation
BAC	Cap	31.34	31.63	+0.93%	28.03	−10.56%	28.30	−9.71%
BAC	Floor	25.56	25.84	+1.09%	29.05	+13.66%	29.37	+14.88%
C	Cap	32.01	34.07	+6.46%	15.71	−50.92%	16.91	−47.17%
C	Floor	28.52	29.96	+5.05%	53.63	+88.06%	56.36	+97.63%
GS	Cap	63.88	65.38	+2.34%	51.86	−18.82%	53.19	−16.74%
GS	Floor	54.64	56.12	+2.71%	67.80	+24.09%	69.44	+27.10%
JPM	Cap	27.61	28.17	+2.02%	23.91	−13.39%	24.41	−11.59%
JPM	Floor	22.87	23.40	+2.34%	26.90	+17.61%	27.51	+20.30%
AXP	Cap	43.34	47.48	+9.57%	26.43	−39.02%	29.50	−31.92%
AXP	Floor	39.34	43.41	+10.34%	62.88	+59.82%	68.86	+75.01%
AIG	Cap	65.01	70.44	+8.35%	37.36	−42.53%	41.37	−36.37%
AIG	Floor	58.63	64.26	+9.60%	98.97	+68.81%	106.63	+81.88%
MS	Cap	83.24	83.60	+0.43%	80.55	−3.23%	80.91	−2.81%
MS	Floor	73.73	74.08	+0.48%	76.55	+3.83%	76.92	+4.33%
MER	Cap	48.25	49.29	+2.16%	41.79	−13.39%	42.72	−11.46%
MER	Floor	42.04	43.07	+2.45%	49.28	+17.21%	50.44	+19.99%

Table 4.14: CVA of 4-year caps and floors for different correlation schemes. The CVA is reported in basis points and variations are computed compared to the no-correlation case.

		$\rho_{V\lambda} = 0,\ \rho_{r\lambda} = 0$	$\rho_{V\lambda} \neq 0,\ \rho_{r\lambda} = 0$		$\rho_{V\lambda} = 0,\ \rho_{r\lambda} \neq 0$		$\rho_{V\lambda} \neq 0,\ \rho_{r\lambda} \neq 0$	
		CVA	CVA	Variation	CVA	Variation	CVA	Variation
BAC	Cap	54.21	54.71	$+0.93\%$	49.01	-9.58%	49.48	-8.72%
BAC	Floor	43.16	43.64	$+1.13\%$	48.73	$+12.91\%$	49.27	$+14.16\%$
C	Cap	47.04	49.78	$+5.83\%$	24.11	-48.75%	26.17	-44.36%
C	Floor	41.44	43.10	$+4.01\%$	76.59	$+84.82\%$	80.76	$+94.87\%$
GS	Cap	102.38	105.08	$+2.64\%$	83.10	-18.84%	85.50	-16.49%
GS	Floor	85.63	88.31	$+3.12\%$	107.47	$+25.50\%$	110.47	$+29.00\%$
JPM	Cap	46.82	47.77	$+2.03\%$	41.11	-12.20%	41.96	-10.37%
JPM	Floor	37.82	38.73	$+2.41\%$	44.14	$+16.71\%$	45.18	$+19.47\%$
AXP	Cap	59.95	65.89	$+9.92\%$	37.69	-37.12%	42.33	-29.39%
AXP	Floor	54.42	60.22	$+10.64\%$	86.16	$+58.32\%$	94.25	$+73.18\%$
AIG	Cap	91.58	99.38	$+8.53\%$	55.01	-39.93%	61.12	-33.26%
AIG	Floor	81.84	90.29	$+10.32\%$	136.36	$+66.62\%$	147.18	$+79.83\%$
MS	Cap	128.77	129.34	$+0.44\%$	124.89	-3.01%	125.45	-2.58%
MS	Floor	111.57	112.14	$+0.51\%$	115.75	$+3.74\%$	116.33	$+4.27\%$
MER	Cap	76.57	78.25	$+2.20\%$	67.07	-12.40%	68.59	-10.42%
MER	Floor	65.11	66.77	$+2.55\%$	75.97	$+16.67\%$	77.85	$+19.56\%$

Table 4.15: CVA of 5-year caps and floors for different correlation schemes. The CVA is reported in basis points and variations are computed compared to the no-correlation case.

All the remarks on the CVA of swaps remain valid for caps and floors. $\rho_{V\lambda}$ has a wrong-way effect for both positions, $\rho_{r\lambda}$ has a right-way effect on caps and a wrong-way effect on floors, and interestingly, the materiatlity of the $\rho_{V\lambda}$ effect is still negligible. This may seem surprising since option exposures are affected by the volatility variable. However, while it is true that the volatility factor affects the exposure, which is an expectation of discounted future cash-flows, the realized cash-flows do not depend on it. Hence, for a given factor to generate significant right-way/wrong-way risk, it should directly influence the cash-flows of the derivative product. We can say that the materiality of right-way/wrong-way risk on the price of counterparty risk is located at the cash-flows level, but neither at the exposure level (expectation of cash-flows), nor at the uncertainty level (volatility of cash-flows).

4.4.3 Impact of correlations on the CVA of collateralized interest-rate swaps

In this sub-section, we examine the CVA of collateralized interest-rate swaps. For fully collateralized swaps and under the assumption that swap positions are replaced only after two weeks upon default, the risk comes from a potential movement of interest rates during the two-week period. If the swap value after two weeks becomes greater than the swap value at the default time, the lastly availabe collateral that is equal to the swap value at the default time cannot cover the new swap value, hence the difference between the two values is considered as a loss. In this context, an increase in interest-rate volatility may have a key effect. Hence, we expect a positive $\rho_{V\lambda}$ to increase the CVA in this case. However, the role of $\rho_{r\lambda}$ in this situation is ambiguous, so that we do not expect it to be relevant. In Table 4.16, we report the CVA of a 5-year collateralized swap for the different correlation schemes considered in this chapter.

As we can see from Table 4.16, $\rho_{V\lambda}$ has a wrong-way effect as expected. However, this effect is not very significant, reaching at the maximum only 12%. In addition, as expected, $\rho_{r\lambda}$ has not a clear effect and the corresponding variation is very small, so that it can be simply caused by sampling

		$\rho_{V\lambda}=0,\ \rho_{r\lambda}=0$	$\rho_{V\lambda}\neq 0,\ \rho_{r\lambda}=0$		$\rho_{V\lambda}=0,\ \rho_{r\lambda}\neq 0$		$\rho_{V\lambda}\neq 0,\ \rho_{r\lambda}\neq 0$	
		CVA	CVA	Variation	CVA	Variation	CVA	Variation
BAC	Payer	4.74	4.85	+2.25%	4.91	+3.52%	4.85	+2.22%
BAC	Receiver	4.80	4.80	+0.13%	4.85	+1.12%	5.03	+4.93%
C	Payer	5.16	5.63	+9.04%	5.66	+9.62%	6.01	+16.41%
C	Receiver	5.18	5.61	+8.35%	5.64	+8.89%	5.95	+14.88%
GS	Payer	9.74	10.12	+3.83%	9.84	+1.05%	10.29	+5.61%
GS	Receiver	9.49	9.93	+4.60%	9.60	+1.14%	10.16	+7.01%
JPM	Payer	4.22	4.33	+2.56%	4.31	+2.18%	4.35	+2.94%
JPM	Receiver	4.17	4.42	+6.00%	4.16	−0.21%	4.52	+8.29%
AXP	Payer	7.06	7.88	+11.75%	7.38	+4.58%	8.19	+16.03%
AXP	Receiver	7.04	7.61	+8.12%	7.26	+3.14%	8.11	+15.25%
AIG	Payer	10.16	11.31	+11.34%	10.64	+4.73%	11.89	+17.02%
AIG	Receiver	10.00	11.07	+10.72%	10.52	+5.19%	11.94	+19.41%
MS	Payer	12.83	12.95	+0.93%	12.97	+1.10%	12.90	+0.50%
MS	Receiver	12.41	12.47	+0.51%	12.35	−0.41%	12.61	+1.63%
MER	Payer	7.22	7.55	+4.60%	7.28	+0.82%	7.72	+6.96%
MER	Receiver	7.19	7.56	+5.05%	7.40	+2.95%	7.51	+4.35%

Table 4.16: CVA of 5-year collateralized swaps for different correlation schemes. The CVA is reported in basis points and variations are computed compared to the no-correlation case.

errors. In sum, the effect of $\rho_{V\lambda}$ dominates the picture, but it is still very small to be taken into consideration, resulting at maximum in a variation of the expected loss of only about 1 basis point. Note that the numbers we obtained are close to the numbers reported in Harris et al. (2015). Harris et al. (2015) analyzed the effect of $\rho_{V\lambda}$ on the expected loss of collateralized swaps with the same assumptions. However, instead of basing their interpretations on the unconditional expected loss, they considered the conditional expected loss, which is defined as the average loss based only on defaulted scenarios. Under this metric, they found the effect of $\rho_{V\lambda}$ to be relevant. Nevertheless, we deem that any conclusion drawn from such findings should be based on the unconditional expected loss, because it is this loss that defines the CVA as a measure for the market price of counterparty risk. Following this view, $\rho_{V\lambda}$ has a minor effect on the price of counterparty risk, whether we consider collateralization or not.

4.5 Sensitivity analysis

In this section, we perform a sensitivity analysis to validate the interpretations drawn in the previous section. We stress the parameters of the interest-rate and the default-intensity models in order to examine to what extent the CVA can be impacted by $\rho_{V\lambda}$ for all the instruments that we consider in this analysis. The key parameters to be stressed are the volatility of the interest-rate volatility process ν_V and the volatility of the default intensity ν_λ. In fact, these are the parameters that amplify the joint random shocks caused by the correlations. We put ν_V equal to 0.03 instead of 0.008. In order to ensure that the interest-rate volatility variable remains strictly positive all the time, we further set $\theta_V = 0.0009$ and $\xi_V = 0.51$. We keep all the other parameters of the interest-rate model at their original values. For the default-intensity parameters, we consider a hypothetical company having a high credit risk profile, for which the default-intensity volatility ν_λ is set equal to 0.4. The stressed parameters of the interest-rate and the default-intensity models are reported in Tables 4.17 and 4.18.

ξ_V	0.51
θ_V	0.0009
ν_V	0.03

Table 4.17: Stressed parameters of the interest-rate model

λ_0	0.17
θ_λ	0.17
ξ_λ	0.5
ν_λ	0.4

Table 4.18: Stressed parameters of the default-intensity model

In Figure 4.1, we can see the incremental effect of $\rho_{V\lambda}$ and $\rho_{r\lambda}$ on the CVA of non-collateralized instruments with a 5-year maturity. In Figure 4.2, we draw the incremental variation of the CVA in % with comparison to the independent case as a function $\rho_{V\lambda}$ and $\rho_{r\lambda}$. Correlation values range from -0.9 to 0.9. It is clear that the effect $\rho_{V\lambda}$ is minor compared to the effect of $\rho_{r\lambda}$ for all instruments. The contribution of $\rho_{V\lambda}$ reaches at maximum around 12% for extreme values, while the effect of $\rho_{r\lambda}$ is much more substantial. This validates the conclusion that the contribution $\rho_{V\lambda}$ is in general small in magnitude, and for non-collateralized instruments, it is always dominated by the contribution of $\rho_{r\lambda}$.

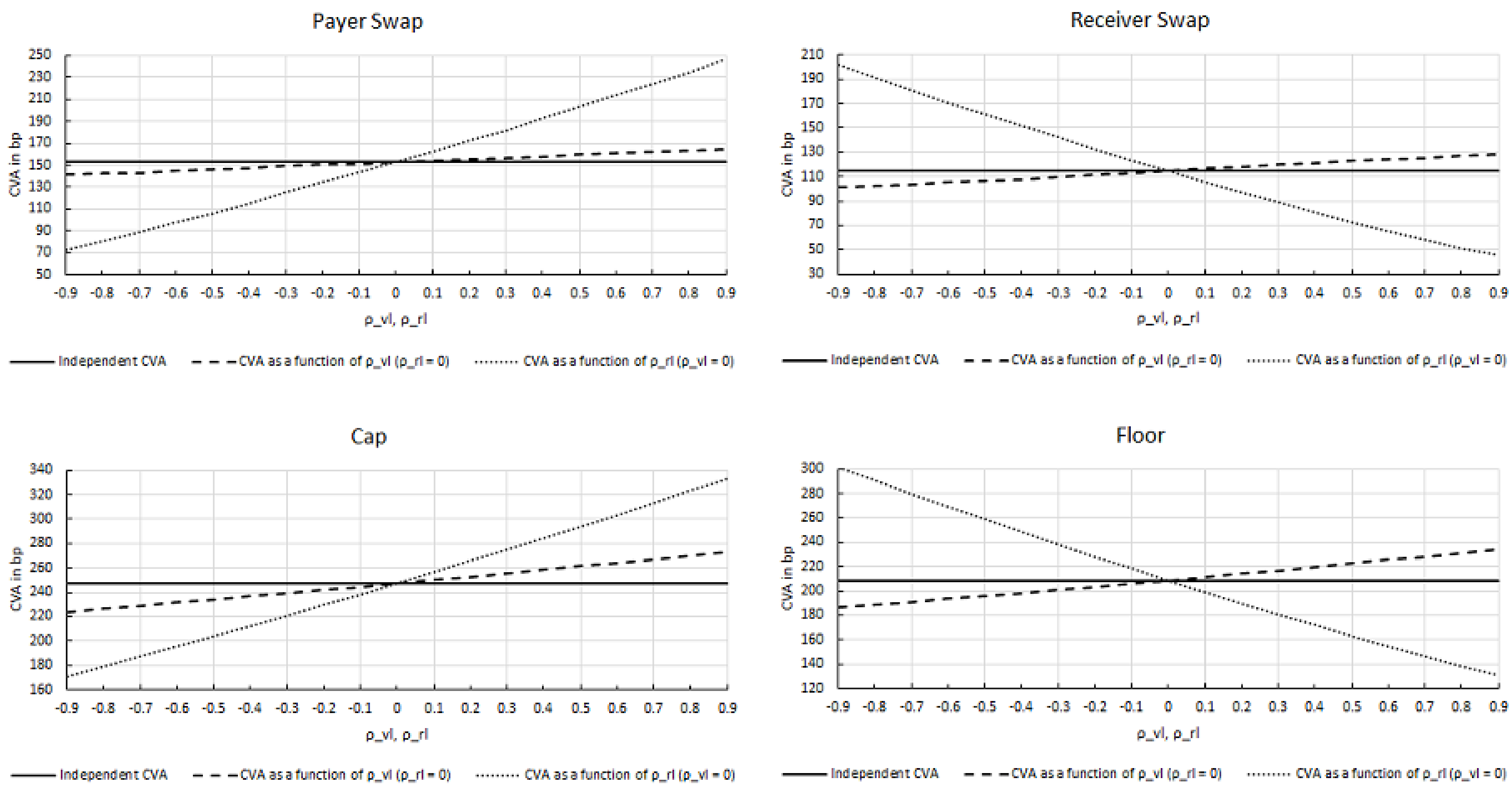

Figure 4.1: CVA as a function of $\rho_{V\lambda}$ and $\rho_{r\lambda}$

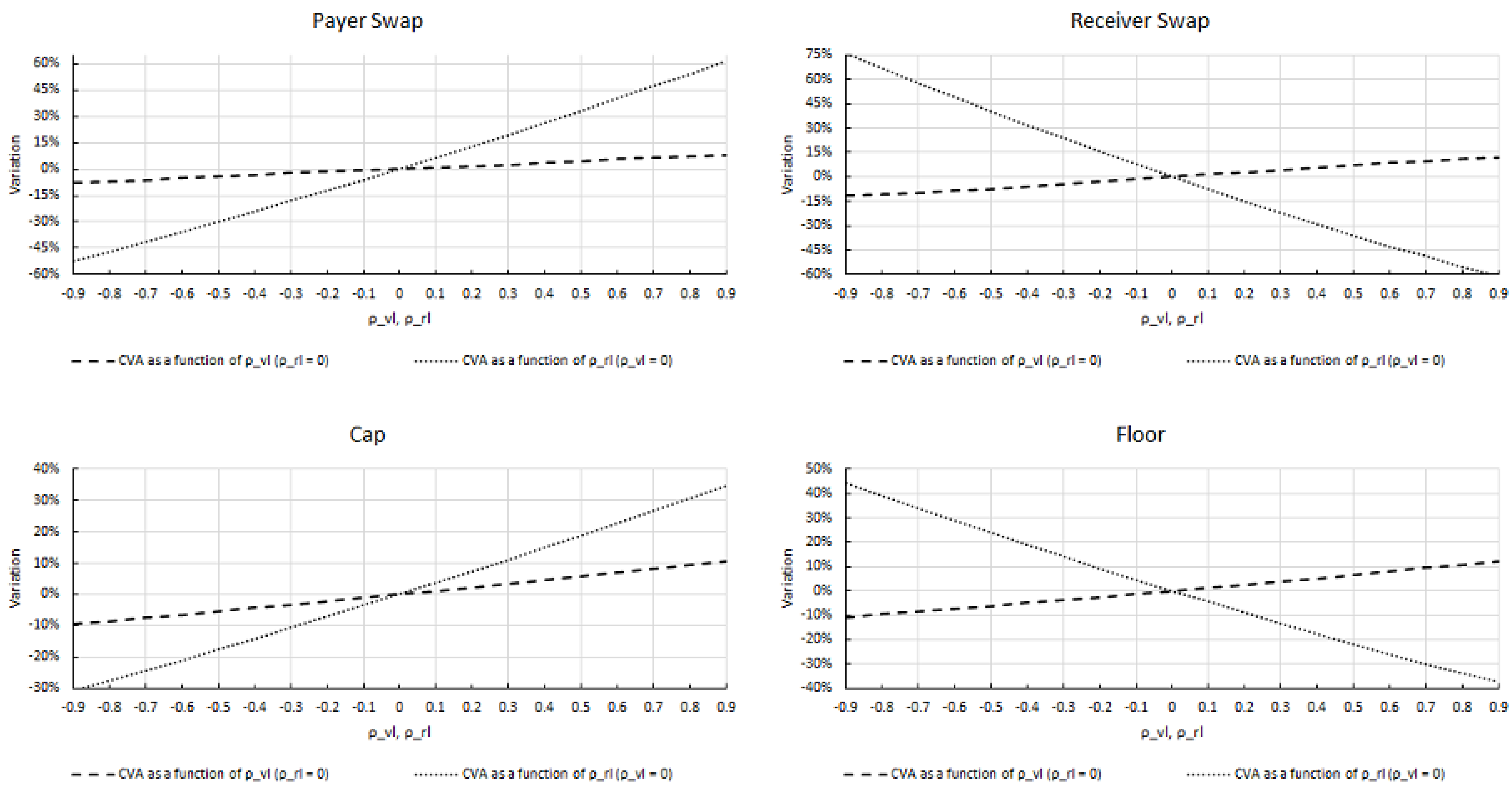

Figure 4.2: Variation of the CVA as a function of $\rho_{V\lambda}$ and $\rho_{r\lambda}$

4.6 Conclusion

In this chapter, we investigated the impact of two kinds of correlation on the right-way/wrong-way risk in the interest-rate market. The first correlation depicts the dependence between the interest-rate level and the default probability, while the second introduces the dependence between the interest-rate volatility and the default probability. We considered an interest-rate model having the USV feature in order to analyze the effects of correlations on both volatility-insensitive products such as interest-rate swaps and volatility-sensitive instruments such as interest-rate caps and floors. We also investigated the effects of correlations on collateralized instruments where gap risk becomes relevant.

We found that a positive correlation between the volatility and the default probability has generally a wrong-way effect. However, this effect is largely dominated by that of the correlation between the interest-rate level and the default probability for non-collateralized instruments, and it is barely contributing to the gap risk for collateralized instruments. This is true for both interest-rate swaps and options. At first glance, this seemed surprising, since option exposures depend on the volatility state. We thus concluded that right-way/wrong-way risk is material at the very bottom level of realized cash-flows, at least for the theoretical setup considered in this study. Our conclusions are backed by the numerical results we reported.

An interesting line of research would be to investigate the effects of the correlations in other markets (equity options, FX, etc.) and to consider a variety of other market models. In particular, it would be interesting to investigate the impact of the volatility correlation on the CVA of timer options, where the cash-flows are directly affected by the volatility variable. We let these extensions for future research.

Chapter 5

General conclusion

In this thesis, we presented several contributions on the topics of counterparty risk.

In the first essay, we suggested a new method to compute the CVA of derivative instruments having early-exercise features. This method is general and can be also applied to derivatives without early-exercise features. The proposed approach is based on a recursive formulation of the CVA. This formulation gives rise to a dynamic programming (DP) algorithm, which is more efficient than standard simulation techniques when the number of risk factors is not high. Moreover, the approach accounts for the change in the exercise strategy caused by the presence of counterparty risk. In particular, we show that the use of the default-free exercise strategy, which keeps the calculation of the CVA as a simple expected loss, may introduce arbitrage opportunities, and thus it is not consistent with financial theory. The CVA in the context of derivatives with early-exercise features is recursive, and its computation has to go through a complete re-evaluation of the optimal value that accounts for counterparty risk. Besides, the major drawback of the dynamic procedure is the curse of dimensionality. When the number of risk factors is quite high, dynamic programming methods are not efficient anymore. This may be a serious problem for the application of our method on the CVA computation for large netted portfolios depending on too many risk factors. However, it is worth noting that netting sets are in general defined at a market level. For instance, interest-rate positions may be netted together, but not with equity options. In this sense, even if a netting set is composed of a high number of different positions, these positions are still depending on the same risk factors, since they belong to the same market. In this situation, our method can be an interesting alternative for simulation, in terms of precision and computational efficiency. Moreover, our method is still very useful to report the incremental CVA of an individual new trade. In any case, there are still some solutions to overcome the dimensionality problem, by the use of parallel computing or heuristic techniques. To finish, an interesting number of extensions can be made to the suggested dynamic model, such as the inclusion of collateral and funding costs. It would be also interesting to adapt the formulation to the bilateral CVA when bilateral counterparty risk is relevant. Another line of research consists in extending the model to cases with multiple stopping times, for instance a portfolio composed of Bermudan options with different maturities. We let these extensions for future research.

In the second essay, we made use of an interesting property of the dynamic algorithm developed in the first essay to build an efficient methodology to estimate the CVA VaR. In fact, the dynamic algorithm provides the CVA as a known function of the risk factors for all dates, in just one execution. This property allows to estimate the CVA VaR by performing only one simple simulation. We studied the complex properties of the CVA VaR through illustrative numerical examples in which we applied the suggested methodology. We showed in particular that ad-hoc assumptions used by practitioners may underestimate the CVA capital charge. This essay is a direct and an elegant risk management application of the first essay. The contribution of this essay can be relevant in regulatory and professional environments, since the CVA capital charge is an important new requirement of the Basel III accords.

Finally, in the third essay, we investigated the role of a correlation between the interest-rate volatility and the default probability in generating right-way/wrong-way risk in the interest-rate derivative market. We considered an interest-rate model featuring unspanned stochastic volatility (USV) in order to analyze, in a first step, the correlation effects on derivatives whose exposures are not affected by the volatility state such as interest-rate swaps, and in a second step, the correlation impact on derivatives whose exposures depend on the volatility variable such as interest-rate caps and floors. We also studied the effects on both collateralized and non-collateralized instruments. We found that, overall, the volatility correlation has a minor effect on the CVA of interest-rate derivatives, and that, for non-collateralized instruments, the impact of the volatility correlation is largely dominated by the effect of a correlation between the interest-rate level and the default probability, which is the main driver of right-way/wrong-way risk. This can be explained by the fact that the cash-flows are driven only by the interest-rate level. These findings can have practical implications, since volatility modeling may not be very relevant to account for serious effects of wrong-way risk. Interesting lines of research would be to further investigate the role of the volatility correlation in other markets, and by considering other models. It would be also interesting to investigate the CVA of timer options, where cash-flows directly depend on the volatility state. We let these extensions for future research.

Bibliography

[1] Andricopoulos, A. D., Widdicks, M., Duck, P. W., and Newton, D. P. (2003). Universal option valuation using quadrature methods. Journal of Financial Economics, Vol. 67, No. 3, pp. 447-471.

[2] Andricopoulos, A. D., Widdicks, M., Newton, D. P., and Duck, P. W. (2007). Extending quadrature methods to value multi-asset and complex path-dependent options. Journal of Financial Economics, Vol. 83, No. 2, pp. 471-499.

[3] Basel Committee on Banking Supervision (BCBS) (2010). Basel III: A global regulatory framework for more resilient banks and banking systems, www.bis.org.

[4] Black, F. (1976). The pricing of commodity contracts. Journal of Financial Economics, Vol. 3, No. 1-2, pp. 167-179.

[5] Breton, M., and de Frutos, J. (2012). Approximation of Dynamic Programs. In: Duan, J.C., Härdle, W., and Gentle, J. E. (Editors), Handbook of Computational Finance, Springer.

[6] Brigo, D., and Alfonsi, A. (2005). Credit Default Swap Calibration and Derivatives Pricing with the SSRD Stochastic Intensity Model. Finance and Stochastics, Vol. 9, No. 1, pp. 29-42.

[7] Brigo, D., and Masetti, M. (2006). Risk Neutral Pricing of Counterparty Risk. In: Pykhtin, M. (Editor), Counterparty Credit Risk Modelling: Risk Management, Pricing and Regulation. Risk Books, London.

[8] Brigo, D., and Mercurio, F. (2001). A deterministic-shift extension of analytically tractable and time-homogeneous short-rate models. Finance and Stochastics, Vol. 5, No. 3, pp. 369-388.

[9] Brigo, D., Morini, M., and Pallavicini, A. (2013). Counterparty Credit Risk, Collateral and Funding: With Pricing Cases For All Asset Classes. Wiley Finance.

[10] Brigo, D., Morini, M., and Tarenghi, M. (2011). Credit calibration with structural models and equity return swap valuation under counterparty risk. In: Bielecki, T., Brigo, D., and Patras, F. (editors) Credit risk frontiers: Subprime crisis, pricing and hedging, CVA, MBS, ratings, and liquidity, pp. 457-484. John Wiley & Sons.

[11] Brigo, D., and Pallavicini, A. (2007). Counterparty Risk under Correlation between Default and Interest Rates. In: Miller, J., Edelman, D., and Appleby, J. (Editors), Numerical Methods for Finance, Chapman Hall.

[12] Brigo, D., Pallavicini, A., and Papatheodorou, V. (2009). Bilateral counterparty risk valuation for interest-rate products: impact of volatilities and correlations. Working Paper, arXiv:0911.3331v3.

[13] Carriere, J. F. (1996). Valuation of the early-exercise price for options using simulations and non-parametric regression. Insurance: mathematics and Economics, Vol. 19, No. 1, pp. 19-30.

[14] Casassus, J., Collin-Dufresne, P., and Goldstein, R. (2005). Unspanned stochastic volatility and fixed income derivatives pricing. Journal of Banking and Finance, Vol. 29, No. 11, pp. 2723-2749.

[15] Cesari, G., Aquilina, J., Charpillon, N., Filipovic, Z., Lee, G., and Manda, I. (2009). Modelling, pricing, and hedging counterparty credit exposure: A technical guide. Springer Finance.

[16] Chen, D., Härkönen, H. J., and Newton, D. P. (2014). Advancing the universality of quadrature methods to any underlying process for option pricing. Journal of Financial Economics, Vol. 114, No. 3, pp. 600-612.

[17] Clenshaw, C. W., and Curtis, R. (1960). A method for numerical integration on an automatic computer. Numerische Mathematik, Vol. 2, pp. 197-205.

[18] Collin-Dufresne, P., and Goldstein, R. (2002). Do Bonds Span the Fixed Income Markets? Theory and Evidence for Unspanned Stochastic Volatility. Journal of Finance, Vol. 57, No. 4, pp. 1685-1730.

[19] Cox, J. C., Ingersoll Jr, J. E., and Ross, S. A. (1985). A theory of the term structure of interest rates. Econometrica, Vol. 53, No. 2, pp. 385-407.

[20] Dai, Q., and Singleton, J. K. (2000). Specification Analysis of Affine Term Structure Models. Journal of Finance, Vol. 55, No. 5, pp. 1943-1978.

[21] Duffie, D., Pan, J., and Singleton, K. (2000). Transform analysis and option pricing for affine jump-diffusions. Econometrica, Vol. 68, No. 6, pp. 1343-1376.

[22] Duffie, D., and Singleton, K. (1999). Modeling term structures of defaultable bonds. Review of Financial Studies, Vol. 12, No. 4, pp. 687-720.

[23] Fong, H. G., and Vasicek, O. A. (1991). Fixed-income volatility management. Journal of Portfolio Management, Vol. 17, No. 4, pp. 41-46.

[24] Gregory, J. (2012). Counterparty Credit Risk and Credit Value Adjustment: A Continuing Challenge for Global Financial Markets. John Wiley and Sons.

[25] Harris, G. R., Wu, T. L., and Yang, J. (2015). The relationship between counterparty default and interest rate volatility and its impact on the credit risk of interest rate derivatives. Journal of Credit Risk, Vol. 11, No. 1, pp. 93-127.

[26] Heath, D., Jarrow, R. and Morton, A. (1992). Bond Pricing and the Term Structure of Interest Rates: A New Methodology for Contingent Claims Valuation. Econometrica, Vol. 60, No. 1, pp. 77-105.

[27] Heston, S. L. (1993). A Closed-Form Solution for Options with Stochastic Volatility with Applications to Bond and Currency Options. The Review of Financial Studies, Vol. 6, No. 2, pp. 327-343.

[28] Hull, J. and White, A. (1990). Pricing Interest Rate Derivative Securities. The Review of Financial Studies, Vol. 3, No. 4, pp. 573-592.

[29] Hull, J., and White, A. (2012). CVA and wrong-way risk. Financial Analysts Journal, Vol. 68, No. 5, pp. 58-69.

[30] Klein, P. (1996). Pricing Black-Scholes options with correlated credit risk. Journal of Banking and Finance, Vol. 20, No. 7, pp. 1211-1229.

[31] Klein, P., and Yang, J. (2013). Counterparty credit risk and American options. Journal of Derivatives, Vol. 20, No. 4, pp. 7-21.

[32] Lando, D. (1998). On Cox Processes and Credit Risky Securities. Review of Derivatives Research, Vol. 2, No. 2, pp. 99-120.

[33] Longstaff, F. A., and Schwartz, E. S. (1992). Interest Rate Volatility and the Term Structure: A Two-Factor General Equilibrium Model. The Journal of Finance, Vol. 47, No. 4, pp. 1259-1282.

[34] Longstaff, F. A., and Schwartz, E. S. (2001). Valuing American options by simulation: A simple least-squares approach. Review of Financial Studies, Vol. 14, No. 1, pp. 113-147.

[35] Merton, R. C. (1974). On the Pricing of Corporate Debt: the Risk Structure of Interest Rates. Journal of Finance, Vol. 29, No. 2, pp. 449-470.

[36] Merton, R. C. (1976). Option pricing when underlying stock returns are discontinuous. Journal of Financial Economics, Vol. 3, No. 1, pp. 125-144.

[37] Nelson, C. R., and Siegel, A. F. (1987). Parsimonious Modeling of Yield Curves. The Journal of Business, Vol. 60, No. 4, pp. 473-489.

[38] Pykhtin, M. (2012). Model foundations of the Basel III standardised CVA charge, Risk, July, pp. 60–66.

[39] Schönbucher, P. J. (2003). Credit derivatives pricing models: models, pricing and implementation. John Wiley and Sons.

[40] Sullivan, M. A. (2000). Valuing american put options using gaussian quadrature. Review of Financial Studies, Vol. 13, No. 1, pp. 75-94.

[41] Svensson, L. E. O. (1994). Estimating and Interpreting Forward Interest Rates: Sweden 1992-1994. IMF Working Paper, WP/94/114.

[42] Svenstrup, M. (2005). On the suboptimality of single-factor exercise strategies for bermudan swaptions. Journal of Financial Economics, Vol. 78, No. 3, pp. 651-684.

[43] Tilley, J. A. (1993). Valuing American options in a path simulation model. Transactions of the Society of Actuaries, Vol. 45, No. 83, pp. 55-67.

[44] Trolle, A., B., and Schwartz, E. S. (2009). A General Stochastic Volatility Model for the Pricing of Interest Rate Derivatives. Review of Financial Studies, Vol. 22, No. 5, pp. 2007-2057.

[45] Tsitsiklis, J. N., and Van Roy, B. (2001). Regression methods for pricing complex American-style options. IEEE Transactions on Neural Networks, Vol. 12, No. 4, pp. 694-703.

[46] Vasicek, O. (1977). An Equilibrium Characterisation of the Term Structure. Journal of Financial Economics, Vol. 5, No. 2, pp. 177-188.